INFORMATION TO USERS

This manuscript has been reproduced from the microfilm master. UMI films the text directly from the original or copy submitted. Thus, some thesis and dissertation copies are in typewriter face, while others may be from any type of computer printer.

The quality of this reproduction is dependent upon the quality of the copy submitted. Broken or indistinct print, colored or poor quality illustrations and photographs, print bleedthrough, substandard margins, and improper alignment can adversely affect reproduction.

In the unlikely event that the author did not send UMI a complete manuscript and there are missing pages, these will be noted. Also, if unauthorized copyright material had to be removed, a note will indicate the deletion.

Oversize materials (e.g., maps, drawings, charts) are reproduced by sectioning the original, beginning at the upper left-hand corner and continuing from left to right in equal sections with small overlaps.

Photographs included in the original manuscript have been reproduced xerographically in this copy. Higher quality 6" x 9" black and white photographic prints are available for any photographs or illustrations appearing in this copy for an additional charge. Contact UMI directly to order.

ProQuest Information and Learning
300 North Zeeb Road, Ann Arbor, MI 48106-1346 USA
800-521-0600

UMI®

CHARACTERIZING FIRE RELATED SPATIAL PATTERNS IN FIRE-PRONE ECOSYSTEMS USING OPTICAL AND MICROWAVE REMOTE SENSING

by

Mary Catherine Henry

A Dissertation Submitted to the Faculty of the

DEPARTMENT OF GEOGRAPHY AND REGIONAL DEVELOPMENT

In Partial Fulfillment of the Requirements
For the Degree of

DOCTOR OF PHILOSOPHY
WITH A MAJOR IN GEOGRAPHY

In the Graduate College

THE UNIVERSITY OF ARIZONA

2002

UMI Number: 3053870

UMI Microform 3053870

ProQuest Information and Learning Company
300 North Zeeb Road
P.O. Box 1346
Ann Arbor, MI 48106-1346

THE UNIVERSITY OF ARIZONA ®
GRADUATE COLLEGE

As members of the Final Examination Committee, we certify that we have read the dissertation prepared by MARY CATHERINE HENRY

entitled Characterizing Fire Related Spatial Patterns in Fire-Prone Ecosystems Using Optical and Microwave Remote Sensing

and recommend that it be accepted as fulfilling the dissertation requirement for the Degree of Doctor of Philosophy

Stephen R. Yool — Date 5/22/02

Stuart E. Marsh — Date 05/23/02

Thomas W. Swetnam — Date 05/23/02

M. Susan Moran — Date 5/23/02

Malcolm J. Zwolinski — Date 5/23/02

Final approval and acceptance of this dissertation is contingent upon the candidate's submission of the final copy of the dissertation to the Graduate College.

I hereby certify that I have read this dissertation prepared under my direction and recommend that it be accepted as fulfilling the dissertation requirement.

Dissertation Director Stephen R. Yool — Date 5/22/02

STATEMENT BY AUTHOR

This dissertation has been submitted in partial fulfillment of requirements for an advanced degree at The University of Arizona and is deposited in the University Library to be made available to borrowers under rules of the Library.

Brief quotations from this dissertation are allowable without special permission, provided that accurate acknowledgment of source is made. Requests for permission for extended quotation from or reproduction of this manuscript in whole or in part may be granted by the head of the major department or the Dean of the Graduate College when in his or her judgment the proposed use of the material is in the interests of scholarship. In all other instances, however, permission must be obtained from the author.

SIGNED: 

ACKNOWLEDGMENTS

I would like to thank my advisor, Dr. Steve Yool, for all of his support throughout my entire PhD experience. I was never short of assistantship opportunities thanks to him. Thank you to my entire committee: Dr. Stuart Marsh (Arid Lands), Dr. Tom Swetnam (Tree-Ring Lab), Dr. Susan Moran (USDA Agricultural Research Station), and Dr. Mal Zwolinski (Renewable Natural Resources). I am fortunate to have had a committee with such diverse areas of expertise and also to have taken classes from almost all of them. Thank you again for serving on my committee.

This dissertation was completed long-distance, which would have been impossible if not for the assistance and cooperation of my entire committee, and especially Rhoda Ray, Linda Koski, and Cathy Weppler of the Geography Department. They were always willing to help with fellowship reimbursement, class registration, and all other administrative issues. Thanks for making the distance as painless as possible.

Thanks to Kathy Schon and Pam Anning of the National Park Service (Saguaro, Rincon Mountain District), who supplied the fire atlas used in this study. I hope my research can be useful to you in some way.

This dissertation would have been much more difficult to complete if not for funding I received from the EPA Science To Achieve Results (STAR) Fellowship Program (Fellowship Number U915601). Thank you to my project officer, Georgette Boddie for all of her help over the past three years.

Lastly, thank you to my family for all of their support during the seemingly endless years school- I'm finally finished!

DEDICATION

For John and Maya,

Who were there through it all.

For my Mom, Judy Roberts,

Thank you for everything.

TABLE OF CONTENTS

ABSTRACT

The use of active and passive remote sensing systems for relating forest spatial patterns to fire history was tested over one of the Arizona Sky Islands. Using Landsat Thematic Mapper (TM), Shuttle Imaging Radar (SIR-C), and data fusion I examined the relationship between landscape metrics and a range of fire history characteristics. Each data type (TM, SIR-C, and fused) was processed in the following manner: each band, channel, or derived feature was simplified to a thematic layer and landscape statistics were calculated for plots with known fire history. These landscape metrics were then correlated with fire history characteristics, including number of fire-free years in a given time period, mean fire-free interval, and time since fire. Results from all three case studies showed significant relationships between fire history and forest spatial patterns. Data fusion performed as well or better than Landsat TM alone, and better than SIR-C alone. These comparisons were based on number and strength of significant correlations each method achieved. The landscape metric that was most consistent and obtained the greatest number of significant correlations was Shannon's Diversity Index. Results also agreed with field-based research that has linked higher fire frequency to increased landscape diversity and patchiness. An additional finding was that the fused data seem to detect fire-related spatial patterns over a range of scales.

CHAPTER 1

INTRODUCTION

Context of the Problem

Fire regime changes have occurred in the southwestern United States following European settlement, fire suppression, and livestock grazing. The shift from frequent low-intensity fires to infrequent stand-replacing crown fires in many forested ecosystems has led contemporary forest managers to reduce fuel loads through prescribed burning and mechanical clearing. Distribution of fuels is spatially variable and impacted by past fire activity. Regularly burned forests are typically more open, often exhibiting a mosaic landscape pattern. In the most extreme cases, fire-excluded forests are very dense with a high proportion of small, young trees. Given the disparate spatial patterns between forests with different fire history, it is likely possible to distinguish forest fire history based on landscape characteristics. Remote sensing may be a viable technique to complement field campaigns and characterize forest conditions at the landscape scale. In this dissertation, I investigated the use of passive and active remote sensing systems for assessing fire-related forest spatial patterns. The major research questions addressed in this dissertation were:

1) Can Landsat Thematic Mapper (TM) data be used to extract fire-related landscape patterns from forest ecosystems?
2) Can Shuttle Imaging Radar (SIR-C) be used to extract fire-related landscape patterns from forest ecosystems?

3) Can fusion of Landsat TM and SIR-C be used to extract fire-related landscape patterns from forest ecosystems?

I also investigated the following sub-questions:

a) Which landscape indices show the strongest link to fire history?

b) Which image data source (TM, SIR-C, or fusion) achieved the best results?

To assess relationships between fire history and spatial patterns, landscape metrics (Table 1) were calculated for areas with known fire history using the image data cited above. These statistics were correlated with a range of fire history variables to determine where significant relationships exist. Fire history data were obtained from the National Park Service, while all image data were acquired from the Arizona Regional Image Archive (ARIA) or purchased from the United States Geological Survey (USGS).

Table 1. Landscape statistics used in this dissertation.

Statistic	Abbreviation	Description
Mean Patch Size	MPS	average patch size
Patch Size Coefficient of Variation	PSCV	patch size standard deviation / mean patch size
Patch-per-Unit Area	PPU	number of patches normalized by area
Mean Patch Fractal Dimension	MPFD	average fractal dimension (area / perimeter calculation)
Area Weighted MPFD	AWMPFD	average fractal dimension weighted by patch area
Shannon's Diversity Index	SDI	sensitive to richness (number of patch types)
Shannon's Evenness Index	SEI	distribution of area among patch types

Dissertation Format

This dissertation is formatted with three publishable papers included as appendices. All three studies were conducted over the same study area, but each used a different data set. In the first paper, I used Landsat TM data to extract landscape patterns.

SIR-C data were used in the second paper, following the same techniques used in the first. Finally, the two data sources were used together to characterize landscape patterns. The data analysis techniques used in each study were kept consistent to facilitate comparison and evaluation of methods. All research described here was conducted solely for the purpose of this dissertation. Funding for the research was provided by the Environmental Protection Agency (EPA) through a Science To Achieve Results (STAR) Graduate Fellowship (Fellowship Number U915601) awarded from September 1999 to August 2002.

CHAPTER 2

PRESENT STUDY

Summary

The literature review, methods, and results of this study are presented in three papers appended to this dissertation. The following is a summary of significant findings from each paper. The goal of this research, as a whole, was to characterize landscape patterns caused by differences in fire history. In all three papers, the approach used was the same: calculate landscape metrics for plots with different fire history and correlate these with various aspects of fire history. The difference between the three case studies was the data used.

Characterizing Fire-Related Spatial Patterns in the Arizona Sky Islands using Landsat TM Data

A Landsat TM scene from May 1996 was used to calculate the Tasseled Cap Transform (Kauth-Thomas, or KT), the Intensity-Hue-Saturation (IHS) components of the KT, and the Normalized Difference Vegetation Index (NDVI). Each of these image enhancements was simplified to a format where landscape metrics could be calculated. Spearman's Rank Correlation Analysis was performed between a range of fire history variables and landscape metrics derived from the simplified image enhancements. Landscape statistics used included: patch size coefficient of variation (PSCV), mean

patch size (MPS), mean patch fractal dimension (MPFD), Shannon's Diversity Index (SDI), and Shannon's Evenness Index (SEI).

Non-spatial analysis (using plot means, rather than landscape metrics) achieved some significant results, but most of the landscape metrics performed better (more significant correlations). Relationships between fire history and landscape patterns agree with results found in related field-based studies. For example, increased fire activity was linked to smaller patch size (MPS), greater patch size variability (PSCV), higher patch shape complexity (MPFD), and higher landscape diversity (SDI).

The Sensitivity of SIR-C Backscatter to Fire-Related Forest Spatial Patterns

SIR-C data (October 1994) and ratios were used in this study to calculate the same landscape metrics used in the first study. The same processing steps were followed to allow comparison between the data types. Significant findings include a lack of significant correlations between mean backscatter (non-spatial analysis) and fire history. Of the landscape metrics, Shannon's Diversity Index (SDI) achieved the greatest number of significant results over all. The relationships found using the SIR-C data agreed with trends found in Landsat TM data and field-based research: landscape diversity is directly related to fire frequency.

Assessing Relationships Between Forest Spatial Patterns and Fire History with Fusion of Landsat TM and SIR-C Data

The third and final study of this dissertation followed the same analysis procedures as the first two studies, but used data fusion of Landsat TM and SIR-C. Because the Landsat TM scene used in the first study was acquired in 1996, a different image was purchased to coincide with the SIR-C data. All comparisons made in this paper between TM, SIR-C, and fused data refer to the 1994 TM analysis. Prior to calculating landscape metrics, the TM and SIR-C data were fused using a range of techniques that resulted in 17 new image features. Details of the fusion techniques are described in Appendix C.

There are several important findings in this paper:

1) fused data obtained correlation results that were better than SIR-C alone in 80% of cases and better than TM data alone in 55% of cases;
2) landscape diversity (SDI) achieved the most consistent results between the data types;
3) different data fusion techniques seem to detect spatial patterns at a range of scales; and
4) relationships between fire history and forest spatial patterns vary with scale.

Conclusions

The results of these studies support the feasibility of relating fire history to forest spatial patterns, using satellite-based remote sensing. Although data fusion obtained the

best results, each data source alone was also able to detect landscape patterns that can be linked to fire history. Future research could assess temporal aspects of these relationships, including how spatial patterns change over time.

APPENDIX A:

Characterizing Fire-Related Spatial Patterns in the Arizona Sky Islands using Landsat TM Data

M. C. Henry and S. R. Yool

Department of Geography and Regional Development, Harvill Building, Box #2, University of Arizona, Tucson, AZ 85721

In press, *Photogrammetric Engineering and Remote Sensing*

ABSTRACT

This research investigates the use of Landsat Thematic Mapper data to characterize spatial patterns in forests experiencing different fire severities and frequencies between 1943 and 1996. Spectral vegetation indices (SVIs) were used to compare spectral characteristics and spatial patterns for four categories of fire history: once burned, twice burned, multiple burned, and unburned. We quantified spatial patterns by calculating spatial statistics from several SVIs for each plot. These statistics were used in Spearman's Rank Correlation Analysis with fire history characteristics. We found significant relationships ($p < 0.05$) between many of the spatial measures (mean patch size, patch size coefficient of variation, mean patch fractal dimension, Shannon's Diversity Index, Shannon's Evenness Index) and fire occurrence in the past ten, thirty, fifty, and fifty-four years, average fire-free interval, most recent fire-free interval, and time since the most recent fire.

INTRODUCTION

Over the last one hundred years, fuels have accumulated to dangerous levels in conifer forest communities of the southwestern United States. Aggressive fire suppression that dominated forest and range management for most of the 20th century is considered largely responsible for the current magnitude of fuel loads (Covington *et al.*, 1997). Prior to fire exclusion, frequent, low intensity lightning-ignited fires burned throughout the late spring and summer, removing dead, decaying plant material. In conifer forest communities, fire return intervals of less than twenty years were common

(Swetnam and Baisan, 1996). However, in the absence of fire, leaves, branch-wood, logs, and other plant debris collect in unnaturally high amounts, creating volatile conditions. A significant number of recent fires have been more intense and uncontrollable than the natural, moderate fires of the past, destroying entire forest stands (Covington *et al.*, 1997; Dahms and Geils, 1997). Fuels continue to increase until they are removed by fire or mechanical clearing.

Prescribed burning has been implemented in many areas in an effort to remove these excess fuels (Hurley, 1995; Swetnam and Baisan, 1996; Fulé *et al.*, 2001). To determine which areas are best-suited (and most critical) for prescribed burning, it is extremely important to assess fuel conditions. Variations in fuel are determined by species composition, fire history, as well as a host of topographically related factors, including site productivity. Fuel amounts are modified each time a fire burns through an area, since some portion (or all) of the fuel is removed. Frequently burned forests have less fuel and often have a more open appearance than forests that have not burned (Romme, 1982). These fire-induced changes are spatially variable in ways that have not been clearly defined (i.e. how are variations in fire severity distributed over space?) and at scales that are not well known (Pyne *et al.*, 1996).

Many ecologists cite the importance of spatial patterns in understanding forest structure and function (Turner, 1989), but much related research has been field-based (Romme, 1982). Remote sensing-based research on fire-related spatial patterns (Minnich *et al.*, 2000) has been conducted in only a few areas, such as Yellowstone National Park (Turner *et al.*, 1994) and the Mediterranean Basin (Chuvieco, 1999; Ricotta and Retzlaff,

2000). These studies demonstrate that the broad perspective afforded by satellite-based remote sensing is appropriate for examining spatial patterns over larger areas than are practical with field work (Schleusner 1994). While the field-based studies are vital to understanding the fundamental effects of anthropogenic fire regime changes, spatially unbiased field sampling is extremely intensive, time-consuming, and it is often difficult to extrapolate these findings to a scale useful for forest managers (Whelan, 1995). For this reason, remote sensing may be the optimal technique for monitoring fire-related landscape dynamics in both a spectral and spatial context.

In this study we extracted landscape metrics from several Landsat Thematic Mapper-derived image enhancements and correlated these with a range of fire history characteristics. We were interested in the following questions:

1) Can Landsat TM data be used to extract meaningful landscape patterns from forested ecosystems?
2) Can these patterns be connected to fire history?
    a) Which landscape metrics show the strongest link to fire history?
    b) Which vegetation indices or image enhancements were best able to extract meaningful landscape patterns?

BACKGROUND

Fire does not have a uniform impact on the landscape. The complexity of fire effects has been documented by many researchers (Whelan, 1995; Pyne *et al.*, 1996) and has been associated with variations in fire frequency and severity (Pyne *et al.*, 1996).

The spatial variability of fire effects is related to current variations in fuel amount and conditions. Fire history is thus also a significant feature of a forest landscape that conditions future fire patterns and severity.

Remote Sensing of Landscape Patterns

The spatially complex nature of fire makes it a good candidate for remote sensing research. Because satellite-based data are acquired over broad areas, the spatial pattern and arrangement of surface features can be easily quantified using a variety of landscape metrics and statistics. Landscape studies have used fractal dimension (Ricotta *et al.*, 1998; Ricotta and Retzlaff, 2000), geographic windows (in contrast to geometric windows) (Dillworth *et al.*, 1994), spatial autocorrelation measures (Chuvieco, 1999), and patch statistics (Chuvievo, 1999; Trani and Giles, 1999; Roy and Tomar, 2000) with varied success. Significant findings from these studies are discussed below.

Ricotta *et al.* (1998) used fractal dimension to quantify landscape structure preceding and following a fire in the Mediterranean basin. They hypothesized that landscape stability was high and that landscape spatial structure was resilient to fire. Due to the fire-tolerant characteristics and regrowth strategies of Mediterranean shrubs, they found that a burned area returned to its pre-fire spatial structure within a relatively short time period (Ricotta *et al.*, 1998). A related study (Ricotta and Retzlaff, 2000) examined scale issues of fractal characteristics and wildfires.

An alternative method to analyzing landscape patterns was discussed by Dillworth *et al.* (1994). The authors compared spatial characteristics derived from traditional

geometric windows (square) to those calculated using geographic windows (irregular shapes determined by landcover). The geographic window sizes vary for each pixel, based on the similarity of surrounding pixels. They found the geographic window technique to be superior for quantifying patch characteristics, because the size and shape of the window was adjusted to fit actual landscape patterns and not constrained by a square or rectangular shape (Dillworth *et al.*, 1994).

Spatial autocorrelation measures the similarities between pixels that are separated by a specified lag distance. These statistics have been used in landscape studies as a measure of landscape heterogeneity. A high degree of spatial autocorrelation is caused by clustering of similar pixel values in space, or landscape homogeneity. Chuvieco (1999) used this technique and others to evaluate landscape patterns preceding and following a large fire in Spain. Results showed that spatial autocorrelation increased following the fire, because most vegetation was removed (Chuvieco, 1999).

Defining a landscape in terms of patches is a commonly used technique in ecological research (Allen 1994). Trani and Giles (1999) studied the effects of deforestation on a host of landscape pattern metrics, including patch statistics. They found that mean patch size, number of patches, mean patch density, and interpatch distance were linked to deforestation. Chuvieco (1999) found that a stand-replacing fire reduced the number of landscape patches.

Despite significant findings from much of this research, Benson and MacKenzie (1995) cite problems with some of these metrics. They found that average patch size, average patch perimeter, and fractal dimension increased when pixel size increased in

their study. These results imply that spatial patterns can be affected significantly by the sensor spatial resolution. Frohn (1998) presents a thorough investigation of problems associated with fractal dimension, particularly with raster data. Ricotta and Retzlaff (2000) also cite a need for techniques to quantify spatial structure, while addressing scale issues. Additionally, some landscape metrics require nominal scale data, which necessitates subjective class definition and labeling (Chuvievo, 1999).

Spectral Enhancements

The image enhancements that we chose to calculate landscape metrics were the Kauth-Thomas Transform (KT), the Normalized Difference Vegetation Index (NDVI), and the Intensity, Hue, and Saturation (IHS) components of the KT. Each of these image enhancements is described below.

The six non-thermal bands of Landsat Thematic Mapper data are transformed into three new components by applying the appropriate KT coefficients (the transform is sensor specific). Examination of the coefficients reveals which characteristics are emphasized. For example, the first component (KT-Brightness, or KT-B) has positive coefficients for all six bands, with the highest value for band 3, or red (0.55177) (Crist and Cicone, 1984). The resulting KT-B image shows areas of bare soil and rock as bright, while vegetated areas are dark. Recent fire scars are usually visible as bright patches in a KT-B image, if a significant fraction of vegetation has been removed.

In contrast, the second component (KT-Greenness, or KT-G) has negative coefficients for all three visible bands, with the heaviest weighting in band 4, or the near-

infrared (0.85468) (Crist and Cicone, 1984). The KT-G image is nearly the opposite of the KT-B image, with bright areas corresponding to live, green biomass and bare areas appearing dark. A severely burned area will appear dark in a KT-G image, shortly following the fire.

The third KT component has been the focus of much controversy, although it is still widely referred to as KT-Wetness (KT-W). The coefficients for KT-W contrast TM bands 1 (blue), 2 (green), 3 (red), and 4 (near-infrared) with band 5 (mid-infrared). The heavy weighting in the mid-infrared is where the "wetness" label originates (these wavelengths are sensitive to moisture content), although this KT component is also responsive to shadowing (Cohen and Spies, 1992). KT-W has been extremely useful in fire-related remote sensing due to its sensitivity to fuel moisture and other forest conditions (Collins and Woodcock, 1996) and structure (Cohen and Spies, 1992).

Some advantages of using KT to study post-fire forested landscapes are illustrated by Patterson and Yool (1998), who compared KT to principal components analysis (PCA) for mapping fire severity. They achieved higher accuracy in a supervised classification using KT rather than PCA. They concluded that KT was superior for post-fire applications, because the coefficients are sensor-based and therefore independent of scene-based variations. Because the precise location of fire perimeters is generally not known, any post-fire image analysis includes both burned and unburned forest. When using a scene-based transform such as PCA, the greatest contrast is likely to occur between the burned and unburned portions of the scene, rather than differentiating fire severity levels within a burned area (Patterson and Yool, 1998).

The NDVI is a ratio vegetation index that accentuates the difference between near-infrared and red reflectances over a target of interest. The resulting values range from −1 to 1, where higher values correspond to healthy, green vegetation. Studies in many different environments have found relationships between NDVI and canopy cover (Larsson 1993), sunlit canopy fraction (Hall *et al.*, 1995) and primary production (Tucker and Sellers, 1986). NDVI has also been used extensively to evaluate fire-related forest conditions (Marchetti *et al.*, 1995; White *et al.*, 1996), including spatial characteristics preceding and following fire (Chuvieco, 1999). Because NDVI is a ratio index, it offers the advantage of minimizing topographic effects.

DATA AND METHODS

Study Area

Our research was conducted in the Rincon Mountains, located just east of Tucson, Arizona, USA. Most of the mountain range is contained within the Rincon Mountain District of Saguaro National Park (Figure 1). The Rincon Mountains represent one of the Arizona Sky Islands, so named because they are literally islands of forest ascending above and surrounded by the Sonoran Desert. Located at a transition between desert types, the vegetation communities found in the Sky Islands are unique and diverse, including desert scrub, oak woodland, pine-oak gallery, pine forest, and mixed conifer forest. The Rincon Mountains range from approximately 900 to 2800 meters in elevation. The present study is concentrated at elevations greater than 2000 meters, where vegetation is restricted to fire-prone oak, pine, or mixed conifer. Precipitation in

the region is bimodal, dominated in winter by frontal storms and in summer by monsoon thunderstorms that bring brief heavy rains. Average annual precipitation varies greatly with elevation and is as high as 760 mm on the mountain peaks.

Field-based fire research has been extensive in the Rincon Mountains (Baisan and Swetnam, 1990), although we are not aware of other forest fire research utilizing remotely sensed data in this area. The abundance of field data makes the Rincon Mountains an ideal location to investigate new techniques for studying fire with remote sensing. Additionally, insight gained here may be applicable to other arid environments throughout the world, where a better understanding of fire is of great importance.

TM Data

We selected an 11 May 1996 Landsat TM scene (Scene ID: LT5036038009613210) from the Arizona Regional Image Archive (ARIA http://aria.arizona.edu) for this project. This scene was chosen for a number of reasons: Late spring is an appropriate season to study forest conditions, since both winter and summer grasses are not at peak greenness (too early for summer rain, too late for winter). If the grasses were green, their strong near-infrared signal could overwhelm reflectance of oak and pine canopies. The late spring image was also entirely cloud-free. This May scene corresponded well with available fire history records: the scene was recent enough to include most fires, but old enough to allow future expansion to a multi-temporal study.

Fire Atlas

Using a digital version of the fire atlas, we chose several sets of overlapping fire polygons (areas that had burned repeatedly) and delineated new polygons within the intersection area. The new plots were not chosen randomly, because we wanted to sample a range of fire histories, while simultaneously avoiding exposed rock and deep shadows. Nine fire plots were chosen in three fire history categories: once burned (single fire), twice burned (two fires), and multiple burns (three or more fires). We selected three plots that had burned only once during the study period. These were labeled as 1.1, 1.2, 1.3 for once burned plots. The plots with two fires were named 2.1, 2.2, 2.3, and the multiple fire plots were called 3.1 for a plot that burned three times, and 5.1 and 6.1 for plots having had five and six fires, respectively (Table 1). The first number corresponds to the number of fires within the study period, and the second distinguishes between plots with the same number of fires.

U.S.G.S. 30-meter Digital Elevation Models (DEMs)

DEMs were used to create shaded relief maps for use in georeferencing. DEMs locationally conform to the National Map Accuracy Standards, and are thus useful to use as reference images for georectification of image data. By creating shaded relief maps matching the solar illumination conditions of the TM scene (elevation: 57.86, azimuth: 107.62), it is possible to select ground control points (GCPs) between the DEM and image. This shaded relief georectification technique is particularly useful in areas with rough terrain, since shadows and sunlit slopes, ridges, and peaks can be used to locate

GCPs. The selected GCPs can be used to calculate a polynomial transformation and convert the image data to match real-world coordinates.

Topographic positions for the nine fire plots were quite variable due to the rugged terrain in the study area. This raised concern over the validity of directly comparing spectral and spatial patterns between the plots. To address this issue, we selected nine analog control plots (one for each fire plot) on an adjacent peak that had not burned during the study period. Each control plot was selected to match the size and topography of a fire plot. Control plot selection was not random, because we attempted to avoid features such as image shadows and large rock exposures, while keeping the control plots within the same elevation ranges as the fire plots. To match topography, we viewed the slope and aspect images while drawing polygons for the control plots. Because this was a subjective process, we also compared average slope and aspect histograms for each fire and control plot pair, after selecting the control plots. This helped to ensure that the topographic patterns were similar between each fire plot and its corresponding control plot. Average aspect was not a useful way to summarize the plot topography, because circular scaling problems occur. 0° and 359° are nearly the same aspect (due north), yet a plot with equal quantities of each value results in an average of 179.5 (due south). We used the control plots to compare patterns between burned and unburned plots with similar topography. The control plots were also used to normalize statistics for the fire plots.

General Approach

The general approach used in this study was to analyze spatial patterns for forested areas having different fire histories over a 54-year period (1943 to 1996). Study plots were chosen to include a range of fire frequencies (one to six fires during the time period) and fire-free intervals (54 years to less than one year). Unburned control plots (no fires between 1943 and 1996- history prior to 1943 is unknown) with similar vegetation and topography were selected from an adjacent mountain peak to pair with each study plot. We used these analog control plots to make comparisons between burned and unburned forest stands and to allow some 'normalization' of the data.

To quantify the spatial patterns in the data, we calculated landscape metrics (see Table 2) for each study plot (fire) and control plot (no fire). We used Rank Correlation Analysis to assess the significance of relationships between fire history and landscape patterns. Details of the image processing and analysis are discussed below.

Preparation of TM Data

TM data were corrected for atmospheric effects using methods described by Chavez (1996) and registered geometrically to corresponding USGS DEMs using a second order transformation (RMSE < 1 pixel). The resulting georectified reflectance image was used to calculate the KT Transform and NDVI (Figure 2). To expand the analysis, we also converted the false color composite of Brightness, Greenness, and Wetness from the KT into Intensity (KT-I), Hue (KT-H), and Saturation (KT-S). In a

recent study in the Mediterranean Koutsias, *et al.* (2000) were successful in mapping fire scars using a similar technique.

Data Analysis

The steps above resulted in seven spectral variables: KT-B, KT-G, KT-W, NDVI, KT-I, KT-H, and KT-S. The next step was to characterize the spatial patterns of these seven images with respect to fire history. The spatial measures we used require data that are thematic so that the landscape can be divided into distinct patches. If the image enhancements were left as continuous floating point data, each pixel would end up as a separate patch and no new information would be revealed. To solve this problem, we masked the image enhancements to 2000 meters and above, and rescaled each image into the range 0 to 10, using the minimum (excluding zero) and maximum values in a linear conversion. Our technique for data reduction differs from that of Chuvieco (1999), who used histogram equalization to reduce continuous data into a thematic map. The Chuvieco (1999) study required data reduction for roughly 250,000 pixels, while our study area only contained about 64,000 pixels after the elevation masking. We felt that a simple linear reduction would best preserve the trends in the data, particularly since we were examining smaller sites within the image subset. Reducing the data value range simplified the image enhancements, but many single pixels were left within most study plots. We used a 3x3 majority filter to avoid having the study results overwhelmed by noise from single pixel "patches". It is worth noting that Chuvieco (1999) found that spatial pattern trends remained fairly constant, irrespective of class reduction. He

calculated statistics for several different class numbers to avoid bias, but found that the number of patches was reduced by a fire, whether the data were reduced to three classes or twelve (Chuvieco, 1999).

Simplified versions of each image were converted into polygon layers and landscape metrics were calculated using the Patch Analyst Extension in ArcView. As a normalization measure, we computed plot ratios (we will refer to as $stat_n$, *e.g.*, MPS_n) for each plot pair ($stat_n$ = *stat* fire plot / *stat* control plot). Because the fire plots were located in variable terrain (disparate slope and aspect) and mixed vegetation (some plots were oak, some pine, some mixed), we felt this normalization was warranted. The resulting normalized plot ratios were used in final correlation analyses.

RESULTS AND DISCUSSION

Plot Specific Spectral Variations

In addition to studying the patch patterns of fire, we thought that it was instructive to also examine the basic statistics for each plot used in the study. Characteristics of spectral data have been the focus of much remote sensing research, so we felt that it would be complementary to include that aspect in this paper. Paired t-tests were used to compare means for each fire and control plot. Because the control plots had been without fire for more than 54 years, we hypothesized that each fire plot mean would be significantly different from its corresponding control plot mean. Bar charts comparing means for fire and control plots are shown in Figure 3 and discussed in this section.

Immediately following a fire that has removed a significant amount of vegetation, we would expect KT-B to be higher (more bare soil) and KT-W, KT-G, and NDVI to be lower (reduction in moisture content of leaves or complete removal of green biomass) for the burned area. For a lower severity or less recent fire, it is not as clear what pattern is expected. Discussion below is limited to NDVI comparison between different fire plots due to topographic differences. We discuss all image enhancements for fire/control plot comparisons. All mean comparisons were significantly different ($p < 0.05$) unless otherwise noted.

Single Fire Plots

Single fire plots (1.1, 1.2, 1.3) exhibited differences that can be explained by fire history. The plot burned in the 1994 Rincon Fire (1.1) had lower mean NDVI than the other two single fire plots (1943 fire, 1989 fire). The 1994 single fire plot (1.1) had not previously burned for a minimum of 52 years (no fires since before 1943), so fuels would have continued to accumulate over that time period. The site's largely southeast aspect makes it drier than more northern exposures, but permits higher site productivity than southwest facing slopes. This combination of factors could allow for considerable fuel accumulation with sufficient desiccation for a high severity fire. Visual assessment of a color infrared digital orthophoto (DOQQ) from June 1996 confirms that the plot was severely burned in the 1994 Rincon Fire (Plate 1).

A single fire plot that stands out was burned in 1943 only (plot 1.3). This long fire-free interval (54 years) makes the stand conditions of this plot potentially similar to

the unburned control plots. If the 1943 Manning Camp Fire was low intensity, there are likely to be older trees in this plot. However, if that fire had been severe, trees on this plot would largely be younger. Comparison of means for the 1943 single fire plot (1.3) and its control plot shows that they were not significantly different for KT-W, NDVI, or KT-S. The extended time without fire would have allowed for significant growth in the understory and considerable fuel accumulation. As a result, the conditions of the forest in this plot are quite different from those found in the 1994 single fire plot (1.1). Descriptive statistics confirm the distinction, with plot 1.3 having higher mean NDVI than the more recently burned plot 1.1.

Twice Burned Plots

Although, fire severity information is unknown for most fires in this study, we expected the twice burned plots to exhibit some resemblances. All three plots had one recent fire (1989 or 1994) and one older fire (1943, 1954, 1972), so there is potential for plot similarities. We thought that the plot that burned in 1972 and 1989 (2.3) would be distinct from the others, because the older fire was more recent. This corresponds to a fire-free interval of at least 30 years prior to the 1972 fire, because the fire-free period preceding 1943 is unknown. This plot also had a shorter interval between fires (17 years). The actual pattern that we observed was different than we had expected: Plots 2.1 (1954, 1994 fires) and 2.3 (1972, 1989 fires) had more similarities, with the third plot (2.2 = 1943, 1994 fires) being more distinct. Plot 2.2 had lower mean NDVI than the other twice burned plots. This trend suggests that plot 2.2 (1943, 1994 fires) was

severely burned in the 1994 Rincon Fire. This plot is located upslope and adjacent to the 1994 single fire plot (1.1), which we concluded had been severely burned in the 1994 Rincon Fire. Like its single fire neighbor, the twice-burned plot (2.2) has a largely south-facing slope, but the slight increase in elevation might allow for higher site productivity. Combined with a 51-year fire-free period, the plot was susceptible to a severe fire under the right weather conditions (low humidity, high winds). To confirm this theory, we examined a color infrared DOQQ from June 1996. The photo clearly shows that a significant portion of the vegetation cover has been removed (Plate 1). Plot 2.1 (1954, 1994 fires) has a similar fire history, with a 40-year fire-free period prior to the 1994 Rincon Fire, but damage was less severe and widespread on that plot (Plate 1).

Multiple Fire Plots

Multiple burn plots had burned three times (3.1), five times (5.1), and six times (6.1) between 1943 and 1996. The most frequently burned plots (5.1, 6.1) had experienced the same fire history, excluding a 1956 fire, which only burned one of them (6.1). Due to the similarities of those two plots (including slope, aspect, elevation, and vegetation), we expected to find spectral similarities. Results revealed that mean NDVI for the frequently burned plots (5.1 and 6.1) was not significantly different ($p > 0.05$). When compared to the other multiple fire plot (3.1), these plots have higher mean NDVI. The difference implies that the frequently burned plots have higher canopy cover and more green biomass than the other multiple burn plot. Visual comparison of the plots confirms that this is the case (Plate 1). The length of the fire-free period preceding the

1994 Rincon Fire is also linked to mean NDVI. Plots burned in the 1994 Rincon Fire that had been without fire more than 50 years preceding the fire have the lowest mean NDVI, while plot 6.1 has the highest mean NDVI. The fact that forest cover appears to be high on the frequently burned plots, also suggests that the numerous fires occurring between 1943 and 1996 were surface (low intensity) fires in those plots. Had either plot experienced a crown fire during that time, it is unlikely that forest cover would be at its current level. The relatively frequent, low intensity fires prevented fuels from accumulating to levels that favor high severity crown fires. These observations illustrate the detrimental impacts that long periods of fire suppression can have on these forests.

Control Plots

The relationships between fire plots and their corresponding control plots varied with fire history, but in most cases means for fire and control plot pairs were significantly different (Figure 3). For example, all control plots had higher mean KT-G than their fire plots ($p < 0.05$), excluding the two frequently burned plots (5.1 and 6.1). These fire plots usually had opposite tendencies than the other fire plots. In most cases, control plots had higher means then their fire plots, but the frequently burned plots had higher means. KT-S had the opposite pattern, with most fire plots having higher means than their control plots. In this case, the frequently burned plots had lower or equal means.

All of the results in this section have confirmed that fire plots 5.1 and 6.1 exhibit spectral similarities to each other and spectral differences from the other fire plots. These two plots have fire histories that more closely resemble pre-settlement fire regimes than

any of the study plots and trends in their spectral patterns have consistently distinguished them from the other plots. Plots 1.1 and 2.2 are also distinct, exhibiting spectral characteristics that suggest higher severity than other plots burned in the 1994 Rincon Fire.

Correlation Analyses of Spectral and Landscape Statistics with Fire History

To assess relationships between forest patterns and fire history, we compared landscape metrics calculated from the image enhancements to several fire history characteristics (Table 3). Due to our small sample size and ordinal nature of some fire history data, we used Spearman's Rank Correlation Analysis to quantify relationships (results shown in Table 4). The following discussion begins with an overview of correlations using the spectral means (non-spatial). Then, we consider which landscape metrics (abbreviations are shown in Table 2) had significant relationships ($p < 0.05$) with fire history. We complete the section with a discussion of which image enhancements best extracted relevant landscape patterns.

Using normalized means (fire plot mean / control plot mean) as input to the correlation analysis, we obtained significant results for only two fire history variables: length of the most recent fire-free interval (last_ffi) and average fire-free interval (avg_ffi). The high number of significant correlations between last_ffi and the non-spatial statistics is likely due to the impact of the 1994 Rincon Fire. In the subjective comparisons of NDVI in the previous section, we noted an inverse relationship between mean NDVI and fire-free period preceding the Rincon Fire. Our observations were

confirmed by the correlation results: an increase in last_ffi was linked to lower KT-G, KT-I, KT-H, and NDVI. In other words, plots that had been without fire over a long time period were more susceptible to vegetation removal (or reduction) in a subsequent fire. KT-G and NDVI are established indicators of green biomass, while the exact nature of KT-I and KT-H has not been established. Our results suggest that these new IHS enhancements may also be linked to related biophysical properties. Visual comparison between NDVI (Figure 2d) and KT-H (Figure 2f) shows remarkable similarities, as well.

Patch size variability ($PSCV_n$) resulted in the greatest number of significant correlations (six) and the highest correlation coefficient (-0.865) for the landscape statistics. Mean patch size (MPS_n) and patch-per-unit area (PPU_n) also performed well with four significant correlations each. Results indicate that more fire-free years (last30 and last50) and longer fire-free intervals (avg_ffi) are linked to a lower number of patches (PPU_n), larger patches (MPS_n), and lower variability in patch size ($PSCV_n$). These trends all point to frequent fire increasing landscape heterogeneity and fire exclusion leading to more homogeneous patterns. Fire ecologists have found that frequently burned forests often have a mosaic pattern due to variability in fire timing and severity across the landscape (Romme, 1982; Turner *et al.*, 1994).

Patch shape complexity ($MPFD_n$) and landscape diversity (SDI_n) were both negatively related to number of fire-free years. Length of most recent fire-fire interval also related inversely to patch complexity. In the case of the most recent fire-free interval (last_ffi), the 1994 Rincon Fire is likely driving the relationships that we observed. Six of the nine fire plots are included within that fire perimeter and their conditions in 1996

(two years after the fire) are strongly linked to the fire-free interval immediately preceding the Rincon Fire. Correlations show that lower fire occurrence during the ten and thirty years preceding 1996 resulted in lower patch shape complexity. Results also indicate that less frequent fire between 1943 and 1996 leads to lower landscape diversity. If frequent fire tends to create heterogeneous landscapes, then we would also expect patch complexity and landscape diversity to increase with fire occurrence.

Landscape evenness (SEI_n) related inversely to time since the most recent fire (last_fire) and directly with last fire-free interval (last_ffi) and average fire-free interval (avg_ffi). This landscape metric indicates how evenly landcover types are distributed over the landscape, without emphasizing richness as SDI does. We can interpret these relationships to mean that long fire-free periods result in more even landscapes. Our results agree with those of Romme (1982), who found that regimes of fire exclusion resulted in greater landscape evenness than natural fire regimes. However, the relationship that we found between how recently a fire has occurred (last_fire) and landscape evenness was inverse, suggesting that evenness decreases with increasing time since fire. Once again, the 1994 Rincon Fire is likely influencing the relationship. The majority of fire plots (two-thirds) had burned only two years prior to image acquisition. If these plots had higher evenness than the other (less recently burned) fire plots, it would seem that evenness declines over time following fire. Although this is contrary to our other results and those of Romme (1982), it is possible that evenness decreases in the short-term following fire, but eventually increases in the long absence of fire. This particular metric is somewhat difficult to put into context with the other statistics,

because a heterogeneous or homogeneous landscape could have high evenness provided that existing cover types are equally distributed (i.e., ten small patches of equal size versus two larger patches of equal size).

The image enhancements that extracted the patterns discussed above included all three KT components (Brightness, Greenness, Wetness) and NDVI. KT-B tends to be higher in non-vegetated areas. This trend can be seen in the grayscale KT-B image (Figure 2a), where severely burned areas (plots 1.1 and 2.2) appear brighter than surrounding forest. Patch size variation ($PSCV_n$) of this image enhancement appears to have a strong link to fire history, as well. KT-W (Figure 2c) has been well established in its utility for fire mapping (Patterson and Yool, 1998), so we expected the spatial patterns of that image enhancement to also be linked to fire history. Both KT-G and NDVI are indicators of canopy cover and green biomass and spatial patterns derived from them are associated with fire history.

Of the IHS components we calculated from the KT Transform, only the Intensity component achieved significant results in the correlation analysis. Image intensity generally contains more spatial information than other image components, so it was expected to be useful for this analysis. KT-I resembles the KT-B image, but with more fine-scale detail and topographic variations visible. Forested areas have greater contrast in the KT-I image, but pixel values follow the same trends as the KT-B image (bare areas have high values, vegetation appears darker). Our results suggest that KT-I is an improvement over KT-B for extracting forest spatial patterns.

CONCLUSIONS

The number of recent wildfires in the western United States underscores the need to reduce fuel loads in many areas and determine which forests are at greatest risk for catastrophic fires. The research presented in this paper represents an important first step in using remote sensing techniques to understand fire-related forest spatial patterns. These vegetation patterns are worthy of study and analysis because they are affected by fire history and they determine future fire behavior. Key findings of our study are summarized below.

The significance of fire frequency and fire exclusion was well illustrated by the results of our spectral comparisons. The most frequently burned plots (5.1 and 6.1) had higher mean spectral values than any other fire plots and many control plots for image enhancements linked to canopy cover and biomass amount. This confirms the beneficial effects of frequent fire in these ecosystems. Conversely, the plots that appeared most damaged by the 1994 Rincon Fire had long fire-free periods prior to that fire.

Rank correlation results showed the strong link between forest spatial patterns (as derived from satellite-based spectral enhancements) and fire history. Patch size (MPS_n), patch size variability ($PSCV_n$), shape complexity ($MPFD_n$), and landscape evenness (SEI_n) obtained significant results for more of the fire history variables than spectral data alone. This is significant and shows that forest spatial patterns can reveal a great deal of information about fire history. The spectral image enhancements that were most useful included KT- Brightness and KT-G, which have both been widely used in other forest research.

An issue that warrants investigation is monitoring spatial patterns for the same plots over time to determine the effects of post-fire regeneration. It would also be instructive to compare spatial patterns before and following fires of differing severity. Similar spatial analysis techniques have proven useful in Mediterranean ecosystems (Chuvieco, 1999), so application of these methods in other forest types may be valuable. Fire is a dynamic process and its temporal impacts on landscape patterns justify further study.

ACKNOWLEDGMENTS

This research was funded by EPA Science to Achieve Results (STAR) Fellowship number U915601 awarded to Mary C. Henry, University of Arizona. Comments on the manuscript from Dr. Tom Swetnam and two anonymous peer reviewers were greatly appreciated. The authors also wish to thank Kathy Schon and Pam Anning of the National Park Service (Saguaro National Park) for supplying the digital fire atlas used in this study.

REFERENCES

Allen, C. D., 1994, Ecological perspective: Linking ecology, GIS, and remote sensing to ecosystem management, *Remote sensing and GIS in ecosystem management*, (V. A. Sample, editor), Island Press, Washington, DC, pp. 111-139.

Baisan, C. H. and T. W. Swetnam, 1990, Fire history on a desert mountain range: Rincon Mountain Wilderness, Arizona, U.S.A., *Canadian Journal of Forest Research*, 20(10):1559-1569.

Benson, B. J. and M. D. MacKenzie, 1995, Effects of sensor spatial resolution on landscape structure parameters, *Landscape Ecology*, 10(2):113-120.

Chavez, P. S., Jr., 1996, Image-based atmospheric corrections – revisited and improved, *Photogrammetric Engineering and Remote Sensing*, 60:1285-1294.

Chuvieco, E., 1999, Measuring changes in landscape pattern from satellite images: short-term effects of fire on spatial diversity, *International Journal of Remote Sensing*, 20(12):2331-2346.

Cohen, W. B. and T. A. Spies, 1992, Estimating structural attributes of Douglas-fir/western hemlock forest stands from Landsat and SPOT imagery, *Remote Sensing of Environment*, 41:1-17.

Collins, J. B. and C. E. Woodcock, 1996, An assessment of several linear change detection techniques for mapping forest mortality using multitemporal Landsat TM data, *Remote Sensing of Environment*, 56:66-77.

Covington, W. W., P. Z. Fulé, M. M. Moore, S. C. Hart, T. E. Kolb, J. N. Mast, S. S. Sackett, and M. R. Wagner, 1997, Restoring ecosystem health in ponderosa pine forests of the Southwest, *Journal of Forestry*, 95:23-29.

Crist, E. P. and R. C. Cicone, 1984, Application of the Tasseled Cap concept to simulated Thematic Mapper data, *Photogrammetric Engineering and Remote Sensing*, 50:343-352.

Dahms, C. W. and B. W. Geils, 1997, *An assessment of forest ecosystem health in the Southwest*, Gen. Tech. Rep. RM-GTR-295, Fort Collins, CO, U.S. Department of Agriculture, Forest Service, Rocky Mountain Forest and Range Experiment Station, 97 p.

Dillworth, M. E., J. L. Whistler, and J. W. Merchant, 1994, Measuring landscape structure using geographic and geometric windows, *Photogrammetric Engineering and Remote Sensing*, 60(10):1215-1224.

Frohn, R. C., 1998, *Remote Sensing for Landscape Ecology: New Metric Indicators for Monitoring, Modeling, and Assessment of Ecosystems*, Lewis Publishers, Boca Raton, Florida, 99 p.

Fulé, P. Z., A. E. M. Waltz, W. W. Covington, and T. A. Heinlein, 2001, Measuring forest restoration effectiveness in reducing hazardous fuels, *Journal of Forestry*, 99:24-29.

Hall, F. G., Y. E. Shimabukuru, and K. F. Huemmrich, 1995, Remote sensing of forest biophysical structure using mixture decomposition and geometric reflectance models, *Ecological Applications*, 5(4):993-1013.

Kauth, R. J. and G. S. Thomas, 1976, The tasseled cap – a graphic description of the spectral-temporal development of agricultural crops as seen by Landsat, *Proceedings: Symposium on Machine Processing of Remotely Sensed Data*, West Lafayette, Indiana, pp. 41-51.

Koutsias, N., M. Karteris, and E. Chuvieco, 2000, The use of intensity-hue-saturation transformation of Landsat-5 Thematic Mapper data for burned land mapping, *Photogrammetric Engineering and Remote Sensing*, 66(7):829-839.

Larsson, H., 1993, Linear regression for canopy cover estimation in Acacia woodlands using Landsat-TM, -MSS and SPOT HRV XS data, *International Journal of Remote Sensing*, 14(11):2129-2136.

Li, H., 1990, *Spatio-temporal pattern analysis of managed forest landscapes: a simulation approach*, Ph.D. Dissertation, Oregon State University, Corvallis, OR.

Marchetti, M., C. Ricotta, and F. Volpe, 1995, A qualitative approach to mapping post-fire regrowth in Mediterranean vegetation with Landsat TM data, *International Journal of Remote Sensing*, 16(13):2487-2494.

McGarigal, K. and B. J. Marks, 1995, *FRAGSTATS: spatial pattern analysis program for quantifying landscape structure*, Gen. Tech. Rep. PNW-GTR-351, Portland, OR: U.S. Department of Agriculture, Forest Service, Pacific Northwest Research Station, 122 pp.

Minnich, R. A., M. G. Barbour, J. Sosa-Ramfrez, 2000, Californian mixed-conifer forests under unmanaged fire regimes in the Sierra San Pedro Matir, Baja California. *Journal of Biogeography*, 27(1):105-130.

Patterson, M. W. and S. R. Yool, 1998, Mapping fire-induced vegetation mortality using Landsat Thematic Mapper data: a comparison of linear transformation techniques. *Remote Sensing of Environment*, 65:132-142.

Pyne, S. J., P. L. Andrews, and R. D. Laven, 1996, *Introduction to Wildland Fire, Second Edition*, John Wiley and Sons, Inc., New York, New York, 769 p.

Ricotta, C., G. C. Avena, E. R. Olsen, R. D. Ramsey, and D. S. Winn, 1998, Monitoring the landscape stability of Mediterranean vegetation in relation to fire with a fractal algorithm, *International Journal of Remote Sensing*, 19(5):871-881.

Ricotta, C. and R. Retzlaff, 2000, Self-similar spatial clustering of wildland fires: the example of a large wildfire in Spain, *International Journal of Remote Sensing*, 21(10):2113-2118.

Romme, W. H., 1982, Fire and landscape diversity in subalpine forests of Yellowstone National Park, *Ecological Monographs*, 52(2):199-221.

Roy, P. S. and S. Tomar, 2000, Biodiversity characterization at landscape level using geospatial modelling technique, *Biological Conservation*, 95:95-109.

Schleusner, D. P., 1994, Resource management perspective: Practical considerations for using GIS and remote sensing at the field level, *Remote sensing and GIS in ecosystem management*, (V. A. Sample, Editor), Island Press, Washington, DC, pp. 140-156.

Shannon, C. and W. Weaver, 1949, *The mathematical theory of communication*, University of Illinois, Urbana, IL, 117 pp.

Swetnam, T. W. and C. H. Baisan, 1996, Historical Fire Regime Patterns in the Southwestern United States since AD 1700, *Proceedings of the Second La Mesa Fire Symposium*, USDA, Forest Service, General Technical Report RM-GTR-286.

Trani, M. K. and R. H. Giles, 1999, An analysis of deforestation: Metrics used to describe pattern change, *Forest Ecology and Management*, 114:459-470.

Tucker, C. J. and P. J. Sellers, 1986, Satellite remote sensing of primary production, *International Journal of Remote Sensing*, 7(11):1395-1416.

Turner, M. G., 1989, Landscape ecology: the effect of pattern on process, *Annual Review of Ecology and Systematics*, 20:171-197.

Turner, M. G., W. W. Hargrove, R. H. Gardner, and W. H. Romme, 1994, Effects of fire on landscape heterogeneity in Yellowstone National Park, Wyoming, *Journal of Vegetation Science*, 5:731-742.

Whelan, R. J., 1995, *The Ecology of Fire*, Cambridge University Press, Cambridge, United Kingdom, 356 p.

White, J. D., K. C. Ryan, C. C. Key, S. W. Running, 1996, Remote sensing of forest fire severity and vegetation recovery, *International Journal of Wildland Fire*, 6(3):125-136.

Table 1. Plot characteristics for each fire plot.

plot	Area (m^2)	Mean Elevation (meters)	Mean Slope (°)	Aspect	Vegetation	Fire History
1.1	488974.5	2111.7	12.18	SE	oak	1994
1.2	334647.0	2114.4	14.20	W-SW	pine/oak	1989
1.3	271291.5	2565.7	7.25	S	pine	1943
2.1	1038867.8	2108.1	10.26	E	oak	1954, 1994
2.2	555579.0	2208.5	12.86	S-SW	pine/oak	1943, 1994
2.3	362263.5	2250.2	16.30	NW	pine/oak	1972, 1989
3.1	986071.5	2152.9	9.00	S-SE	pine	1943, 1954, 1994
5.1	175446.0	2168.1	11.71	E	pine/oak	1943, 1950, 1972, 1993, 1994
6.1	273728.3	2152.1	14.07	E	pine/oak	1943, 1950, 1956, 1972, 1993, 1994

Table 2. Landscape statistics used in this study.

Statistic	Abbreviation	Description	Reference
Mean Patch Size	MPS	average patch size	McGarigal and Marks, 1995
Patch Size Coefficient of Variation	PSCV	patch size standard deviation / mean patch size	McGarigal and Marks, 1995
Patch-per-Unit Area	PPU	number of patches normalized by area	Frohn, 1998
Mean Patch Fractal Dimension	MPFD	average fractal dimension (area and perimeter calculation)	Li, 1990
Shannon's Diversity Index	SDI	sensitive to richness (number of patch types)	Shannon and Weaver, 1949
Shannon's Evenness Index	SEI	distribution of area among patch types	Shannon and Weaver, 1949

Table 3. Description of fire history variables.

Variable	Description
last10	number of fire free years in the last 10 years
last30	number of fire free years in the last 30 years
last50	number of fire free years in the last 50 years
last54	number of fire free years in the last 54 years
last_fire	time since the most recent fire
last_ffi	length of most recent fire-free period
avg_ffi	average length of fire-free period

Table 4. Significant (p<0.05) results of Spearman's Rank Correlation Analysis. Correlations significant at 0.01 are shown in italics.

metric	band	last10	last30	last50	last54	last fire	last ffi	avg ffi
$mean_n$	KT-G						*-0.911*	-0.678
	KT-W						0.785	
	KT-I						-0.734	
	KT-H						-0.734	
	KT-S						*0.836*	
	NDVI						*-0.886*	
MPS_n	KT-G			0.690				0.797
	KT-I		0.771					
	NDVI						0.760	
$PSCV_n$	KT-B		-0.771	-0.725				*-0.865*
	KT-I		-0.743	-0.759				*-0.881*
PPU_n	KT-G			-0.690				-0.797
	KT-I		-0.771					
	NDVI						-0.760	
$MPFD_n$	KT-W	-0.757	*-0.881*					
	KT-I						-0.760	
SDI_n	KT-G				-0.707			
SEI_n	KT-B							0.763
	KT-I					-0.677	0.734	

FIGURE CAPTIONS

Figure 1. Location of Saguaro National Park, Rincon Mountain District.

Figure 2. Grayscale versions of each image enhancement with fire plot locations shown. a) KT-Brightness, b) KT-Greenness, c) KT-Wetness, d) NDVI, e) KT-Intensity, f) KT-Hue, g) KT-Saturation. Plot labels shown in a).

Figure 3. Bar charts showing means for each of the seven image enhancements. Paired means that are not significantly different ($p>0.05$) are marked with *.

PLATE CAPTIONS

Plate 1. Color Infrared Digital Orthophoto from June, 1996 showing fire plot locations (yellow) and partial perimeter of 1994 Rincon Fire (magenta).

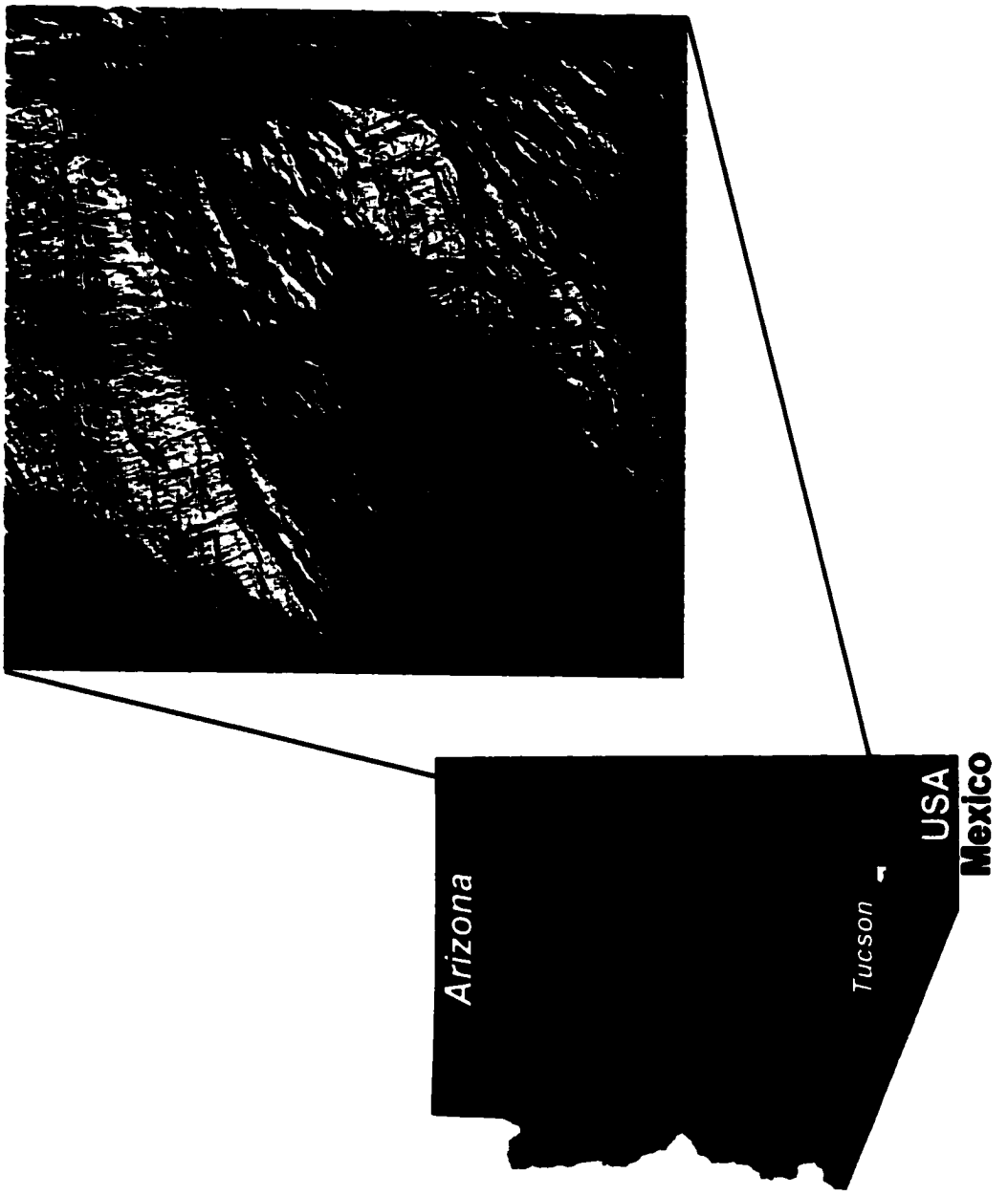

Figure 1

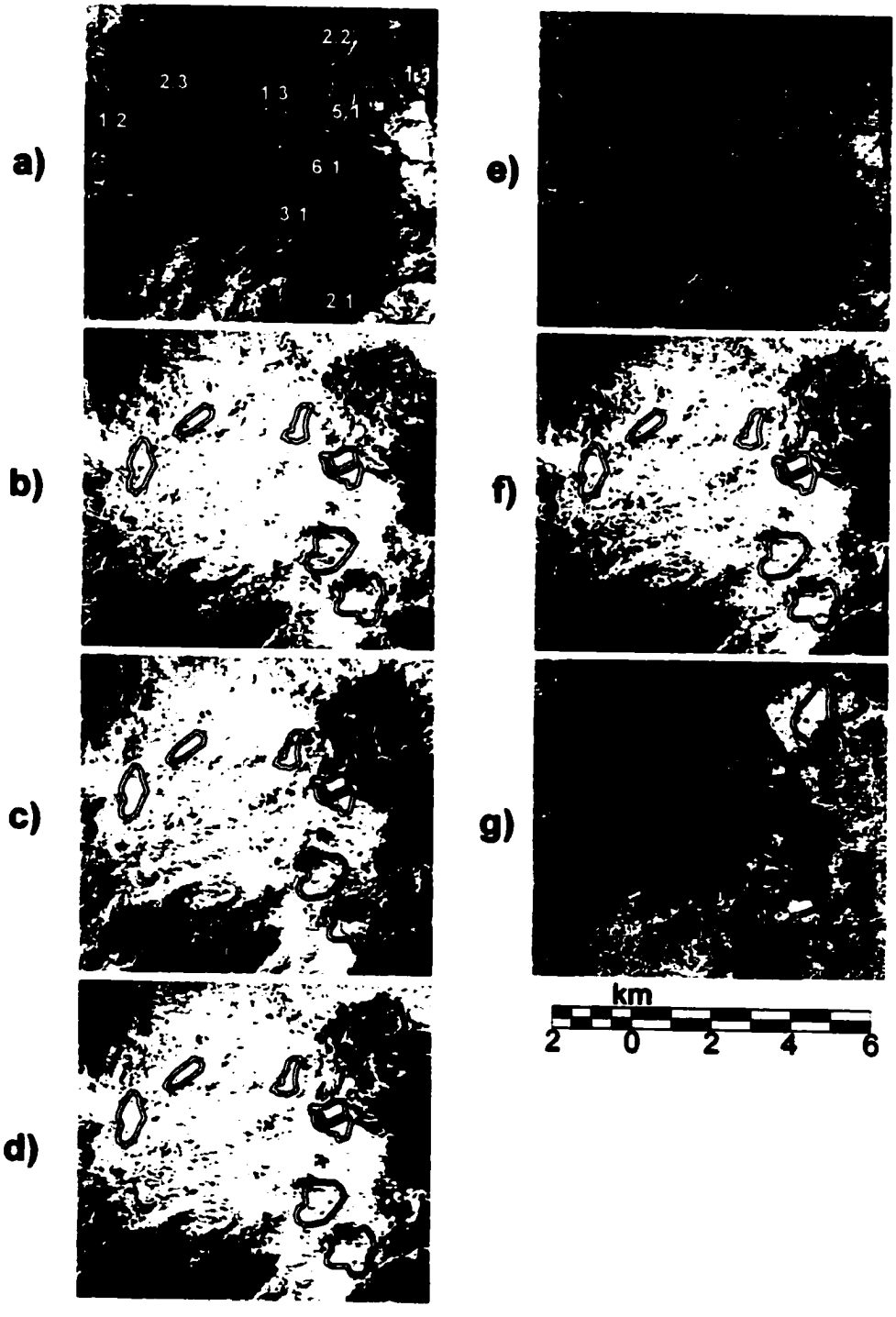

Figure 2

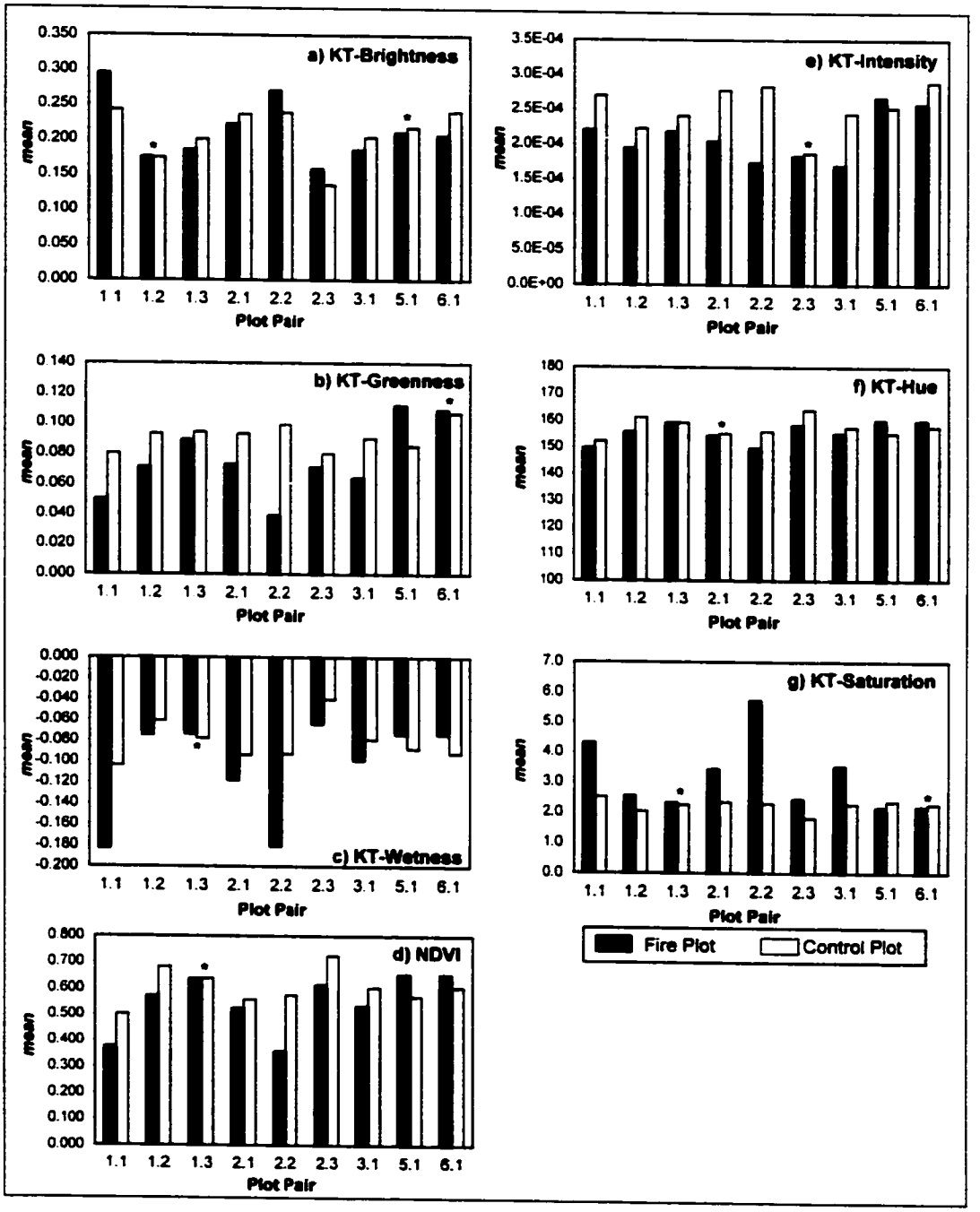
a) KT-Brightness
b) KT-Greenness
c) KT-Wetness
d) NDVI
e) KT-Intensity
f) KT-Hue
g) KT-Saturation
mean
Plot Pair
1.1 1.2 1.3 2.1 2.2 2.3 3.1 5.1 6.1
Fire Plot
Control Plot

Figure 3

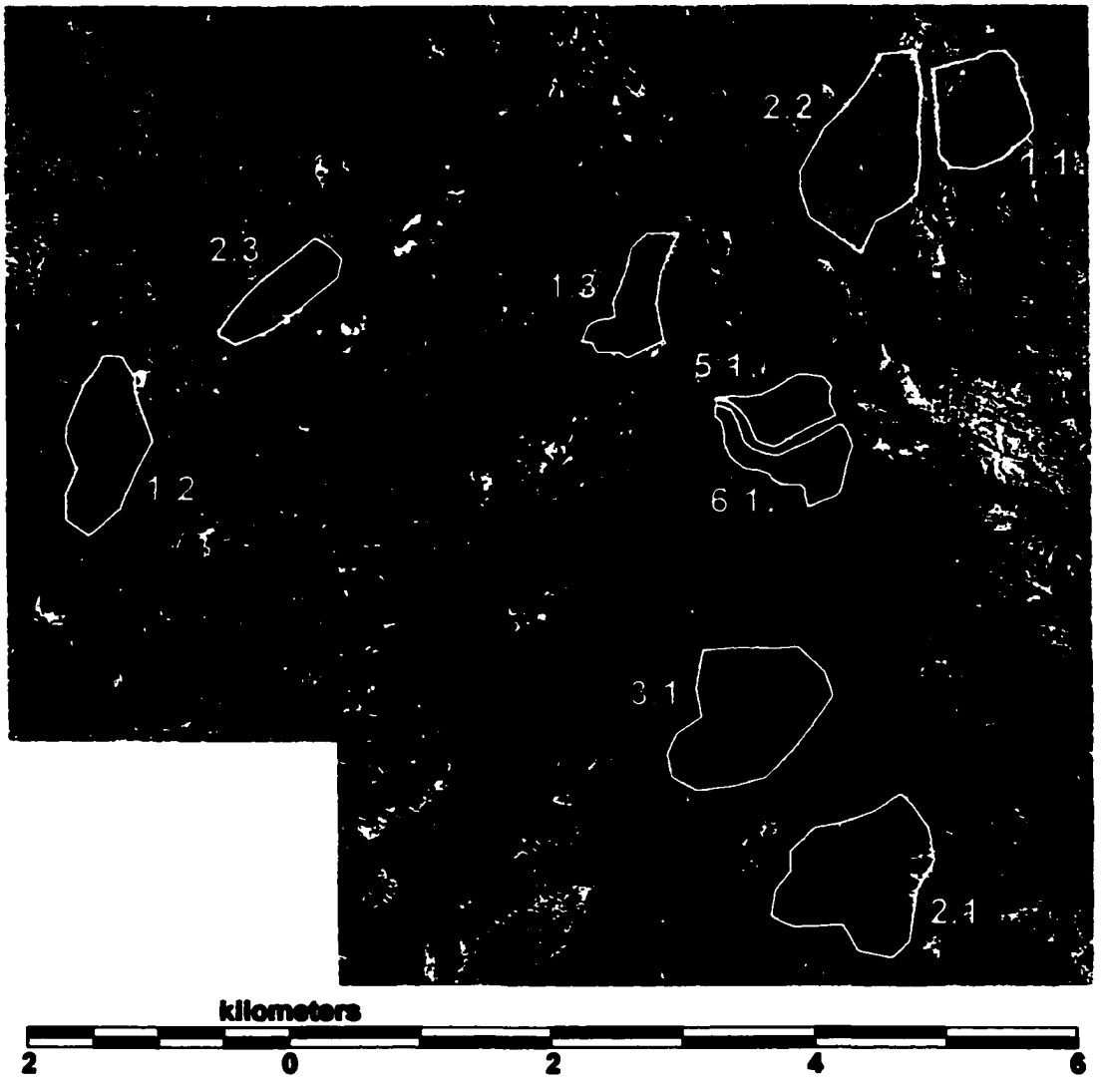

Plate 1

APPENDIX B:

The Sensitivity of SIR-C Backscatter to Fire-Related Forest Spatial Patterns

M. C. Henry and S. R. Yool

Department of Geography and Regional Development, Harvill Building, Box #2,
University of Arizona, Tucson, AZ 85721

To be submitted to *Remote Sensing of Environment*

ABSTRACT

The effects of fire on the landscape are extremely complex and have a significant impact on future fires. A variety of remote sensing techniques have been used to successfully map fire perimeters, but little remote sensing research has examined the impacts of fire history on forest spatial patterns. This research investigates the use of Shuttle Imaging Radar (SIR-C) data to analyze and compare spatial patterns in forests experiencing different fire histories between 1943 and 1994. C-HH, C-HV, L-HH, and L-HV band data and ratios of those data were used to calculate mean backscatter (σ°) and several spatial statistics for four categories of fire history: once burned, twice burned, multiple burned, and unburned. Spatial statistics included mean patch size, mean patch fractal dimension, coefficient of variation of patch size, Shannon's Diversity Index, and Shannon's Evenness Index. Using Spearman's Rank Correlation Analysis, we assessed the relationship between σ° and fire history, as well as spatial patterns and fire history. Both ratios and individual bands were analyzed. Significant ($p < 0.05$) results were obtained for spatial statistics derived from σ° and several fire history variables, although the ratios performed better over all. We did not find significant relationships ($p < 0.05$) between mean backscatter and fire occurrence during the study period.

INTRODUCTION

Remote sensing techniques have been used widely to study various aspects of forest fire, including fire detection (Cahoon and Stocks, 1996; Harris, 1996), fire perimeter delineation (Pozo et al., 1997), and fire hazard monitoring (Maselli et al.,

1996). Little of this work, however, has examined the spatially complex patterns that fire creates on the landscape. These patterns are worthy of study, because they are linked to fire history and have a significant impact on future fire occurrence and behavior (Pyne et al., 1996). It is particularly difficult to find research that uses synthetic aperture radar (SAR) data to characterize forest spatial patterns (Sun and Ranson, 1998), especially with respect to fire history. We believe synthetic aperture radar (SAR) data are well-suited to pattern resolution because SAR backscatter is largely a function of forest structural components (Wang et al., 1994; Kasischke et al., 1995; Imhoff et al., 1997), and fire history has a significant impact on forest structure (Romme, 1982; Pyne et al., 1996). In this paper, we test the potential of Shuttle Imaging Radar (SIR-C) to detect relationships between forest spatial patterns and fire history over the last half of the 20th century.

SAR BACKSCATTER MODELING

Many backscatter models have been developed to enhance understanding and interpretation of SAR backscatter from vegetated surfaces (Leckie and Ranson, 1998). These initially modeled vegetation as horizontally homogeneous continuous layers (Attema and Ulaby, 1978; Fung and Ulaby, 1978), but more recently have become more complex (Ulaby et al., 1990) to model landscapes that are not horizontally homogeneous. Early work on these models includes Sun et al. (1991) who developed a backscatter model for open forest conditions. In their model, each tree is treated as an individual scatterer, rather than being viewed as part of a continuous scattering medium. During the 1990s researchers developed models that are appropriate for a range of discontinuous

vegetation cover, including forest (Sun and Ranson, 1995; Ranson et al., 1997), woodland (Wang et al., 1993), and shrubland (Wang et al., 2000).

The significance of these modeling developments is that they underscore the importance of tree spatial arrangement in resulting backscatter from a given surface- both at the pixel and sub-pixel scale (Sun and Ranson, 1995). In our research, we consider the impact of forest spatial patterns on SAR backscatter over areas with known fire history. This enables two issues to be considered: 1) Are forest spatial patterns impacted by fire history in a predictable, quantifiable way? 2) Can significant forest spatial patterns be detected using spaceborne SAR systems? We feel that the potential for using SAR to characterize fire-related spatial patterns is high, and backscatter modeling research has helped lead to this conclusion.

FOREST ATTRIBUTE ESTIMATION FROM SAR DATA

SAR technology has been favored by many forest researchers due to its ability to image through cloud cover (Ranson and Sun, 1994; Kasischke et al., 1997) and sensitivity to forest structural properties (Dobson et al., 1995; Harrell et al., 1995; Castel et al., 2002). A large body of literature now exists on modeling relationships between SAR backscatter and vegetation structural components (Prevot et al., 1993; Wang et al., 1994; Kasischke et al., 1995; Moran et al., 1998). For a good review of SAR forestry applications see Waring et al. (1995), Kasischke et al. (1997), and Baltzer (2001). Relevant findings of several recent studies are discussed below.

Many researchers have worked to characterize relationships between SAR backscatter and biophysical vegetation characteristics, such as biomass, height, and basal area (Ranson and Sun, 1994; Harrell et al., 1997). Working in the Northern Great Lakes region, located at a transition between north temperate and boreal forest, Bergen and Dobson (1999) derived equations for predicting height, crown biomass, and basal area using SIR-C backscatter and field data. These predicted variables were used in a Net Primary Production (NPP) Model. They found SAR sensitive to variations in tree structure (leaf type and orientation, branch configuration). The SAR frequency-polarization combinations used in each model varied with tree architecture, even within different hardwoods or conifers. Specifically, L-HV showed sensitivity to height and basal area for all conifer communities except one, while C-VV was sensitive to forest structure in maple-beech forest, but not aspen (Bergen and Dobson, 1999). These results are significant because they underscore the impact that subtle structural differences have on backscatter.

In the Western Great Lakes region, Chipman et al. (2000) found significant relationships between cross-polarized L-band backscatter and tree size and density class. Their study area presented challenges due to the complex mixture of conifer and deciduous tree species present. The dual frequency configuration of SIR-C enabled different forest components to be examined, because the higher frequency C-band interacts with the canopy, while lower frequency L-band backscatter is due largely to double-bounce scattering from tree trunk to ground to sensor (Chipman et al., 2000).

In a pine plantation in southern France, Castel et al. (2001b) incorporated a plant architectural model (AMAP) to calculate additional forest parameters and create 3-dimensional stand simulations. SIR-C L-HV, the AMAP model, and a combination of the two were used to estimate stand age and bole volume. Better results were obtained for AMAP-derived quantities calculated from field-based measurements rather than SIR-C derived quantities: The authors cite their previous work stating that L-HV backscatter shows sensitivity to bole volume, age, and height, but that inversion of these relationships remains difficult. They had best success in younger stands with bole volume below 300 m^3/ha because SAR becomes insensitive to biomass differences above this level (Castel et al., 2001b).

In addition to measuring and modeling forest characteristics using SAR data, some researchers have examined explicitly the impacts of forest gaps and spatial patterns on SAR backscatter. Green (1998) studied the effect of forest windthrow gaps on AIRSAR backscatter over a Sitka spruce plantation in central Wales finding significant correlations between C-HH backscatter and total gap area, as well as gap perimeter to area ratio. Gap perimeter to area ratio also correlated significantly with C-VV and L-HH backscatter (Green, 1998). These results are particularly relevant to our study, because they show that spatial pattern (gap shape) has an impact on co-polarized C- and L-band backscatter.

Sun and Ranson (1998) conducted related research using AIRSAR over an experimental forest in Maine with a variety of management practices. A 3-dimensional simulated stand was also modeled, so that tree positions could be altered and the

subsequent backscatter changes monitored. They calculated quartiles for simulated image data for a random and clumped tree pattern. Each quartile image was converted to a binary image and spatial patterns quantified using lacunarity (distribution of gap sizes) analysis. Results showed that gaps (and tree clumps) can be identified from backscatter images, but the impact of these patterns on backscatter weakens as spatial resolution becomes coarser (Sun and Ranson, 1998).

The research described above demonstrates that the spatial arrangement of trees has a strong impact on SAR backscatter. Fulé and Covington (1998) provide one example of fire history impacts on forest spatial patterns. In a field-based study, Fulé and Covington (1998) observed fire-related spatial patterns in pine-oak forests of Mexico's Sierra Madre Occidental. They studied forest plots that fell into three different fire history categories: fire-excluded (FE), fire-excluded with fire recently returned (FR), and frequent fire (FF). One particular characteristic they noted was that tree density was strongly influenced by fire history, with FE plots having nearly eight times the tree density of the FF plots (Fulé and Covington, 1998). This variation in density could have a significant impact on SAR backscatter given the increased scattering potential in the denser, unburned forest. In the understory, there were additional differences in species and overall density that could also impact backscatter.

FIRE RESEARCH USING SAR DATA

SAR data have been used widely in two categories of fire research: Studies using SAR data to map stand-replacing fire perimeters (Bourgeau-Chavez et al., 1997;

Kasischke et al., 1994) and predicting fire danger through fuel moisture assessment (Bourgeau-Chavez et al., 1999). These two approaches illustrate the potential of SAR for fire-related research, but differ from our methods, which examine gap structure. Kasischke et al., (1994) used SAR to detect surface roughness differences between burned (stand-replaced) and unburned forest. Bourgeau-Chavez et al. (1999) investigated the sensitivity of SAR backscatter to moisture conditions to determine fire risk.

Most SAR-based fire perimeter mapping has been in boreal forest regions of Alaska (Kasischke et al., 1992; Kasischke et al., 1994) and Siberia. SAR is an attractive option for these areas, because cloud cover at these high latitudes often precludes extensive use of optical remote sensing. Tropical regions present similar cloud problems, so some researchers have turned to SAR for fire perimeter mapping in those areas (Sugardiman et al., 1999; Siegert and Hoffman, 2000).

Recent advances in fire-related SAR research have occurred in fire hazard monitoring. Bourgeau-Chavez et al. (1999) and Couturier et al. (2001) used ERS data to monitor moisture conditions in two different forest environments. Bourgeau-Chavez et al. (1999) compared drought index with average backscatter in a boreal forest environment for 15 images over three growing seasons in Alaska. They found significant relationships between backscatter and the drought measures. Accurate prediction required stratification of low vegetation cover. Couturier et al. (2001) employed similar techniques to monitor fire risk in Indonesia. ERS (C-VV) backscatter correlated significantly with a daily drought index, especially in disturbed forests.

STUDY SITE AND DATA

Rincon Mountains

We conducted our research using data acquired over the Rincon Mountains, just east of Tucson, Arizona. Most of the area is contained within Saguaro National Park's Rincon Mountain District (Figure 1). Vegetation in the area consists of desert scrub at the lowest elevations (900 meters), which changes gradually into oak, pine-oak gallery, and mixed conifer as elevation increases to a maximum of about 2800 meters. Annual precipitation averages 760 mm at the highest elevations, falling mostly in winter and late summer. Rincon Mountain topography is more variable than in most prior studies. Implications of this variability are discussed in the following sections.

Shuttle Imaging Radar (SIR-C) Data

SIR-C data were obtained over the Rincon Mountains for 04 October 1994 (Figure 2). Data were acquired in C-band (5.8 cm) and L-band (23.5 cm) for both horizontal send-horizontal receive (HH) and horizontal send-vertical receive (HV) polarizations. The Space Shuttle Endeavour was in a descending orbit (144.468° from north) with a left-looking view direction and 50.8° incidence angle at the scene center when the data were acquired. The resulting look direction is shown in Figure 2a. The data were provided in terrain corrected format and had also been calibrated and converted to radar backscatter (σ°). Personnel from the Office of Arid Lands Studies at the University of Arizona completed multi-look processing resulting in 30-meter pixel spacing before our analysis.

SIR-C data have great potential for forestry research due to the dual frequency/polarization design of the system: The shorter C-band wavelength interacts with smaller tree components and the cross-polarized data are typically affected by canopy volume scattering (Ranson and Sun, 1994). The longer L-band signal interacts with larger tree components (trunk, large branches) and often indicates trunk-ground double bounce scattering (Pulliainen et al., 1999). SAR sensitivity to moisture (dielectric properties) can often be a confounding issue in such research, because increases in soil moisture or vegetation water content increase backscatter, particularly at higher frequencies (Harrell et al., 1997; Pulliainen et al., 1999). Our research focused on forest structural parameters, so backscatter variations due to moisture differences would be considered "noise" in this context. Fortunately, no precipitation was recorded for at least a month prior to image acquisition and relative humidity levels are typically low in this region.

USGS Digital Elevation Model

USGS 30-meter Digital Elevation Models (DEMs) were used to create shaded relief maps for use in georeferencing, as well as slope and aspect images for use in the analysis. Because DEMs conform to National Map Accuracy Standards, they are useful as reference images for georectification of image data in areas with variable terrain. By creating shaded relief maps to match the look direction and incidence angle of the SIR-C image, it is possible to match ground control points (GCPs) between the DEM and image. These GCPs can then be used to calculate a polynomial transformation that converts the

image data to real-world coordinates. Ranson et al. (2001) employed the same technique to georectify SIR-C data to a DEM in Siberia.

Fire Atlas

Locations of plots with different fire histories were selected from a digital fire atlas of the Rincon Mountains. The Rincon fire atlas contains perimeters for all fires occurring since 1943. Plot selection favored a range of different fire histories. It was necessary to exclude areas with extensive rock outcrops or dark shadowing. We selected nine plots (see Table 1) with three categories of fire history: single fire plots (1.1, 1.2, 1.3), twice burned plots (2.1, 2.2, 2.3), and multiple fire plots (3.1, 5.1, 6.1). Although this is a small sample size, we chose plots for their unique fire history characteristics. The goal of the research was not to analyze all areas that had burned in the last half century, but to study in depth a range of fire histories that were all unique. The plots themselves were chosen so that the number of pixels would allow a statistically valid analysis (the smallest plot, 5.1, contains 339 pixels).

In addition to these fire plots, unburned control plots with similar topography and vegetation were selected from an adjacent peak; each control plot was chosen to match one fire plot. We used these control plots to compare forest without fire during the study period to more frequently burned forest. By choosing topographic analogs, we hoped to minimize differences due to local incidence angle. The same fire and control plots were used for a previous study. Additional site selection details are described in Henry and Yool (in press).

ANALYSIS PROCEDURES

SIR-C Data Processing

Georectification was performed using a shaded relief map generated from the DEM (RMSE was less than half a pixel). Following georeferencing, a Local Region filter (3 by 3 window) was applied to reduce image speckle (Nagao and Matsuyama, 1979). This algorithm is an edge-preserving smoothing filter that assigns the output pixel value from the mean of one quadrant (minimum variance) of the filter window. Speckle is caused by the backscatter of many individual objects within a single ground resolution cell being added incoherently. It is necessary to reduce this effect before analyzing a SAR image, particularly for our research examining spatial patterns. Failure to remove this image speckle would have strongly skewed our results and likely cause most plots to appear extremely heterogeneous. By applying the speckle reduction filter, the signal-to-noise ratio for the image was increased. We used the small window size for speckle suppression to ensure that a minimum of fine-scale detail would be removed (Wu and North, 2001). Although the smaller window size preserves more noise, we felt that subsequent processing steps for topographic effects would further reduce speckle noise.

Castel et al. (2001a) found that L-band detection of biomass was highly dependent on local incidence angle (based on slope with respect to sensor incidence angle). In a study to determine the most effective method for reducing topographic effects in SAR data, Ranson et al. (2001) compared uncorrected backscatter, DEM-radiometric corrected backscatter, and band ratios for mapping landcover. They achieved

the highest accuracy using principle components calculated from the band ratios. In light of their results, we chose to include band ratios in our analysis (Figure 3).

Spatial Analysis

Calculation of spatial statistics for a landscape is often done using a landcover map. To eliminate the need for subjective class labeling, we opted to simplify the original data to a thematic format. Image data acted as a surrogate for landcover, with landscape patches consisting of contiguous groups of similar pixel values. Similarly, Ranson and Sun (1998) used quartile images of L-band data to calculate lacunarity.

We masked each of the four original bands and six ratio images to include only areas above 2000 meters. We chose to mask the area by elevation for two reasons: 1) We wanted to include only oak, pine, and mixed conifer, and 2) elevation contours provide a natural break in the scene (rather than an arbitrarily drawn rectangle or polygon). This reduction in image area lowered the dynamic range of input values used for rescaling, enabling a greater range of values in the resulting simplified image. Each masked image was then rescaled from 0 to 10 to reduce the number of values (classes) in the scene. A 3-by-3 majority filter was applied to each resulting image to remove single inconsistent pixels. We converted each simplified thematic version of the original image data to individual polygon coverages for each fire and control plot.

Spatial statistics (see table 2) were calculated for each fire and control plot for all single band and ratio images (18 plots x 10 bands). To normalize for topographic and

vegetation differences, resulting statistics for each fire plot were divided by the statistic for the corresponding control plot.

To quantify relationships between resulting spatial measures and fire history, we used Spearman's Rank Correlation Analysis. The Spearman's method was selected because some of the fire history variables were ordinal data (i.e., number of years without fire in a given time period).

RESULTS AND DISCUSSION

Plot-Specific Backscatter (σ^o) Variations

Prior to calculating spatial statistics for the original and ratioed SIR-C data, we examined mean backscatter for all fire and control plots. We compared each fire plot to the other fire plots and corresponding control plots using difference of means tests. Bar charts showing means for all plots are shown in Figure 4. A summary of fire plot means is shown in Table 3.

Results from Single Fire Plots

Mean backscatter for the single fire plots does not follow a pattern that is clearly defined by fire history differences. For both C-band polarizations (C-HH and C-HV), the 1989 fire plot (plot 1.2) had higher mean backscatter than the other two single fire plots (burned 1943 and 1994). One explanation for this pattern is that the 1989 fire plot (plot 1.2) is on the illuminated slope of the mountain (facing west-southwest with 14.20° slope). It would follow that more energy would be reflected back to the sensor from this

position than from the other plots which face away from the sensor (plot 1.1 facing southeast with 12.18° slope; plot 1.3 facing south with 7.25° slope). Mean backscatter for the other plots 1.1 and 1.3 was not significantly different, despite that fact that one plot had burned earlier that year (plot 1.1, 1994) and the other had burned in 1943 (plot 1.3). This comparison attests to the strong impact that local incidence angle (as mediated by topography) has on backscatter.

Mean backscatter for L-band showed distinctive patterns that appear to be related to fire history: For both polarizations (L-HH and L-HV), the less recently burned plots (1.2, 1989; 1.3, 1943) are not significantly different and produce higher mean backscatter than the 1994 fire plot. After examining a color aerial photo of the study area from 1996 (two years after the SIR-C image), it is clear that the 1994 single fire plot (1.1) was still nearly devoid of vegetation cover. Because L-band interacts with larger forest components, such as trunks and large branches, it follows that a nearly treeless plot would have a weaker L-band return than forested plots.

Results from Twice Burned Plots

Mean backscatter for the co-polarized C-band (C-HH) was not significantly different for all three twice burned plots (Figure 4). This pattern cannot be explained clearly by fire history or topographic pose. Two of the plots burned in 1994 (2.1 and 2.2), while the third burned in 1989 (plot 2.3). Though all three plots had burned between 1985 and 1994, there were noteworthy differences in fire history prior to that

time. The 1994 twice burned plots had not burned for at least 40 years prior to the 1994 fire: the 1989 twice burned plot (plot 2.3) had burned in 1972.

Backscatter for the other C-band polarization (C-HV) and both L-band polarizations (L-HH and L-HV) followed trends matching each other, with differences potentially due to fire history differences: Plot 2.3 (1972 and 1989) had the highest mean backscatter of the three plots, followed by plot 2.1 (1954 and 1994) and plot 2.2 (1943 and 1994). As with the 1994 single fire plot (plot 1.1), plot 2.2 was burned severely and appeared to be nearly bare in the 1996 color aerial photo. C-HV backscatter is largely a function of volume scattering within a vegetation canopy, so a general lack of vegetation cover would result in a low return signal. As with the 1994 single fire plot, the lack of tree cover would also cause less L-band backscatter. Such conditions likely explain in part why plot 2.2 had consistently lower mean backscatter than the other twice burned plots.

Results from Multiple Fire Plots

The rank order of the three multiple fire plots held fairly constant between the different wavelengths and polarizations studied: In all cases, the plot that had burned three times (plot 3.1) had the highest mean backscatter, although for C-HV it was not significantly different from the mean for plot 5.1. Although there were fire history differences between the multiple fire plots, there was no clear link between backscatter and fire history. It is possible that plot 3.1 has higher backscatter because its topographic pose faces the sensor more directly (south-southeast facing slope) than the other multiple

burn plots (which face east). The more frequently burned plots (plots 5.1 and 6.1) have steeper slopes (11.71° and 14.07° for 5.1 and 6.1, respectively) than plot 3.1 (9.00°) and face away from the sensor.

The most frequently burned plots (plots 5.1 and 6.1) served as useful comparisons because their topography, vegetation, and fire history are extremely similar. Accordingly, we expected these plots to exhibit similar characteristics- both spatially and with regard to backscatter. It was only in the case of L-HV backscatter that the means of these plots were not significantly different. When we compared means for C-HH, C-HV, and L-HH, plot 5.1 had higher mean backscatter. The effects of topography on SAR backscatter may play a role in these differences, because plot 6.1 has a steeper slope than plot 5.1- even though they both generally face away from the sensor.

Results from Control Plots

For the majority of plot pairs, mean backscatter was higher for the fire plots than corresponding control plots. The most likely cause of this pattern is that the control plots were all located on steeper slopes than the fire plots. Exceptions to this trend included a few cases where the means for a fire/control plot pair were not significantly different. For both C-band polarizations, fire and control plots 6.1 were not significantly different. Plot pair 3.1 was a rare case where mean backscatter for both C-band polarizations was higher for the control plot than the fire plot. Although the control plot is located on a steeper slope than the fire plot, it has a larger number of pixels that are more west-facing

(toward the sensor). This difference in slope and aspect could account for the higher backscatter.

Considering the findings from the previous sections, it is important not to overemphasize the significance of these relationships. Differences in mean backscatter between fire and control plots may be largely a function of topography. Although the control plots were selected to match the topographic pose of each fire plot, we have seen in this study (and others have seen similar effects) that even slight changes in slope and aspect can result in significant backscatter differences. We demonstrate in the following sections that spatial patterns in backscatter not appear to be as sensitive to topographic effects and may be a better indicator of fire history than the magnitude of the backscatter.

Correlation Analysis of Spatial Statistics and Fire History

We ran Spearman's Rank Correlation Analysis on several fire history variables and spatial statistics derived from original SIR-C data and ratios. Spatial statistics and topographic effects were normalized by dividing values for fire plots by values for corresponding control plots. Correlation analysis was also used on normalized mean backscatter, but no significant relationships were found. Several spatial statistics also resulted in no significant correlations, but the measures that were successful are shown in Table 4 and discussed in this section.

It is useful to view the correlation results from two perspectives: First, by examining the spatial statistics and their relationship to fire history, second considering which individual bands and ratios were able to extract these patterns. Three of the spatial

statistics resulted in one or two significant correlations: mean patch size (MPS), mean patch fractal dimension (MPFD), and Shannon's Evenness Index (SEI). Patch-per-Unit area (PPU) has been omitted from this discussion because the correlations were the same magnitude as MPS, but with inverse values. MPS increased as length of the most recent fire-free period increased. Specifically, the longer a plot had been without fire prior to its most recent fire, the larger landscape patches tended to be. This relationship is well illustrated by the two plots that were burned severely in the 1994 Rincon Fire (plots 1.1 and 2.2). The single fire plot (1.1) had not burned since before 1943 (> 51 years), while the twice burned plot (2.2) had not burned since 1943 (51 years). Both plots sustained a high level of damage in the 1994 Rincon Fire, leaving the landscape relatively homogeneous (not patchy). In such a condition (as can be seen on color aerial photos), there would neither be much on the surface for a SAR signal to interrogate, nor would there be much variation in this structure over space.

Correlations using MPFD had two significant results: Average patch complexity was related inversely to the number of fire-free years in the study period. MPFD was also related inversely to how long a plot had been without fire. The more frequently an area burned over the 52 years, the more complex patch shapes tended to be. Moreover, the longer it had been since a fire occurred, the less complex patch shapes were. Both these relationships suggest fire increases landscape complexity when it occurs regularly.

Shannon's Evenness Index (SEI) is a measure of how evenly different cover types are distributed in an area. In this case the cover types are not labeled, but there was a significant correlation between time since the most recent fire and SEI: As time passes

following a fire, evenness increases in the absence of another fire. Rather than describing the number of cover types, SEI gives an indication of their distribution over the landscape. This relationship may indicate that these forests tend toward a particular spatial pattern in the absence of fire.

The most successful of the spatial statistics we tested was Shannon's Diversity Index (SDI), which resulted in significant correlations for 75% (six of eight) of the fire variables that we studied. SDI gives a relative measure of richness, or the number of cover types present. The number of fire-free years in all cumulative time periods (from the last ten years to the last 52 years) was correlated negatively with SDI: The more frequent fire was in any time period, the higher the current SDI (Figure 5). In addition, there was a significant negative correlation between the average length of fire-free intervals and SDI. Thus, the longer a plot was unburned between fires, the lower the landscape diversity. This finding follows the pattern of the time intervals as well, because more frequent fire increases plot diversity.

Results of our correlation analysis correspond well with related field based studies. Frequent, low-intensity fires tend to increase heterogeneity, while fire exclusion leads to greater homogeneity (Romme, 1982; Hemstrom, 2001). As a result, we would expect higher fire frequency to be linked to greater landscape patchiness. The strong negative correlations between number of fire-free years and Shannon's Diversity Index (SDI) follow this pattern. Because the other landscape metrics resulted in so few significant correlations, it is more difficult to assess trends, although relationships we found point toward frequent fire regimes increasing landscape heterogeneity.

In the above correlation analysis, ratios of the SIR-C data performed better than the individual channels. C-HV and L-HH were the only single frequency/polarizations that achieved significant correlations. Researchers have found relationships between C-HV and leaf area index (Imhoff et al., 1995), crown biomass (Saatchi and Moghadden, 2000), and woody volume (Ferrazzoli and Guerriero, 1995) in a range of forest types. L-HH backscatter has been linked to trunk-ground scattering (Sun and Ranson, 1998), biomass (Kasischke et al., 1995), and stem density (Castel et al, 2002). These biophysical characteristics are important indicators of stand structure and would vary spatially under different fire regimes (Fulé and Covington, 1994). The ratio of L-HH to C-HV also obtained two significant correlations for MPFD (Figure 5). No other single channels or ratios obtained significant results for that landscape metric, so combining the two channels appears to enhance their sensitivity to structural characteristics.

All two-channel ratios obtained at least one significant correlation with a fire history variable, with L-HV/C-HV performing particularly well when SDI was calculated. These results complement those of Ranson and Sun (1994), who found that L-HV/C-HV was sensitive to standing biomass in a mixed forest in Maine. Harrell et al. (1997) also found links between loblolly pine biomass and L-HV/C-HV. The L-HH/L-HV ratio, which has been correlated with percent canopy closure (Green, 1998a), also had some significant correlations when used to calculate SDI.

The C-HH/L-HH ratio was the only ratio or single channel to obtain a significant correlation using Shannon's Evenness Index (SEI). Green (1998b) found that C-HH backscatter is sensitive to canopy gaps, while L-HH has been linked to stem density and

volume (Castel et al., 2002). Our results show that time since fire is positively correlated with SEI, or landscape evenness is lower immediately following fire. In a landscape simulation study, Keane et al. (1999) found that fire exclusion leads to increased evenness in standing biomass. While our results are not a comparison of fire exclusion to frequent fire, the positive relationship between SEI and time implies that long fire-free periods (fire exclusion) results in higher landscape evenness. C-HH/L-HH also obtained a significant correlation between Mean Patch Size (MPS) and length of the most recent fire-free interval (Figure 5). The longer the last fire-free interval, the larger patches tended to be. This result suggests that longer fire-free periods result in a more homogenous landscape.

The higher success rate for the ratios is likely due to the complementary nature of C- and L-band backscatter. The combinations of C- and L-band contain information about smaller forest components (C-band) and trunk-ground, or large branch scattering (L-band). The prevalence of the SIR-C band ratios in the significant correlations is not surprising, given the highly variable topography in the study area. By calculating ratios from the SAR image data, we were able to combine information from different frequencies and polarizations, while eliminating many of the strong topographic effects observed in the original data.

Limitations

The results we obtained in this study demonstrate significant relationships between SAR-derived forest spatial patterns and fire history. However, it is useful to

address some limitations of this work. Fire perimeters obtained from the Park Service were compiled from various sources and are of undetermined accuracy. Our fire polygons were delineated inside fire perimeter boundaries to reduce the likelihood of potential inaccuracies.

Much of the uncertainty associated with this study is produced by the study area's highly variable terrain. The incidence angle of the energy received at each location is determined by the geometry between the sensor and topography. Each study plot (fire and control) was located over a range of slope and aspects, each receiving the signal at a different range of incidence angles. This angle affects how the incident microwave energy interacts with the surface, so backscatter could differ between plots for this reason rather than forest spatial pattern differences. Our incorporation of analog control plots helped minimize this effect. Additionally, by evaluating spatial patterns in backscatter over each plot, the importance of the actual backscatter magnitude was also reduced. Our correlation analysis of mean backscatter (normalized with control plots) to fire history obtained no significant results. It is possible that the magnitude of backscatter was strongly impacted by topographic variations, which overwhelmed any differences due to forest structure.

We used a small number of fire plots in this study due to environmental constraints such as elevation and rock outcrops. Future studies would benefit from analysis of a larger sample size and the associated increase in statistical power. Despite our small sample, fire histories the plots represent cover a wide range of variability that is likely indicative of other portions of the study area.

SUMMARY AND CONCLUSIONS

In this study we investigated the use of SIR-C data to quantify forest spatial patterns and relate them to fire history. Using original and channel ratio data, we calculated spatial statistics for nine fire and control plot pairs and compared ratios of these (normalized data) to several fire history variables. We used Spearman's Rank correlation analysis to determine relationships between forest spatial patterns and fire history characteristics, such as fire-free years in the preceding ten, thirty, forty, fifty, and fifty-two year periods, time since fire, most recent fire-free interval, and average fire-free interval. Pertinent findings include:

1. Mean backscatter showed no significant relationships with any of the fire history variables that we tested;
2. Channel ratios performed better than individual band/polarizations;
3. Our results demonstrate that enhanced SAR data can produce results consistent with patterns that other researchers have measured in the field;
4. Shannon's Diversity Index (SDI) had the strongest link to fire history, with all significant correlations showing a positive relationship between fire occurrence and landscape diversity.

Several options exist to follow up the results of this study, including conducting a sensitivity analysis of spatial statistics to various despeckle algorithms and window sizes. It may be possible to determine an optimum algorithm for extracting fire-related spatial patterns from SAR data. The effects of topography were apparent in this study, so it may be useful to test the effectiveness of topographic normalization on SAR data as well.

Finally, it would be informative to conduct a similar study with other types of SAR data, because SIR-C data are only available from the two missions in 1994.

ACKNOWLEDGEMENTS

This research was funded by EPA Science to Achieve Results (STAR) Fellowship number U915601 awarded to Mary C. Henry, University of Arizona. The authors also wish to thank Dr. Susan Moran, Dr. Thomas W. Swetnam, Dr. Stuart Marsh, and Dr. Malcolm J. Zwolinski for reviewing the manuscript and Kathy Schon and Pam Anning of the National Park Service (Saguaro National Park) for supplying the fire atlas used in this study.

REFERENCES

Attema, E. P. and Ulaby, F. T. (1978) Vegetation modeled as a water cloud. *Radio Science*. 13(2):357-364.

Balzter, H. (2001), Forest mapping and monitoring with interferometric synthetic aperture radar (InSAR). *Progress in Physical Geography*. 25(2):159-177.

Bergen, K.M., Dobson, M.C. (1999), Integration of remotely sensed radar imagery in modeling and mapping of forest biomass and net primary production. *Ecological Modelling*. 122(3):257-274.

Bourgeau-Chavez, L. L., Harrell, P. A., Kasischke, E. S., and French, N. H. F. (1997), The detection and mapping of Alaskan Wildfires using a spaceborne imaging radar system. *International Journal of Remote Sensing*. 18:355-373.

Bourgeau-Chavez, L. L., Kasischke, E. S., Rutherford, M. D. (1999), Evaluation of ERS SAR Data for Prediction of Fire Danger in a Boreal Region. *International Journal of Wildland Fire*. 9(3):183-194.

Cahoon, D. R. Jr., and Stocks, B. J. (1996), The Use of AVHRR Satellite Imagery to Monitor Boreal Ecosystem Forest Fires. *Accuracy Assessment in Natural Resources and Environmental Sciences: Second International Symposium*. Fort Collins, Colorado, pp. 383-390.

Castel, T., Beaudoin, A, Stach, N., Stussi, N. (2001a), Sensitivity of space-borne SAR data to forest parameters over sloping terrain. Theory and experiment. *International Journal of Remote Sensing*. 22(12):2351-2376.

Castel, T.; Caraglio, Y.; Beaudoin, A.; Borne, F. (2001b), Using SIR-C SAR Data and the AMAP Model for Forest Attributes Retrieval and 3-D Stand Simulation. *Remote Sensing of Environment*. 75: 279-290.

Castel, T., Guerra, F., Caraglio, Y., and Houllier, F. (2002), Retrieval biomass of a large Venezuelan pine plantation using JERS-1 SAR data. Analysis of forest structure impact on radar signature. *Remote Sensing of Environment*. 79:30-41.

Chipman, J. W.; Lillesand, T. M.; Gage, J. D.; Radcliffe, S. (2000), Spaceborne Imaging Radar in Support of Forest Resource Management. *Photogrammetric Engineering and Remote Sensing*. 66(11)1357-1366.

Couturier, S.; Taylor, D.; Siegert, F.; Hoffmann, A.; Bao, M. Q. (2001), ERS SAR backscatter: a potential real-time indicator of the proneness of modified rainforests to fire. *Remote Sensing of Environment*. 76:410-417.

Dobson, M. C., Ulaby, F. T., and Pierce, L. E. (1995), Land-cover classification and estimation of terrain attributes using synthetic aperture radar. *Remote Sensing of Environment*. 51:199-214.

Ferrazzoli, P. and Guerriero, L. (1995), Radar sensitivity to tree geometry and woody volume: a model analysis. IEEE Transactions on Geoscience and Remote Sensing. 33(2):360-371.

French, N. H. F., Bourgeau-Chavez, L. L., Wang, Y., and Kasischke, E. S. (1999), Initial observations of Radarsat imagery at fire-disturbed sites in interior Alaska. *Remote Sensing of Environment*. 68:89-94.

Frohn, R. C. (1998), *Remote Sensing for Landscape Ecology: New Metric Indicators for Monitoring, Modeling, and Assessment of Ecosystems*. Lewis Publishers, Boca Raton, Florida, 99 p.

Fulé, P. Z. and Covington, W. W. (1994), Fire-regime disruption and pine-oak forest structure in the Sierra Madre Occidental, Durango, Mexico. *Restoration Ecology*. 2(4):261-272.

Fulé, P. Z. and Covington, W. W. (1998), Spatial patterns in Mexican pine-oak forests under different recent fire regimes. *Plant Ecology*. 134:197-209.

Fung, A. K. and Ulaby, F. T. (1978) A scatter model for leafy vegetation. *IEEE Transactions on Geoscience and Remote Sensing*. 16:281-286.

Green, R. M. (1998a), Relationships between polarimetric SAR backscatter and forest canopy and sub-canopy biophysical properties. *International Journal of Remote Sensing*. 19(12):2395-2412.

Green, R. M. (1998b), The sensitivity of SAR backscatter to forest windthrow gaps. *International Journal of Remote Sensing*. 19(12):2419-2425.

Harrell, P. A., Bourgeau-Chavez, L. L., Kasischke, E. S., French, N. H. F., and Christensen, N. L., Jr. (1995), Sensitivity of ERS-1 and JERS-1 radar data to biomass and stand structure in Alaskan boreal forest. *Remote Sensing of Environment*. 54:247-260.

Harrell, P. A., Bourgeau-Chavez, L. L., Kasischke, E. S., Haney, E. M., and Christensen, N. L., Jr. (1997), Evaluation of approaches to estimating aboveground biomass in southern pine forests using SIR-C data. *Remote Sensing of Environment*. 59:223-233.

Harris, A. J. L. (1996), Towards automated fire monitoring from space: semi-automated mapping of the January 1994 New South Wales wildfires using AVHRR data. *International Journal of Wildland Fire*. 6(3):107-116.

Hemstrom, M. A. (2001) Vegetative patterns, disturbances, and forest health in eastern Oregon and Washington. *Northwest Science*. 75(special issue):91-109.

Henry, M. C. and Yool, S. R. (in press) Characterizing fire-related spatial patterns in the Arizona Sky Islands using Landsat TM Data. *Photogrammetric Engineering and Remote Sensing*.

Hessburg, P. F., Smith, B. G., Salter, R. B., Ottmar, R. D., and Alvarado, E. (2000), Recent changes (1930s-1990s) in spatial patterns of interior northwest forests, USA. *Forest Ecology and Management*. 136:53-83.

Imhoff, M. L., Sisk, T. S., Milne, A., Morgan, G., and Orr, T. (1997), Remotely sensed indicators of habitat heterogeneity: use of synthetic aperture radar in mapping vegetation structure and bird habitat. *Remote Sensing of Environment*. 60:217-227.

Kasischke, E. S., Bourgeau-Chavez, L. L., and French, N. H. F. (1994), Observations of variations in ERS-1 SAR image intensity associated with forest fires in Alaska. *IEEE Transactions on Geoscience and Remote Sensing*. 32(1):206-210.

Kasischke, E. S., Christensen, N. L. Jr., and Bourgeau-Chavez, L. L. (1995), Correlating radar backscatter with components of biomass in loblolly pine forests. *IEEE Transactions on Geoscience and Remote Sensing*. 33(3):643-659.

Kasischke, E. S., Melack, J. M., and Dobson, C. M. (1997), The use of imaging radar for ecological applications- a review. *Remote Sensing of Environment*, 59:141-156.

Keane, R. E., Morgan, P., and White, J. D. (1999) Temporal patterns of ecosystem processes on simulated landscapes in Glacier National Park, Montana, USA. *Landscape Ecology*. 14:311-329.

Leckie, D. G. and Ranson, K. J. (1998), Forestry applications using imaging radar. In: Henderson, F. M. and Lewis, A. J. (Editors), *Principles and Applications of Imaging Radar: Manual of Remote Sensing, Third Edition, Volume 2*. John Wiley & Sons, Inc., New York, New York, 435-509.

Li, H. (1990), *Spatio-temporal pattern analysis of managed forest landscapes: a simulation approach*. Ph.D. Dissertation, Oregon State University, Corvallis, OR.

Maselli, F., Rodolfi, A., and Conese, C. (1996), Evaluation of forest fire risk by the analysis of environmental data and TM Images. *International Journal of Remote Sensing*. 17(7):1417-1423.

McGarigal, K. and Marks, B. J. (1995), *FRAGSTATS: spatial pattern analysis program for quantifying landscape structure*. Gen. Tech. Rep. PNW-GTR-351, Portland, OR: U.S. Department of Agriculture, Forest Service, Pacific Northwest Research Station, 122 pp.

Moran, M.S., Vidal, A., Troufleau, D., Inoue, Y., and Mitchell, T. (1998), Ku- and C-band SAR for discriminating agricultural crop and soil conditions. *IEEE Transactions on Geoscience and Remote Sensing*. 36:265-272.

Nagao, M. and Matsuyama, T. (1979) Edge preserving smoothing. *Computer Graphics and Image Processing*. 9(4):394-407.

Pozo, D., Olmo, F. J., and Alados-Arboledas, L. (1997), Fire detection and growth monitoring using a multitemporal technique on AVHRR mid-infrared and thermal channels. *Remote Sensing of Environment*. 60(2):111-120.

Prevot, L., DeChambre, M., Taconet, O., Vidal-Madjar, D., Normand, M., and Galle, S. (1993), Estimating characteristics of vegetation canopies with airborne radar measurements. *International Journal of Remote Sensing*. 14(15):2803-2818.

Pulliainen, J. T., Kurvonen, L., and Hallikainen, M. T. (1999) Multitemporal behavior of L- and C-band observations of boreal forests. . *IEEE Transactions on Geoscience and Remote Sensing*. 37(2):927-937.

Pyne, S. J., Andrews, P. L., and Laven, R. D. (1996), *Introduction to Wildland Fire, Second Edition*. John Wiley and Sons, Inc., New York, New York, 769 pp.

Ranson, K. J., Sun, G. (1994) Mapping biomass of a northern forest using multifrequency SAR data. *IEEE Transactions on Geoscience and Remote Sensing*. 32(2):388-396.

Ranson, K. J., Sun, G., Kharuk, V. I., Kovacs, K. (2001), Characterization of forests in western Sayani Mountains, Siberia from SIR-C Data. *Remote Sensing of Environment*. 75:188-200.

Ranson, K. J., Sun, G., Weishampel, J. F., and Knox, R. G. (1997) Forest biomass from combined ecosystem and radar backscatter modeling. *Remote Sensing of Environment*. 59:118-133.

Romme, W. H. (1982), Fire and landscape diversity in subalpine forests of Yellowstone National Park. *Ecological Monographs*. 52(2):199-221.

Saatchi, S. S. and Moghaddam, M. (2000), Estimation of crown and stem water content and biomass of boreal forest using polarimetric SAR imagery. *IEEE Transactions on Geoscience and Remote Sensing*. 38(2):697-709.

Shannon, C. and Weaver, W. (1949), *The mathematical theory of communication*. University of Illinois, Urbana, IL, 117 pp.

Siegert, F. and Hoffman, A. A. (2000), The 1998 forest fire in East Kalimantan (Indonesia): A quantitative evaluation using high resolution, multitemporal ERS-2 SAR images and NOAA-AVHRR hotspot data, *Remote Sensing of Environment*. 72(1):64-77.

Sugardiman, R. A., Hoekman, D., Schut, V., Vissers, M. (1999), Landcover change and fire damage monitoring using ERS-1/2 Multitemporal data sets in East Kalimantan. *European Space Agency*. 489:41-46.

Sun, G. and Ranson, K. J. (1995), A three-dimensional radar backscatter model of forest canopies. *IEEE Transactions on Geoscience and Remote Sensing*. 33(2):372-382.

Sun, G. and Ranson, K. J. (1998), Radar modeling of forest spatial patterns. *International Journal of Remote Sensing*. 19(9):1769-1791.

Sun, G., Simonett, D. S., and Strahler, A. H. (1991), A radar backscatter model for discontinuous coniferous forests. *IEEE Transactions on Geoscience and Remote Sensing*. 29(4):639-650.

Turner, M. G., Hargrove, W. W., Gardner, R. H., and Romme, W. H., (1994), Effects of Fire on Landscape Heterogeneity in Yellowstone National Park, Wyoming. *Journal of Vegetation Science*. 5: 731-742.

Ulaby, F. T., Sarabandi, K., McDonald, K., Whitt, M., and Dobson, M. C. (1990) Michigan microwave canopy scattering model. *International Journal of Remote Sensing*. 11(7):1223-1253.

Wang, Y., Day, J., and Sun, G. (1993) Santa Barbara microwave backscattering model for woodlands. *International Journal of Remote Sensing*. 14(8):1477-1493.

Wang, Y., Kasischke, E. S., Bourgeau-Chavez, L. L., O'Neill, K. P., and French, N. H. F. (2000), Assessing the influence of vegetation cover on soil-moisture signatures in fire-disturbed boreal forests in interior Alaska: modelled results. *International Journal of Remote Sensing*. 21(4):689-708.

Wang, Y., Kasischke, E. S., Melack, J. M., Davis, F. W., and Christensen, N. L., Jr. (1994), The effects of changes in loblolly pine biomass and soil moisture on ERS-1 SAR backscatter. *Remote Sensing of Environment*. 49:25-31.

Waring, R. H., Way, J., Hunt, R. J., Jr., Ranson, K. J., Weishampel, J. F., Oren, R., and Franklin, S. E. (1995), Imaging radar for ecosystem studies. *Bioscience*. 45(10):715-723.

Wu, Q. X. and North, H. C. (2001), A multi-scale technique for detecting forest-cover boundary from L-band SAR images. *International Journal of Remote Sensing*. 22(5):757-772.

Table 1. Plot characteristics for each fire plot.

plot	Area (m^2)	Mean Elevation (meters)	Mean Slope (°)	Aspect	Vegetation	Fire History
1.1	488974.5	2111.7	12.18	SE	oak	1994
1.2	334647.0	2114.4	14.20	W-SW	pine/oak	1989
1.3	271291.5	2565.7	7.25	S	pine	1943
2.1	1038867.8	2108.1	10.26	E	oak	1954, 1994
2.2	555579.0	2208.5	12.86	S-SW	pine/oak	1943, 1994
2.3	362263.5	2250.2	16.30	NW	pine/oak	1972, 1989
3.1	986071.5	2152.9	9.00	S-SE	pine	1943, 1954, 1994
5.1	175446.0	2168.1	11.71	E	pine/oak	1943, 1950, 1972, 1993, 1994
6.1	273728.3	2152.1	14.07	E	pine/oak	1943, 1950, 1956, 1972, 1993, 1994

Table 2. Landscape statistics used in this study.

Statistic	Abbreviation	Description	Reference
Mean Patch Size	MPS	average patch size	McGarigal and Marks, 1995
Patch Size Coefficient of Variation	PSCV	patch size standard deviation / mean patch size	McGarigal and Marks, 1995
Patch-per-Unit Area	PPU	number of patches normalized by area	Frohn, 1998
Mean Patch Fractal Dimension	MPFD	average fractal dimension (area and perimeter calculation)	Li, 1990
Shannon's Diversity Index	SDI	sensitive to richness (number of patch types)	Shannon and Weaver, 1949
Shannon's Evenness Index	SEI	distribution of area among patch types	Shannon and Weaver, 1949

Table 3. Cases where fire plot mean backscatter (σ°) was not significantly different.

	Single Fire Plots			Two Fire Plots			Multiple Fire Plots		
PLOT	**1.1**	**1.2**	**1.3**	**2.1**	**2.2**	**2.3**	**3.1**	**5.1**	**6.1**
1.1			C-HH C-HV	C-HH	C-HH L-HV	C-HH		C-HH	C-HV
1.2			L-HH L-HV			L-HH	L-HH L-HV		
1.3	C-HH C-HV	L-HH L-HV				L-HH L-HV	L-HH	C-HH	C-HV
2.1	C-HH				C-HH	C-HH	C-HV	C-HH C-HV	L-HH
2.2	C-HH L-HV			C-HH		C-HH		C-HH	C-HV
2.3	C-HH	L-HH	L-HH L-HV	C-HH	C-HH		C-HV L-HH	C-HH C-HV	
3.1		L-HH L-HV	L-HH	C-HV		C-HV L-HH		C-HV	
5.1	C-HH		C-HH	C-HH C-HV	C-HH	C-HH C-HV	C-HV		L-HV
6.1	C-HV		C-HV	L-HH	C-HV			L-HV	

Table 4. Spearman's Rank Correlation Coefficients for Mean Patch Size, Mean Patch Fractal Dimension, Shannon's Evenness Index, and Shannon's Diversity Index as derived from single band and band ratio SIR-C data. All correlations shown are significant at the 0.05 level. Correlations significant at the 0.01 level are indicated in italics.

Mean Patch Size		Mean Patch Fractal Dimension			Shannon's Evenness Index	
	last FFI		last 52	last fire		last fire
C-HH / L-HH	0.785	L-HH / C-HV	-0.707	-0.777	C-HH / L-HH	0.777

Shannon's Diversity Index						
	last10	last30	last40	last50	last52	avg FFI
C-HV	-0.767	-0.798	-0.785	-0.707		-0.780
L-HH		-0.688	-0.676			
C-HH / L-HV		-0.716	-0.694			
L-HV / C-HV		-0.743	-0.767	*-0.863*	*-0.811*	*-0.932*
L-HH / L-HV	-0.697	-0.688	-0.694			

last10 *= number of fire-free years in previous ten years*
last30 *= number of fire-free years in previous thirty years*
last40 *= number of fire-free years in previous forty years*
last50 *= number of fire-free years in previous fifty years*
last52 *= number of fire-free years in previous fifty-two years*
avg FFI *= average length of time between fires*
last fire *= time since most recent fire*
last FFI *= length of most recent fire-free period*

FIGURE CAPTIONS

Figure 1. Location of Saguaro National Park, Rincon Mountain District.

Figure 2. Grayscale versions of four original bands of SIR-C data with fire plot locations shown

Figure 3. Grayscale versions of six ratios calculated from original bands of SIR-C data with fire plot locations shown. a) C-HH/C-HV, b) C-HH/L-HH, c) C-HH/L-HV, d) L-HH/C-HV, e) L-HV/C-HV, f) L-HH/L-HV. Plot locations are labeled in a).

Figure 4. Mean backscatter (σ°) for fire plots (black bars) and control plots (white bars). All fire/control plot pairs had significantly different means, unless indicated otherwise. Means that were not significantly different ($p > 0.05$) are marked with *.

Figure 5. Scatter plots for selected image enhancements, showing relationships between landscape metrics and fire history variables: average fire-free interval (AVG_FFI), fire-free years in the past 52 years (LAST52), length of the most recent fire-free interval (LAST_FFI). a) Mean Patch Fractal Dimension (normalized) derived from LHH/CHV, b) Shannon's Diversity Index (normalized) derived from LHV/CHV, c) Shannon's Diversity Index (normalized) derived from CHV, d) Mean Patch Size (normalized) derived from CHH/LHH.

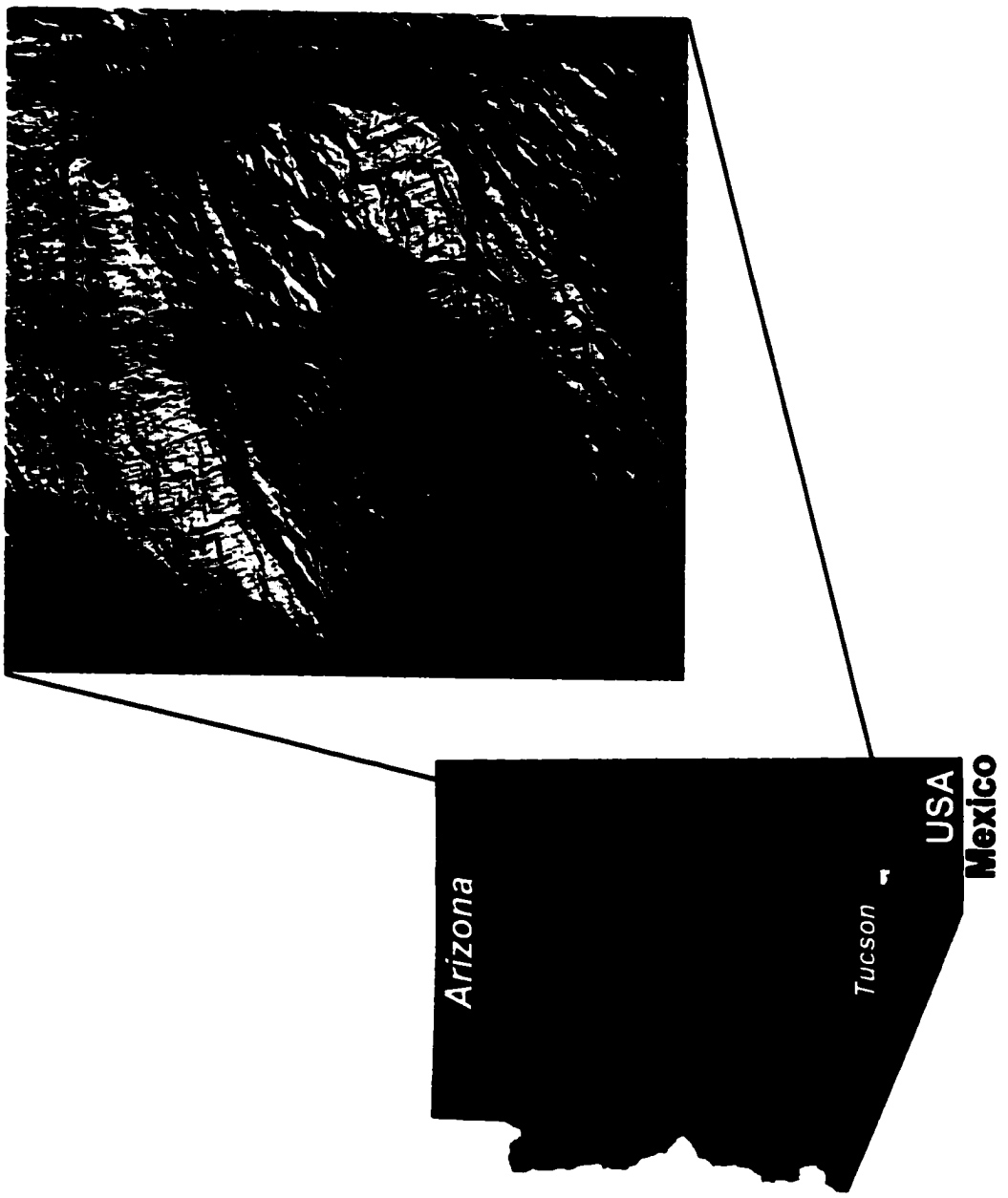

Figure 1

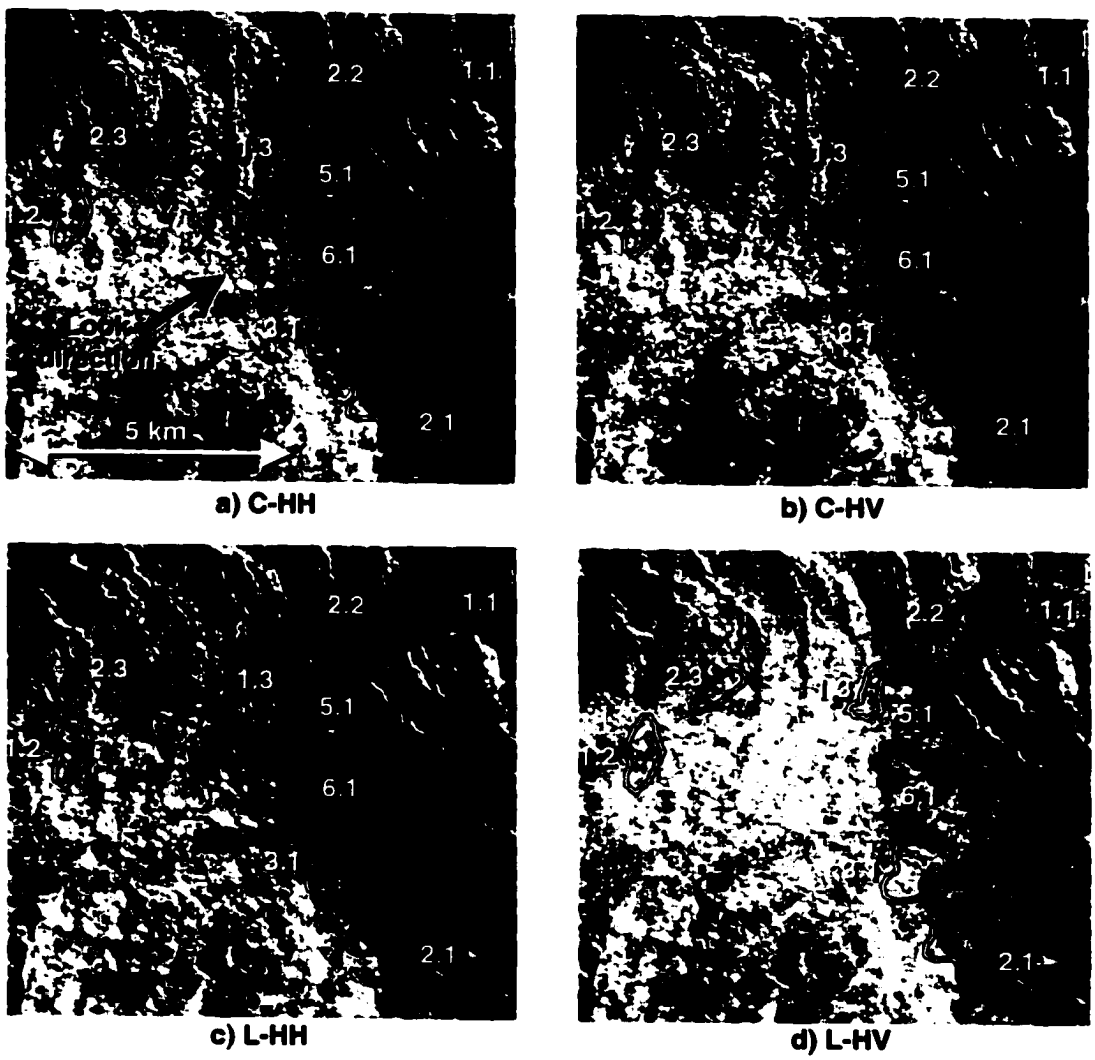

Figure 2

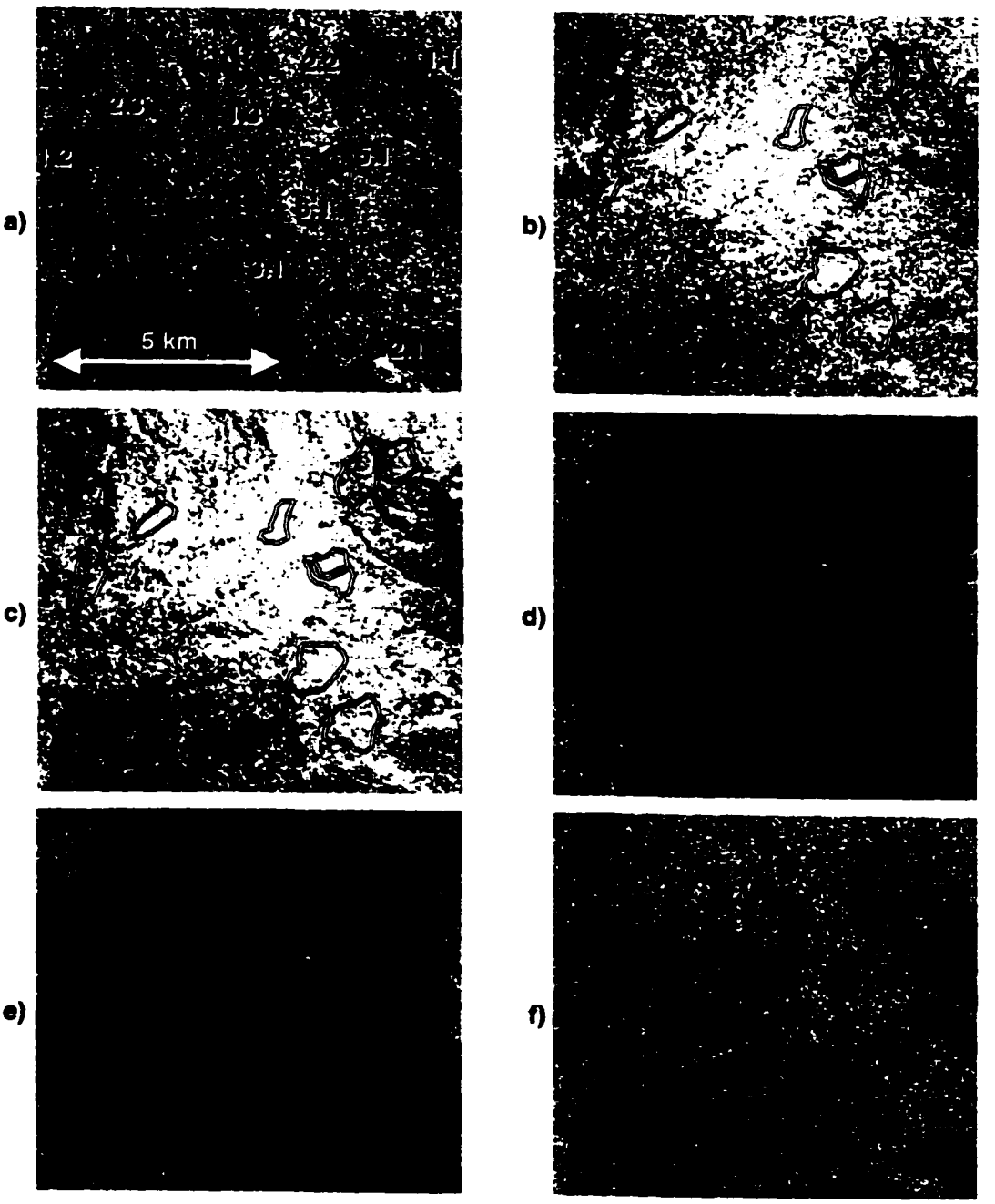

Figure 3

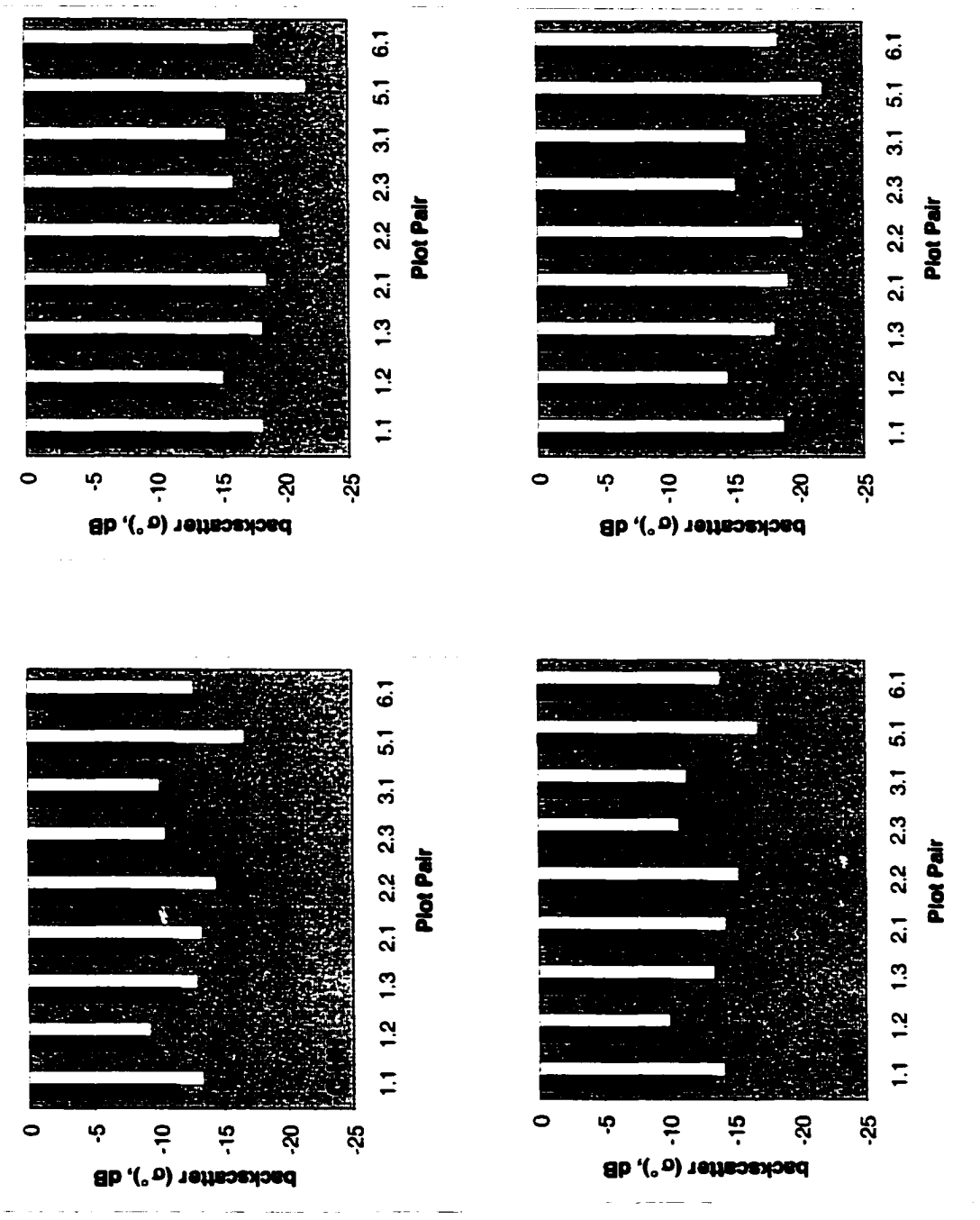
backscatter (σ°), dB
0
-5
-10
-15
-20
-25
1.1 1.2 1.3 2.1 2.2 2.3 3.1 5.1 6.1
Plot Pair

Figure 4

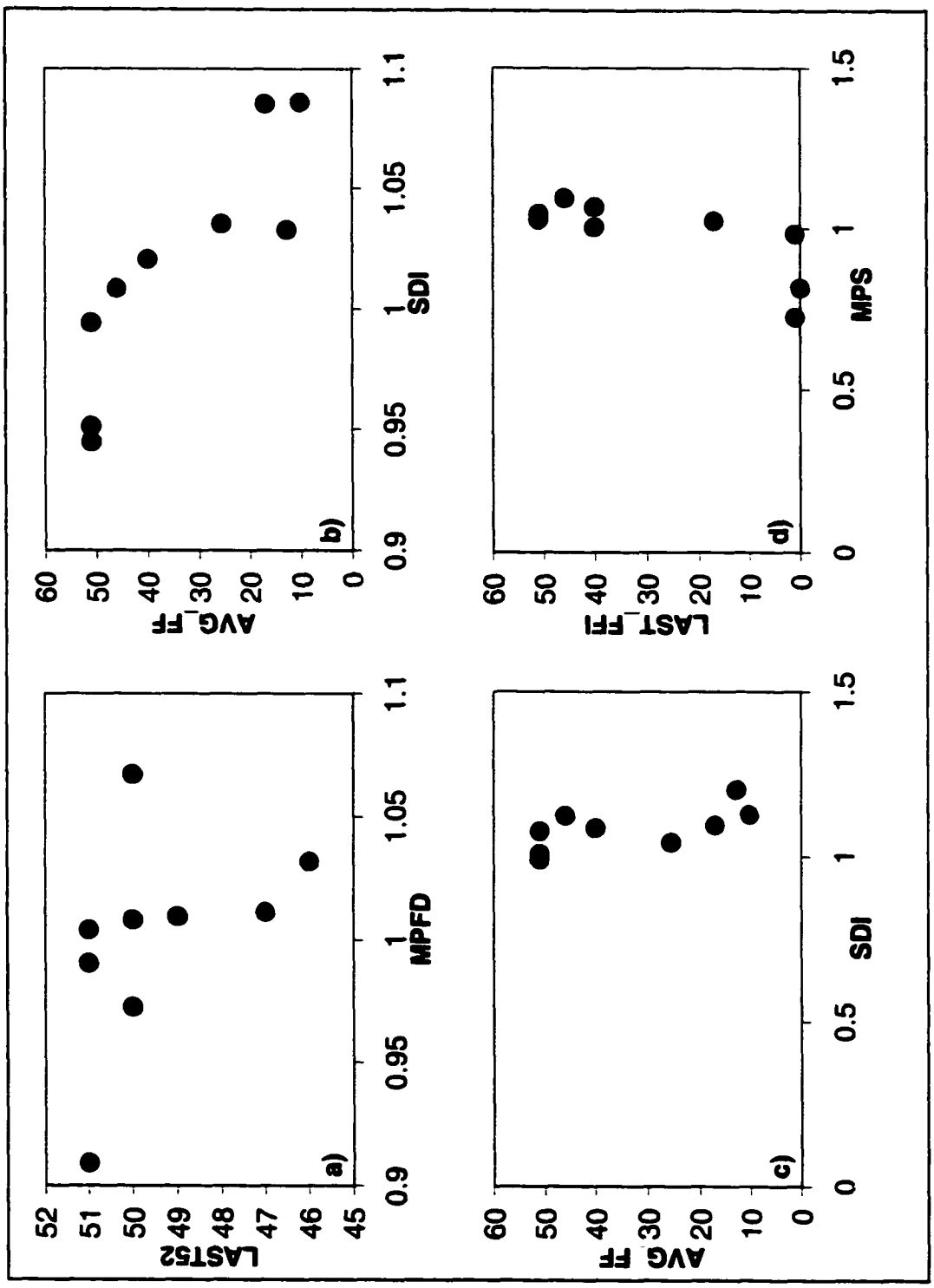

Figure 5

APPENDIX C:

Assessing Relationships Between Forest Spatial Patterns and Fire History with Fusion of Landsat TM and SIR-C Data

M. C. Henry and S. R. Yool

Department of Geography and Regional Development, Harvill Building, Box #2, University of Arizona, Tucson, AZ 85721

To be submitted to *International Journal of Wildland Fire*

ABSTRACT

In this paper, we tested the use of active and passive sensor fusion for relating forest fire history to landscape spatial patterns. A range of data fusion techniques was implemented to combine Landsat Thematic Mapper (TM) and Shuttle Imaging Radar (SIR-C) data from October 1994. Plots with known fire history were chosen from four categories: unburned, once burned, twice burned, and multiple burned. We calculated landscape metrics for each plot, including mean patch fractal dimension, mean patch size, Shannon's Diversity Index, and Shannon's Evenness Index. Spearman's Rank Correlation Analysis was used to compare the landscape statistics to fire history characteristics, such as time since fire, average fire-free interval, and number of fire-free years in different time periods. Results showed that landscape patterns derived from fused data were significantly ($p < 0.05$) related to fire history and typically performed better (more significant correlations) than the single source data.

INTRODUCTION

Forest fires are a common concern in many different environments from tropical ecosystems to boreal forests. In the American Southwest fire regimes have shifted dramatically since European settlement, due chiefly to livestock grazing and fire suppression. The reduction in fire occurrence has increased forest density and created conditions more favorable to stand-replacing crown fires (Covington et al., 1997; Dahms and Geils, 1997). There are many factors that impact how easily a forest can burn, such as weather (wind, humidity) and fuel conditions (including moisture, amount, connectivity). Although weather often dictates when fires will occur, fuel conditions

mediate fire intensity. The spatial arrangement of fire fuels (connectivity) is a product of many factors (species composition, site productivity) and affects the spread of fire from one area to another (Miller and Urban, 2000). Fire history also has a significant direct impact on spatial arrangement of fuels, current species composition and age structure. Ecologists acknowledge the importance of spatial pattern, but it is often difficult to characterize over large areas.

Multispectral sensors such as Landsat Thematic Mapper (TM) have been used extensively for forestry applications such as monitoring forest mortality (Collins and Woodcock, 1996), post-fire damage (Rogan and Yool, 2001) and regeneration (Jakubauskas, 1996; White et al., 1996; Riaño et al, 2002) and Synthetic Aperture Radar (SAR) systems such as the Shuttle Imaging Radar (SIR-C) have shown strong relationships with forest structural characteristics (Dobson et al, 1995; Green, 1998a; Castel et al, 2002). There is certainly great potential for combining these datasets to obtain detailed forest information. We tested in this study the capability of fused Landsat TM and SIR-C data to extract forest spatial patterns and report here whether these patterns can be linked to fire history. Specifically, we investigated the following question: Is optical and active microwave data fusion an effective technique for extracting fire-related forest patterns? We addressed this question in three parts:

1) Which landscape metrics show the strongest relationships to fire history?
2) Does data fusion achieve better results than Landsat TM or SIR-C alone?
3) Which fusion technique obtains the best results?

OPTICAL/MICROWAVE DATA FUSION

Multisensor data fusion may be well suited to examine some aspects of fire-induced spatial patterning. Image data fusion is a technique where data from two different sensors are combined with the goal of extracting information about a landscape. The major appeal of these fusion methods is the potential for synergy- that the fused data will provide more information than either data source alone.

Multispectral data have been used in conjunction with SAR data for a variety of applications including monitoring coal subsidence areas (Prakash et al, 2001), detecting oceanic plankton blooms (Svejkovsky and Shandley, 2001), monitoring crop conditions (Moran et al, 2002), mapping flooded areas (Townsend and Walsh, 1998; Töyrä et al, 2001), and landcover mapping (Pohl and Van Genderen, 1999; Kuplich et al, 2000; Le Hégarat-Mascle et al., 2000). The logic for fusion lies in the distinct and complementary qualities of these data: SAR systems can image despite cloud cover, thus are especially desirable for high latitude (Kasischke et al, 1994) and tropical research (Majumdar and Mohanty, 1999; Siegert and Hoffman, 2000; Couturier et al, 2001). The microwave energy emitted by the system penetrates and interacts with forest structural components (stems, branches, leaves), while optical systems record sunlight reflected from the top of the forest canopy (or any exposed surface). Differences between microwave and optical data modalities can thus be fused to obtain structural and color information about an area of interest.

A variety of approaches have been used to fuse multisensor datasets. Many of these techniques employ pixel-based image fusion (Pohl and van Genderen, 1999), while

others combine datasets in a supervised or unsupervised classification (Rignot et al, 1997; Kuplich et al, 2000). Methods available for merging datasets at the pixel-level vary widely, and include principal components analysis, mathematical operators, and image transformation/insertion techniques (Pohl and Van Genderen, 1998). Thorough discussion of these techniques is beyond the scope of this paper. For a review of sensor data fusion techniques and applications, refer to Pohl and Van Genderen (1998).

Various researchers have used optical and SAR data in fusion studies to determine whether the two data types are more valuable in combination than they are independently. Much of this research has compared single sensor and data fusion for landcover or resource mapping. In most cases, data fusion provided higher accuracy than single sensors. Researchers have found that data fusion produced small to moderate increases in accuracy from multispectral image mapping and significant accuracy improvements over SAR data alone (Schistad Solberg et al, 1994). For instance, Lozano-Garcia and Hoffer (1993) compared classification of SIR-B data (L-HH at three different incidence angles), Landsat TM, and multisensor fusion for mapping landcover in Florida. The best accuracy they achieved for the fused data was only slightly higher than the best results for the TM alone, but a great improvement over SIR-B alone. Le Hégarat-Mascle et al. (2000) observed similar trends when they compared image classifications of multitemporal European Remote Sensing (ERS) Satellite (C-VV), Landsat TM, and fusion for identifying crops in France. They found that SAR data (ERS) produced the poorest results, TM identified crop types better, and the fused data classification was an improvement over either single data source.

Our research is unique for two reasons: 1) we are not aware of any other studies that have used data fusion to assess spatial patterns; and 2) very little fire-related research has investigated data fusion (Siegert and Hoffmann, 2000). Our technique for comparing datasets also differs from previous work: In many cases where image data have been fused at the pixel level, it was for interpretation purposes (Yesou et al, 1993) or resolution improvement (Carper et al, 1990; Chavez et al, 1991). We combine these two approaches, fusing datasets at the pixel level and comparing results to each input dataset.

DATA AND METHODS

Our strategy was to extract landscape spatial statistics from plots with known fire history, then compare these spatial patterns with different fire history characteristics. For example, several fire history variables were defined by fire occurrence in particular time spans. We examined also how the amount of time since the most recent fire related to spatial patterns. The impact of time since fire varies considerably with fire severity. We included this variable to see if a simple measure, such as time since fire, adequately defines forest spatial patterns with respect to fire history. Detailed descriptions of the fire history variables can be found in the Results section.

Study Area

Saguaro National Park's Rincon Mountain District is located just east of Tucson, Arizona, USA (Figure 1). The Rincon Mountains exemplify southern Arizona's Sky Islands, which support a diverse flora and fauna in isolated forest ecosystems above the

Sonoran Desert. Vegetation communities in the Rincons include desert scrub on the desert floor, which grade into grassland, oak woodland, pine-oak communities, and mixed conifer at the higher elevations. Climate for the southern Arizona region is semi-arid, with low relative humidity throughout much of the year. Precipitation is bimodal, with one peak in late summer and one in winter. Average annual precipitation at the highest elevations in the study area is approximately 760 mm.

Study Plot Selection

Using a fire atlas from the National Park Service that covered fires from 1943 to 1996, we selected nine fire plots, each with a distinct fire history (see Table 1). Plot selection was challenging for several reasons: 1) it was important to avoid rock outcrops, as these would certainly affect spatial patterns in the area of interest; 2) we wanted each fire plot to be a fairly simple shape (no long narrow features); 3) we wanted each plot to be large enough to be considered a statistically valid size (near 300 pixels minimum); 4) we needed to select sites located above 2000 meters elevation, to ensure shrub-dominated vegetation would be excluded (due to a potentially different fire regime and recovery sequence). Nine plots met these requirements.

Topographic and forest type variability in the study area affect site productivity. We chose unburned plots to coincide with each fire plot, controlling for site productivity differences. We selected the control plots from another part of the mountains that had not burned during the study period. Control plots were used to normalize landscape statistics calculated for each fire plot (fire plot statistic / control plot statistic).

TM Data

In other recent work, we analyzed a 1996 TM scene and found significant relationships between spatial patterns and fire history. For this study, we obtained a TM scene that coincided in time with the SIR-C data. The new TM image (Figure 2a) was obtained October 13, 1994 (scene ID: LT5036038009428610). We followed the same processing steps as with the 1996 image, except that we also applied a C-factor topographic normalization (Teillet et al., 1982) to reduce shadows (Figure 2b). This algorithm is a modified cosine correction, which provides a better result than other non-Lambertian normalization techniques (Meyer et al., 1993).

Following this preprocessing, we calculated the Kauth-Thomas (KT) Transform (Crist and Ciccone, 1984) to obtain a Brightness (KT-B), Greenness (KT-G), and Wetness (KT-W) image. We opted to use the KT, because it has proved useful in other fire-related work (Patterson and Yool, 1998). A KT-B, KT-G, and KT-W composite image was also transformed into its Intensity, Hue, and Saturation components. Koutsias et al. (2000) successfully mapped fire scars in the Mediterranean using a similar technique. Finally, we also calculated the Normalized Difference Vegetation Index (NDVI), which has been widely used in other fire-related research (Marchetti et al., 1995; Chuvieco, 1999). These seven image enhancements were used in our previous work, so we attempted to maintain consistency in image processing. We found many landscape statistics calculated from the 1996 TM enhancements were correlated with fire history.

SIR-C Data

SAR data were obtained during the second of the 1994 SIR-C missions (October 4, 1994) for an area that included the Rincon Mountains (Figure 3). This SAR system used C-band (5.8 cm) and L-band (23.5 cm) wavelengths with horizontal send-horizontal receive (HH) and horizontal send-vertical receive (HV) polarizations. The look direction of the image was 54.5° (from north) and incidence angle was 50.8° (Figure 3). Data were terrain corrected and calibrated before purchase from NASA's Jet Propulsion Laboratory. Additional general processing steps included georectification to a DEM using shaded relief that matched SAR illumination conditions, application of a speckle suppression filter, and calculation of band ratios (Figure 4).

The main advantage of this dataset over commercially available spaceborne SAR data is the multifrequency multipolarization format: By combining shorter C-band data with L-band, different forest components can be evaluated. C-band backscatter is impacted by smaller tree components in the upper part of the canopy, while L-band backscatter is affected most by larger parts of the tree and trunk-ground scattering (Chipman et al, 2000). In our previous work, we found significant relationships between fire history and spatial patterns derived from SIR-C data. By fusing SIR-C with the TM data, we hoped to enhance our ability to detect fire-related forest spatial patterns.

Data Fusion Methods

In a number of data fusion studies, researchers have fused multispectral data with a single SAR channel (Kuplich et al., 2000, Moran et al., 2002). Commercially available

satellite SAR systems operate at single frequency and polarization, so in many cases there is only one channel to use. In our study we had the advantage of two bands and two polarizations, thus four different channels to analyze. While these data provide much more information than a single band/polarization, we were faced with an excess of data, particularly once we began forming data combinations between the two sensors. Given the richness of this dataset, we tested a variety of fusion methods, assessing which techniques were optimal for extracting fire-related forest patterns. In the following sections, we outline the fusion approaches we used to merge the TM and SIR-C data (Table 2), including methods to reduce our data.

Principal Components Analysis

Principal Components Analysis (PCA) has been used in many different remote sensing studies, including data fusion. By using data from two (or more) datasets as input to PCA, it is possible to reduce the number of bands for use in later analysis, as well as generate images that contain vital information from both input datasets. In our analysis we ran PCA using three different combinations of bands (Table 2). The first PCA (called PCA) included all of the original TM bands (1-5, 7) and SIR-C bands (C-HH, C-HV, L-HH, L-HV). The first three components accounted for 96.43% of the total variance and were used in the spatial analysis. Based on statistical and visual assessments, these first three components contained potentially useful information and were retained for analysis (Figure 5).

The second set of inputs we used in PCA consisted of all derived image data from the two datasets (called allPCA). This allPCA set included the seven image enhancements used in the TM analysis, the original SIR-C bands, and SIR-C ratios (Table 2). This combination is composed of each of the separate datasets that were analyzed independently (TM only, SIR-C only). The first principal component (PC1) had extremely low dynamic range, with most fire plots containing pixels of the same value. It was clear that landscape statistics derived from this image would not differentiate the plots, so it was excluded from further analysis. PC2, PC3, and PC4 showed apparently non-random spatial variability, and therefore appeared to contain better information than PC1 (Figure 6). These components were used in later analysis.

The final PCA (subPCA) used a subset of the derived images. We selected three image enhancements from each dataset, based on which bands performed well in earlier analysis. We chose NDVI, KT-H, and KT-S from the TM image enhancements and C-HV, C-HH/L-HH, and L-HV/C-HV from the SIR-C data. These image enhancements had the highest number of significant correlations in the individual TM and SIR-C analyses, so we felt that they could achieve good results when fused. The second PC had the same dynamic range problems that allPC1 had, so only PC1 and PC3 were used in the analysis.

Multisensor Unsupervised Classification

Because much landscape analysis is conducted using landcover maps, we included an unsupervised classification in our fusion methods. The same six bands used

in the subPCA described above were used also in a clustering algorithm to obtain 25 classes. No attempts to label the classes were made, but we believed that this processing would reveal the dominant spatial patterns in the study area. The output from the classifications will be called CLASS in the remaining discussion.

Intensity-Hue-Saturation Conversion

The Intensity-Hue-Saturation (IHS) enhancement has been used in many data fusion studies (Harris et al., 1990), including those using optical and SAR data. In most studies, a three-band color composite image from the multispectral dataset is converted into IHS space. The SAR image is then substituted for one of the components, and transformed back into RGB space. Intensity is typically used because it is associated with image spatial variability. A major limitation of this method is that only three multispectral bands and one SAR band can be used as input. Because our TM data consisted of six bands and our SAR data contained four bands, it was not practical to combine the two datasets in this manner. We employed instead a direct IHS method, where a three band composite formed from two TM bands and one SIR-C band was converted to IHS space. Analyses focused on the Intensity component, because of its link to spatial pattern.

We began initially by converting all images generated from unique three-band composites of two TM bands (3, 4, 5, and 7) and one SIR-C channel, but after transforming several, it became clear that there were no differences in the Intensity images derived from composites containing the same SAR band (regardless of channel

assignments in RGB space). As a result, we chose only one three-band composite for each SIR-C band and analyzed the Intensity component from each. A summary of the bands input to these transformations is shown in Table 3.

Data Multiplication

Mathematical operators such as ratios or image differencing readily combine pairs of bands or channels (Pohl and van Genderen, 1999). Accordingly, we multiplied each of the TM bands, except TM1 (blue) and TM2 (green) by each SIR-C channel to generate sixteen new images. There were noticeable similarities between features that had been multiplied by the same TM band (i.e., TM3 x CHH was similar to TM3 x LHV). To reduce sixteen images and eliminate redundancy, each feature set that had included a given TM band was input to PCA. PC1 from each PC run was used in the final spatial analysis. Final image names are MULTI3, MULTI4, MULTI5, and MULTI7. Figure 7 shows a summary of the processing steps to create these images.

Data Simplification and Statistical Analysis

From the individual optical and microwave analyses, TM data supplied seven image enhancements, while the SIR-C data had four original bands plus six ratio images. The processing steps describe below and summarized in Figure 8 were completed for all 17 TM, SIR-C, and fused image features.

Landscape analyses often require discrete data as input. This was the case with our study: Most fused image data were continuous, requiring simplification prior to

analysis. We strove to simplify all image features in an objective and consistent manner. Each image feature was masked to elevations above 2000 meters and rescaled to the range 0 to 25 using a standard deviation stretch. Following rescaling, we applied 3-by-3 majority filters to the resulting thematic images, and finally converted them to polygon coverages. Each of the seventeen polygon coverages was clipped to match the nine fire plots and nine control plots.

The final input data for landscape analysis consisted of 306 polygon coverages (18 plots x 17 channels). Six different landscape statistics were calculated for each of the 306 coverages (Table 4). We normalized the landscape statistics (and reduced data volume) by dividing statistics for each fire plot by the same statistic for corresponding control plot. For example, mean patch size for fire plot 1.1 was divided by mean patch size for control plot 1.1. We used this same technique in the individual dataset studies to help control for topographic differences between fire plots. For the final procedure, we ran Spearman's Rank Correlation analysis between various fire history variables (e.g., fire occurrence in a given time period) and these normalized landscape statistics (Figure 8).

RESULTS AND DISCUSSION

The goal of these analyses was to assess relationships between fire history and forest spatial patterns as quantified by landscape spatial statistics. Other studies have compared the use of data fusion to single data sources, using classification accuracies to evaluate the performance of one method over another (Lozano-Garcia and Hoffer, 1993;

Le Hegarat-Mascle et al., 2000). Our results differ in that we have correlation coefficients to compare for a multidimensional dataset. To produce valid comparisons among techniques, we present results from multiple perspectives, discussing individual variables where appropriate. We describe the landscape spatial statistics used in Table 4. Fire history variables are shown in Table 5.

Correlation Analysis of Fused Data

Fractal Dimension

Results of correlations between area-weighted mean patch fractal dimension (AWMPFD) and mean patch fractal dimension (MPFD) were significant ($p < 0.05$), but the nature of the relationships (direct or inverse) was different (Table 6). For example, an increase in fire occurrence (fewer fire-free years) was associated with a decrease in patch complexity measured by AWMPFD. The opposite relationship was found for the non-weighted version of the statistic. Similarly, a shorter average fire-free period was linked to a decrease in patch complexity for AWMPFD, but an increase in MPFD. These results suggest patch size has an impact on patch patterns: when all patch sizes are weighted equally, greater patch complexity is associated with frequent fire. When larger patches are given more weight, fire frequency decreases patch complexity. Considering that fire-induced spatial patterns are not consistent across scales, the differences in these relationships between MPFD and AWMPFD may be caused by scale differences (Hemstrom, 2001).

Because specific fusion algorithms diverged consistently in these correlations, it is possible certain fusion techniques detect patterns at distinct resolution scales: Patch complexity appears to increase with increasing fire occurrence at a fine scale, but a different pattern may operate at coarser scales. The fusion technique that linked fire occurrence to higher patch complexity (MPFD) was higher order PCA (allPC4 and allPC3). PCs of this order are more likely to have a "salt and pepper" appearance than lower order PCs and correspond to higher order image statistics. As a result, these higher order PCs may correspond to finer scale (pixel level) variations in the landscape.

To investigate relationships between fusion method and spatial scale, we calculated a grand mean as the average mean patch size (MPS) for each fusion technique (individual features) and found that there are large differences in patch size across fusion methods (Figure 9). MULTI7 had the highest mean MPS (10.89 ha) and PC3 had the smallest patches (0.22 ha). This investigation confirmed also our perception regarding higher order PCs. In all cases, mean MPS was higher for the first PC and decreased with each subsequent (higher order) component.

Patch Statistics

Mean patch size (MPS) and patch size coefficient of variation (PSCV) showed greater divergence in the nature of relationships between fire occurrence and spatial patterns than fractal dimension (Table 6). Some fusion methods showed increasing patch size and patch size variability with higher fire frequency, but others produced the opposite pattern. Band multiplication tended to show relationships the opposite of what

we had expected, such as fewer fires being linked to smaller patch size and greater patch size variability. It seems feasible that these patterns do exist, but at a coarser resolution scale than we intended to detect. Hessburg et al. (2000) found that patch sizes at the subwatershed scale tend to be smaller under current fire regimes (suppression) than historical conditions. This contradicts patterns often found at stand scales, such as frequent fire regimes increasing forest density (Fulé and Covington, 1998). Three of the MULTI images are in the top four highest mean MPS, so this fusion method appears to detect coarser scale patterns than the other fusion methods. This could explain the conflicting significant correlations we obtained in our analysis.

Diversity and Evenness Measures

Correlation results from Shannon's Diversity Index (SDI) and Shannon's Evenness Index (SEI) also produced mixed results (Table 6), though trends were consistent in terms of fusion technique: MULTI3 and PC1 linked increasing fire occurrence with decreasing diversity, while other fusion methods had the opposite relationship. We had expected SDI to increase with fire occurrence and this trend was observed with several fusion techniques (and previous analysis of both TM and SIR-C). Scale differences appear to play a role in these discrepancies. Fulé and Covington (1998) found clustering of trees at fine spatial scales (12 meters and below) with frequent fire, but Romme (1982) determined fire exclusion and natural fire regimes had nearly the same diversity. The important distinction is that Romme (1982) studied patterns using 5-hectare units. At the subwatershed scale, Hessburg et al. (2000) found higher diversity

under current fire regimes than at historical conditions. These studies demonstrate that relationships between landscape diversity and fire history vary across scales.

Our results showed that increased fire occurrence is linked to a decrease in SEI (landscape evenness). TM and SIR-C did not obtain any significant results for this landscape spatial statistic, so it is not possible to compare these figures with others. However, the observed relationship suggests that landscape evenness decreases with higher fire frequency. Keane et al. (1999) found that evenness based on leaf area index, biomass, and cover type increased under fire exclusion. Our results are in agreement also with Romme (1982), who found fire exclusion increased landscape evenness.

Performance of Fusion Techniques

PC2 was the best-performing fusion method based on total number of significant correlations (12) and percentage of fire history variables with significant correlations (87.5%). Loadings for PC2 were high for C-HH (-0.66), which is sensitive to canopy caps (Green, 1998b) and L-HV (0.63), which is linked to biomass (Castel et al., 2002) and woody volume (Ferrazzoli and Guerriero, 1995). Most significant correlations were obtained using area-weighted mean patch fractal dimension (AWMPFD) and mean patch size (MPS) as landscape spatial statistics. The combination of these two SIR-C channels also produced significant results as a ratio (C-HH/L-HV). However, PC2 obtained more significant results across a range of landscape spatial statistics than the ratio of these two channels. While the ratio consists of only two channels, PC2 corresponds to image variance using all TM and SIR-C channels (although loadings were highest for C-HH and

L-HV). Mean MPS (Figure 9) is smaller for PC2 than C-HH/L-HV, so this fusion method is likely sensitive to finer scale variations than the ratio.

Following PC2, CHHi also performed well, with a total of 10 significant correlations for 87.5% of fire history variables. CHHi was derived from C-HH, which is responds to canopy gaps (Green, 1998b), TM3 (red), and TM4 (near infrared), which when used to calculate NDVI are linked to primary production (Prince, 1991). CHHi obtained many of its significant correlations using Shannon's Diversity Index (SDI) and Shannon's Evenness Index (SEI). For two fire history variables, CHHi was the only image enhancement (including TM and SIR-C alone) to obtain a significant correlation. These correlations found that landscape evenness increases with higher fire frequency. Keane et al. (1999) found that landscape evenness based on net primary production decreased under fire suppression. CHHi may not be directly related to primary production, but the patterns we found are in agreement with Keane et al. (1999).

The third best fusion algorithm we tested was MULTI3, which was derived from TM3 (red) and all four SIR-C channels. The final version of this enhancement was calculated from PCA, where loadings were higher for C-HV (0.51) and L-HV (0.65). The prevalence of both cross-polarized channels explains the success of MULTI3 (9 significant correlations for 75% of fire history variables): L-HV has been linked to biomass (Kasischke et al., 1995; Castel et al., 2002) and C-HV is sensitive to leaf area index (Imhoff et al., 1997) and crown biomass (Saatchi and Moghadden, 2000). Each MULTI enhancement includes different TM bands, with MULTI3 (including TM3, or red) performing better than the others. TM3 is sensitive to chlorophyll, so when

combined with the cross-polarized SIR-C channels, both structural and reflectance information can be obtained. All the MULTI enhancements showed different relationships between fire history and landscape patterns, such as MULTI3 showing increased landscape diversity with lower fire frequency. This is one of the cases where coarser scale patterns are possibly being detected. Hessberg et al. (2000) found that landscape diversity at the subwatershed scale increased under current fire regimes (suppression). This trend is different than those observed at finer scales, but matches our results for many of the fusion methods.

Comparison of Fused Data to TM and SIR-C

There were few cases where the SIR-C correlations were stronger than those of the fused data. TM-derived landscape statistics, however, showed stronger relationships in several cases. Fused data achieved significant correlations for 75% (six of eight) of the fire variables when area weighted mean patch fractal dimension (AWMPFD) was measured, however, TM-derived correlations were stronger in four of those cases. The TM data also out-performed fused data when mean patch size (MPS) was evaluated. There were five instances where TM correlations were stronger than fused data. For all other landscape statistics we tested, fused data produced the highest correlation coefficients for the majority of fire history variables. The best image enhancement (from TM, SIR-C, or fusion) for each landscape metric is shown in Figure 10. The fire history variable shown is average fire-free interval, which is a good summary indicator of fire frequency over the study period.

The best of the fusion techniques obtained stronger correlations than TM and SIR-C in most cases, although PC2 was only better than TM 8.3% of the time. Compared to SIR-C alone, PC2 achieved higher correlation coefficients in 100% of cases. Many of the significant correlations for PC2 occurred using landscape metrics where TM performed very well. For example, MPS derived from NDVI showed significant relationships to fire frequency (fire-free years in a given interval, mean fire-free interval). NDVI has been linked to primary production (Justice et al., 1985; Tucker and Sellers, 1986; Prince, 1991). Keane et al. (1999) showed that patch density derived from net primary production decreases under a regime of fire suppression. This relationship was stronger in our analysis than that between PC2 and fire frequency. CHHi and MULTI3 were more consistent, with higher correlations than TM 80% and 77.8% of the time, respectively. Compared to SIR-C correlations, CHHi was higher in 60% of comparisons, while MULTI3 was higher 100% of the time.

It is interesting to note that C-HH was important in calculating the two best fusion methods (PC2 and CHHi), yet it did not achieve a single significant correlation alone. The inclusion of TM3 (red) and TM4 (near infrared) in CHHi may have reduced some topographic effects present in C-HH, because the TM image had been topographically normalized. Another difference can be illustrated by summary statistics for one of the frequently burned plots (5.1). Standardized skewness shows that C-HH is nearly in the normal range (2.32) and CHHi is more skewed to the right (2.78). The right skewness of CHHi distributes high values over a greater range than those of C-HH, potentially revealing more within-plot variations.

There were specific TM-derived variables that performed best. KT-Hue showed strong sensitivities between fire history variables and spatial pattern in several cases: AWMPFD, MPS, PSCV (patch size coefficient of variation), and SEI (Shannon's Evenness Index). NDVI also obtained high correlation coefficients for AWMPFD, MPS, and SDI (Shannon's Diversity Index). KT-Hue is the enhancement that resulted in the highest number of significant correlations for all three datasets (16) for 87.5% of the fire history variables. These results are better than those for NDVI, but the two enhancements followed similar trends. All significant correlations from NDVI correspond to fire history/landscape metrics also explained by KT-Hue. In two cases, NDVI had higher correlations coefficients, but KT-Hue performed better for all others. KT-Hue was calculated from the original KT composite, where brightness was red, greenness was green, and wetness was blue. The hue component of that color composite corresponds to the color (or dominant wavelength) created by the combination of the three bands. As a result, KT-Hue combines information about exposed soil (brightness), vegetation cover (greenness), and moisture content (wetness). The spatial patterns of all three KT components correspond to spatial variations in a range of forest characteristics and our results indicate these are linked to fire history.

Another way to compare the results of the correlation analysis is to assess which technique produced the strongest relationships between spatial pattern and each fire history variable. We summarized these results in Table 7. Fused data produced highest correlation coefficients, or tied with TM for the highest for every fire history variable tested. Although the strength of the correlations was the same for TM and fused data in

many cases, fused data had the sole highest correlations for the remaining fire history variables.

It is useful to discuss the cases where fused data obtained significant correlations and TM or SIR-C alone did not: When PSCV was used as the spatial pattern indicator, neither TM nor SIR-C correlated with time since fire (last_fire), but the fused data (PC3) were able to accomplish this (-0.757, $p = 0.018$). In the SDI analysis, MULTI5 showed a significant relationship with last_FFI (0.836, $p = 0.005$), and with SEI, both subPC3 (-0.734, $p = 0.024$) and MULTI5 (0.785, $p = 0.012$) produced significant results.

The preceding analysis and discussion demonstrates that TM / SIR-C data fusion enhances forest spatial patterns that are linked to fire history. The relationships between landscape statistics derived from the fused data were in many cases stronger than those of TM-derived patterns. There were only a few cases where SIR-C based correlations were stronger than data fusion. Results from this new application agree with many other studies: Fused data are a significant improvement over SAR data alone, but only slightly better than multispectral data (Schistad Solberg et al., 1994). Researchers have found SAR data are typically inferior to optical data for most landcover mapping applications (Rignot et al, 1997; Kuplich et al, 2000). Although we did not actually map landcover, we used SAR backscatter as a surrogate for different landcover types to evaluate surface spatial patterns. It is noteworthy that SAR research is not at the same stage of advancement as optical remote sensing techniques, so future improvements to SAR systems or processing may help resolve these issues.

Although our findings are significant and suggest that active/passive sensor fusion is an effective technique for extracting fire-related spatial patterns from the landscape, there are limitations. First, it would be beneficial for future studies to focus on areas where it is possible to obtain a larger sample size. In our study, we were restricted to a fairly small area, where rock outcrops are abundant. This made it difficult to obtain a larger sample. Parametric statistics would be feasible if more study plots could be used, thereby increasing the statistical power of the results. Secondly, it is important to consider the nature of the fire atlas used in the study: The fire perimeters were delineated over the course of many years, likely by many individuals, so the accuracy of these boundaries is largely unknown. Despite these considerations, our results were significant and indicate landscape patterns can be linked to fire history using remote sensing.

Implications of Results

The preceding results have an interesting implication: TM/SIR-C data fusion may be able to detect fire-related forest patterns at multiple scales. Trends observed in MPS support this idea: All image enhancements and fusion techniques with mean MPS below 1.0 ha showed a positive relationship between fire-free years and patch size (more fires lead to smaller patches). In contrast, fused data with mean MPS greater than 1.0 ha had the opposite pattern. We can interpret these results, concluding that frequent fire increases patchiness at a fine scale, but results in a homogeneous pattern at coarser scales.

Another example of scale dependence is illustrated with the SDI results: For most enhancements, diversity increased with increasing fire occurrence. The only exceptions

to this pattern occur in MULTI3 and PC1, with PC1 only showing significant correlations in two time periods. Mean MPS for MULTI3 is 1.3 ha, while all other enhancements have mean MPS below 1.0 ha. Mean MPS for PC1 is the only issue that prevents a clear scale division from being defined, because it is also below 1.0 ha (and smaller than many of the other mean MPS). Using a 5.0 ha minimum cell size, however, Romme (1982) found no clear distinction between landscape diversity for fire excluded areas and frequently burned areas. Hessburg et al. (2000) found increasing landscape diversity with lower fire frequency at the subwatershed scale. It is evident that scale relationships between fire history and spatial patterns have not been clearly defined. Furthermore, it is likely that these relationships vary across ecosystems. While our results were significant over a range of scales and image enhancements, the direction and nature of the relationship cannot be recognized clearly and we can conclude that spatial patterns are not consistent across all scales (Hemstrom, 2001).

SUMMARY AND RECOMMENDATIONS

We explored in this study the potential of multispectral/SAR data fusion for assessing fire-related forest spatial patterns. We quantified relationships between data fusion-derived landscape statistics and a range of fire history variables and compared these results to those of each data source alone. We found the following:

1) Optical and active microwave data fusion successfully extracted forest spatial patterns linked to fire history;

2) Shannon's Diversity Index was consistent in characterizing forest patterns related to fire history;
3) Data fusion performed better than SIR-C in most cases, and better than TM in many cases;
4) Band multiplication and PCA were among the most effective data fusion techniques for extracting forest spatial patterns;
5) Fusion techniques appear to detect fire-related spatial patterns at multiple scales from less than one-quarter hectare to over ten hectares.

The robustness of these data fusion techniques from fine to coarse resolution suggests data fusion offers excellent potential for additional study and provides unique information not obtained from independent passive and active data sources. Future work could include fusion of Landsat TM with commercially available SAR data, to determine whether including single frequency and polarization data is sufficient to characterize fire-related spatial patterns. If so, it would also be possible to conduct multitemporal studies, assessing forest spatial patterns before and after fire.

ACKNOWLEDGMENTS

This research was funded by EPA Science to Achieve Results (STAR) Fellowship number U915601 awarded to Mary C. Henry, University of Arizona. The authors wish to thank Dr. Stuart Marsh, Dr. Tom Swetnam, Dr. Susan Moran, and Dr. Mal Zwolinski for comments and suggestions on the manuscript. We would also like to thank Kathy Schon

and Pam Anning of the National Park Service (Saguaro National Park) for supplying the fire atlas used in this study.

REFERENCES

Carper WJ, Lillesand TM, Kiefer RW (1990) The use of intensity-hue-saturation transformations for merging SPOT Panchromatic and Multispectral image data. *Photogrammetric Engineering and Remote Sensing* **56**, 459-467.

Castel T, Guerra F, Caraglio Y, Houllier F (2002) Retrieval biomass of a large Venezuelan pine plantation using JERS-1 SAR data. Analysis of forest structure impact on radar signature, *Remote Sensing of Environment* **79**, 30-41.

Chavez PS, Sides SC, Anderson JA (1991) Comparison of 3 different methods to merge multiresolution and multispectral data- Landsat TM and SPOT Panchromatic. *Photogrammetric Engineering and Remote Sensing* **57**, 295-303.

Chipman JW, Lillesand TM, Gage JD, Radcliffe S (2000) Spaceborne imaging radar in support of forest resource management. *Photogrammetric Engineering and Remote Sensing* **66**, 1357-1366.

Chuvieco E (1999) Measuring changes in landscape pattern from satellite images: short-term effects of fire on spatial diversity. *International Journal of Remote Sensing* **20**, 2331-2346.

Collins JB, Woodcock CE (1996) An assessment of several linear change detection techniques for mapping forest mortality using multitemporal Landsat TM data. *Remote Sensing of Environment* **56**, 66-77.

Couturier S, Taylor D, Siegert F, Hoffmann A, Bao M Q (2001) ERS SAR backscatter: a potential real-time indicator of the proneness of modified rainforests to fire. *Remote Sensing of Environment* **76**, 410-417.

Covington WW, Fulé PZ, Moore MM, Hart SC, Kolb TE, Mast JN, Sackett SS, Wagner MR (1997) Restoring ecosystem health in ponderosa pine forests of the Southwest. *Journal of Forestry* **95**, 23-29.

Crist EP, Cicone RC (1984) Application of the Tasseled Cap concept to simulated Thematic Mapper data. *Photogrammetric Engineering and Remote Sensing* **50**, 343-352.

Dahms CW, Geils BW (1997) 'An assessment of forest ecosystem health in the Southwest.' General Technical Report RM-GTR-295, U. S. Department of Agriculture, Forest Service, Rocky Mountain Forest and Range Experiment Station, Fort Collins, CO.

Dobson MC, Ulaby FT, Pierce LE (1995) Land-cover classification and estimation of terrain attributes using synthetic aperture radar. *Remote Sensing of Environment* **51**, 199-214.

Ferrazzoli P, Guerriero L (1995) Radar sensitivity to tree geometry and woody volume: a model analysis. *IEEE Transactions on Geoscience and Remote Sensing* **33**, 360-371.

Fulé PZ, Covington WW (1998) Spatial patterns in Mexican pine-oak forests under different recent fire regimes. *Plant Ecology* **134**, 197-209.

Green RM (1998a) Relationships between polarimetric SAR backscatter and forest canopy and sub-canopy biophysical properties. *International Journal of Remote Sensing* **19**, 2395-2412.

Green RM (1998b) The sensitivity of SAR backscatter to forest windthrow gaps. *International Journal of Remote Sensing* **19**, 2419-2425.

Harris JR, Murray R, Hirose T (1990) IHS transform for the integration of radar imagery with other remotely sensed data. *Photogrammetric Engineering and Remote Sensing* **56**, 1631-1641.

Hemstrom MA (2001) Vegetative patterns, disturbances, and forest health in eastern Oregon and Washington. *Northwest Science* **75SI**, 91-109.

Hessburg PF, Smith BG, Salter RB, Ottmar RD, Alvarado E (2000) Recent changes (1930s-1990s) in spatial patterns of interior northwest forests, USA. *Forest Ecology and Management* **136**, 53-83.

Imhoff ML, Sisk TS, Milne A, Morgan G, and Orr T (1997) Remotely sensed indicators of habitat heterogeneity: use of synthetic aperture radar in mapping vegetation structure and bird habitat. *Remote Sensing of Environment* **60**, 217-227.

Jakubauskas ME (1996) Thematic Mapper characterization of lodgepole pine seral stages in Yellowstone National Park, USA. *Remote Sensing of Environment* **56**, 118-132.

Justice CO, Townshend JRG, Holben BN, and Tucker CJ (1985) Analysis of the phenology of global vegetation using meteorological satellite data. *International Journal of Remote Sensing* **6**, 1271-1318.

Kasischke ES, Bourgeau-Chavez LL, French NHF (1994) Observations of variations in ERS-1 SAR image intensity associated with forest fires in Alaska. *IEEE Transactions on Geoscience and Remote Sensing* **32**, 206-210.

Kasischke ES, Christensen NL Jr, Bourgeau-Chavez LL (1995) Correlating radar backscatter with components of biomass in loblolly pine forests. *IEEE Transactions on Geoscience and Remote Sensing* **33**, 643-659.

Keane RE, Morgan P, and White JD (1999) Temporal patterns of ecosystem processes on simulated landscapes in Glacier National Park, Montana, USA. *Landscape Ecology* **14**, 311-329.

Koutsias N, Karteris M, Chuvieco E (2000) The use of intensity-hue-saturation transformation of Landsat-5 Thematic Mapper data for burned land mapping. *Photogrammetric Engineering and Remote Sensing* **66**, 829-839.

Kuplich TM, Frietas CC, Soares JV (2000) The study of ERS-1 and Landsat TM synergism for land use classification. *International Journal of Remote Sensing* **21**, 2101-2111.

Le Hégarat-Mascle S, Quesney A, Vidal-Madjar D, Taconet O (2000) Land cover discrimination from multitemporal ERS images and multispectral Landsat images: a study case in an agricultural area in France. *International Journal of Remote Sensing* **21**, 435-456.

Li H (1990) *Spatio-temporal pattern analysis of managed forest landscapes: a simulation approach*. Ph.D. thesis, Oregon State University, Corvallis, OR.

Lozano-Garcia DF, Hoffer RM (1993) Synergistic effects of combined Landsat-TM and SIR-B data for forest resources assessment. *International Journal of Remote Sensing* **14**, 2677-2694.

Majumdar TJ, Mohanti KK (1999) Textural classification of single band SIR-B data over a part of Brahmaputra Basin, India. *Geocarto International* **14**, 62-66.

Marchetti M, Ricotta C, Volpe F (1995) A qualitative approach to mapping post-fire regrowth in Mediterranean vegetation with Landsat TM data. *International Journal of Remote Sensing* **16**, 2487-2494.

McGarigal K, Marks BJ (1995) 'FRAGSTATS: spatial pattern analysis program for quantifying landscape structure.' General Technical Report PNW-GTR-351, U.S. Department of Agriculture, Forest Service, Pacific Northwest Research Station Portland, OR.

Meyer P, Itten KI, Kellenberger T, Sandmeier S, Sandmeier R (1993) Radiometric corrections of topographically induced effects on Landsat TM data in an alpine environment. *ISPRS Journal of Photogrammetry and Remote Sensing* **48**, 17-28.

Miller C, Urban DL (2000) Connectivity of forest fuels and surface fire regimes. *Landscape Ecology* **15**, 145-154.

Moran MS, Hymer DC, Qi J, Kerr Y (2002) Comparison of ERS-2 SAR and Landsat TM imagery for monitoring agricultural crop and soil conditions. *Remote Sensing of Environment* **79**, 243-252.

Patterson MW, Yool SR (1998) Mapping fire-induced vegetation mortality using Landsat Thematic Mapper data: a comparison of linear transformation techniques. *Remote Sensing of Environment* **65**, 132-142.

Pohl C, Van Genderen JL (1998) Multisensor image fusion in remote sensing: concepts, methods, applications. *International Journal of Remote Sensing* **19**, 823-854.

Pohl C, Van Genderen JL (1999) Multi-sensor image maps from SPOT, ERS, and JERS. *Geocarto International*, **14**, 34-41.

Prakash A, Fielding EJ, Gens R, Van Genderen JL, Evans DL (2001) Data fusion for investigating land subsidence and coal fire hazards in a coal mining area. *International Journal of Remote Sensing* **22**, 921-932.

Prince SD (1991) A model of regional primary production for use with coarse resolution satellite data. *International Journal of Remote Sensing* **12**, 1313-1330.

Riaño D, Chuvieco E, Ustin S, Zomera R, Dennison P, Roberts D, and Salas J (2002) Assessment of vegetation regeneration after fire through multitemporal analysis of AVIRIS images in the Santa Monica Mountains. *Remote Sensing of Environment* **79**, 60-71.

Rignot E, Salas WA, Skole DL (1997) Mapping deforestation and secondary growth in Rondonia, Brazil, using imaging radar and Thematic Mapper data. *Remote Sensing of Environment* 59, 169-179.

Rogan JM, Yool SR (2001) Mapping fire-induced vegetation depletion in the Peloncillo Mountains, Arizona and New Mexico. *International Journal of Remote Sensing* **22**, 3101-3121.

Romme WH (1982) Fire and landscape diversity in subalpine forests of Yellowstone National Park. *Ecological Monographs* **52**, 199-221.

Saatchi SS, Moghaddam M (2000) Estimation of crown and stem water content and biomass of boreal forest using polarimetric SAR imagery. *IEEE Transactions on Geoscience and Remote Sensing* **38**, 697-709.

Schistad Solberg AH, Jain AK, Taxt T (1994) Multisource classification of remotely sensed data: fusion of Landsat TM and SAR images. *IEEE Transactions on Geoscience and Remote Sensing* **32**, 768-778.

Shannon C, Weaver W (1949) 'The mathematical theory of communication.' (University of Illinois: Urbana, IL)

Siegert F, Hoffmann AA (2000) The 1998 forest fires in East Kalimantan (Indonesia): a qualitative evaluation using high resolution, multitemporal ERS-2 SAR images and NOAA-AVHRR hotspot data. *Remote Sensing of Environment* **72**, 64-77.

Svejkovsky J, Shandley J (2001) Detection of offshore plankton blooms with AVHRR and SAR imagery. *International Journal of Remote Sensing* **22**, 471-485.

Teillet PM, Guindon B, Goodenough DG (1982) On the slope-aspect correction of multispectral scanner data. *Canadian Journal of Remote Sensing* **8**, 84-106.

Townsend PA, Walsh SJ (1998) Modeling floodplain inundation using an integrated GIS with radar and optical remote sensing. *Geomorphology* 21, 295-312.

Töyrä J, Pietroniro A, Martz LW (2001) Multisensor hydrologic assessment of a freshwater wetland. *Remote Sensing of Environment* **75**, 162-173.

Tucker CJ, Sellers PJ (1986) Satellite remote sensing of primary production. *International Journal of Remote Sensing* **7**, 1395-1416.

White JD, Ryan KC, Key CC, Running SW (1996) Remote sensing of forest fire severity and vegetation recovery. *International Journal of Wildland Fire* **6**, 125-136.

Yesou H, Besnus Y, Rolet J, Pion JC, Aing A (1993) Merging Seasat and SPOT imagery fr the study of geological structures in a temperate agricultural region. *Remote Sensing of Environment* **43**, 265-279.

Table 1. Plot characteristics for fire plots.

plot	Area (m^2)	Mean Elevation (meters)	Mean Slope (°)	Aspect	Vegetation	Fire History
1.1	488974.5	2111.7	12.18	SE	oak	1994
1.2	334647.0	2114.4	14.20	W-SW	pine/oak	1989
1.3	271291.5	2565.7	7.25	S	pine	1943
2.1	1038867.8	2108.1	10.26	E	oak	1954, 1994
2.2	555579.0	2208.5	12.86	S-SW	pine/oak	1943, 1994
2.3	362263.5	2250.2	16.30	NW	pine/oak	1972, 1989
3.1	986071.5	2152.9	9.00	S-SE	pine	1943, 1954, 1994
5.1	175446.0	2168.1	11.71	E	pine/oak	1943, 1950, 1972, 1993, 1994
6.1	273728.3	2152.1	14.07	E	pine/oak	1943, 1950, 1956, 1972, 1993, 1994

Table 2. Summary of data fusion methods used in this study.

Fusion Channel	Description	TM Inputs	SIR-C Inputs
PC1	Principle Component 1 from all original bands	TM1, TM2, TM3, TM4, TM5, TM7	CHH, CHV, LHH, LHV
PC2	Principle Component 2 from all original bands	TM1, TM2, TM3, TM4, TM5, TM7	CHH, CHV, LHH, LHV
PC3	Principle Component 3 from all original bands	TM1, TM2, TM3, TM4, TM5, TM7	CHH, CHV, LHH, LHV
subPC1	Principle Component 1 from six enhancements	KT-H, KT-S, NDVI	CHV, CHH/LHH, LHV/CHV
subPC3	Principle Component 3 from six enhancements	KT-H, KT-S, NDVI	CHV, CHH/LHH, LHV/CHV
allPC2	Principle Component 2 all enhancements	KT-B, KT-G, KT-W, KT-I, KT-H, KT-S, NDVI	CHH, CHV, LHH, LHV, CHH/CHV, CHH/LHH, CHH/LHV, LHV/CHV, LHH/CHV, LHH/LHV
allPC3	Principle Component 3 all enhancements	KT-B, KT-G, KT-W, KT-I, KT-H, KT-S, NDVI	CHH, CHV, LHH, LHV, CHH/CHV, CHH/LHH, CHH/LHV, LHV/CHV, LHH/CHV, LHH/LHV
allPC4	Principle Component 4 all enhancements	KT-B, KT-G, KT-W, KT-I, KT-H, KT-S, NDVI	CHH, CHV, LHH, LHV, CHH/CHV, CHH/LHH, CHH/LHV, LHV/CHV, LHH/CHV, LHH/LHV
CLASS	Unsupervised Classification of six enhancements	KT-H, KT-S, NDVI	CHV, CHH/LHH, LHV/CHV
CHHi	Intensity component of TM/SIR-C composite containing CHH band	TM3, TM4	CHH
CHVi	Intensity component of TM/SIR-C composite containing CHV band	TM4, TM5	CHV
LHHi	Intensity component of TM/SIR-C composite containing LHH band	TM5, TM7	LHH
LHVi	Intensity component of TM/SIR-C composite containing LHV band	TM4, TM7	LHV
MULTI3	Principle Component 1 from TM3 multiplied by SIR-C bands	TM3	CHH, CHV, LHH, LHV
MULTI4	Principle Component 1 from TM4 multiplied by SIR-C bands	TM4	CHH, CHV, LHH, LHV
MULTI5	Principle Component 1 from TM5 multiplied by SIR-C bands	TM5	CHH, CHV, LHH, LHV
MULTI7	Principle Component 1 from TM7 multiplied by SIR-C bands	TM7	CHH, CHV, LHH, LHV

Table 3. Color assignments for input channels in IHS transformation.

	Red	Green	Blue
CHHi	TM4	TM3	CHH
CHVi	TM4	CHV	TM5
LHHi	LHH	TM7	TM5
LHVi	TM4	LHV	TM7

Table 4. Summary of Spatial Statistics used in analysis.

Statistic	Abbreviation	Description	Reference
Mean Patch Fractal Dimension	MPFD	average fractal dimension (area and perimeter calculation)	Li, 1990
Area Weighted MPFD	AWMPFD	average fractal dimension weighted by patch area	Li, 1990
Mean Patch Size	MPS	average patch size	McGarigal and Marks, 1995
Patch Size Coefficient of Variation	PSCV	patch size standard deviation / mean patch size	McGarigal and Marks, 1995
Shannon's Diversity Index	SDI	sensitive to richness (number of patch types)	Shannon and Weaver, 1949
Shannon's Evenness Index	SEI	distribution of area among patch types	Shannon and Weaver, 1949

Table 5. Description of fire history variables.

Variable	Description
last10	number of fire free years in the last 10 years
last20	number of fire free years in the last 20 years
last30	number of fire free years in the last 30 years
last40	number of fire free years in the last 40 years
last50	number of fire free years in the last 50 years
last52	number of fire free years in the last 52 years
last_fire	time since the most recent fire
last_ffi	length of most recent fire-free period
avg_ffi	average length of fire-free period

Table 6. Significant results ($p < 0.05$) of Spearman's Rank Correlation Analysis for all fire history variables, spatial measures, and image bands or enhancements. Correlations significant at 0.01 are in italics. $n = 9$.

		last10	last30	last40	last50	last52	last_fire	last_ffi	avg_ffi
AWMPFD	NDVI		0.771	0.749	*0.828*	*0.845*			*0.831*
	KT-I							-0.684	
	KT-H	*0.837*	*0.853*	*0.840*	*0.949*	*0.897*			*0.949*
	KT-S						-0.727		
	PC2	0.687			*0.845*	*0.845*	0.727		0.712
	subPC1								0.678
	allPC4							-0.709	
MPFD	KT-B								-0.678
	KT-W							-0.709	
	KT-I								-0.695
	KT-H							-0.734	
	KT-S							-0.709	
	LHH/CHV					-0.707	-0.777		
	CHHi		-0.688	-0.676					
	CHVi						0.777		
	allPC3							*-0.937*	-0.746
	allPC4	-0.767	-0.743	-0.749					
MPS	NDVI		0.743	0.712	*0.811*				*0.881*
	KT-H		0.798	*0.803*	0.690				*0.831*
	KT-S						*0.837*		
	CHH/LHH							0.785	
	PC2		0.688	0.676	0.742	0.759			0.678
	PC3						-0.777		
	subPC1							0.76	
	MULTI3				-0.776	-0.742			-0.797
	MULTI5							*-0.861*	
	MULTI7					*-0.845*			
	CHVi						0.757		
PSCV	KT-W	-0.677	-0.688	-0.676					-0.695
	KT-H								0.797
	KT-S	-0.687	-0.716	-0.730					-0.729
	PC3						-0.757		
	MULTI7	0.700	*0.802*	0.798	0.736	*0.823*			
	allPC2	-0.767	-0.743	-0.730	-0.759	-0.759			-0.695
SDI	NDVI				-0.725				-0.695
	KT-I	-0.677							-0.695
	KT-H				*-0.828*	-0.742			*-0.865*
	KT-S						*-0.837*		
	CHV	-0.767	-0.798	-0.785	-0.707				-0.78
	LHH		-0.688	-0.676					
	CHLV		-0.716	-0.694					
	LHCV								
	LVCV		-0.743	-0.767	*-0.863*	*-0.811*			*-0.932*
	LHLV	-0.697	-0.688	-0.694					
	PC1		0.716	0.694					
	PC2						*0.837*		
	CLASS				-0.725				-0.797
	subPC1				-0.725				*-0.831*
	MULTI3	*0.837*	*0.853*	*0.840*	*0.949*	*0.897*			*0.949*
	MULTI5							*0.836*	
	MULTI7								0.706
	CHHi	-0.767	-0.743	-0.730	-0.759	-0.914			-0.712
	LHHi							-0.684	
	LHVi							-0.684	
SEI	KT-I					0.759	*0.807*		
	KT-H								-0.695
	KT-S						*-0.837*		
	CHLH						0.777		
	PC2						0.777		
	subPC3							-0.734	
	MULTI5							0.785	
	CHHi		-0.688	-0.712					
	LHVi						*0.807*		

Table 7. Strongest correlations for each fire history variable. $n = 9$.

Fire History Variable	Spearman's ρ, p	Image Band	Spatial Measure
last10	0.837, 0.005	KT-H	AWMPFD
last10	0.837, 0.005	MULTI3	SDI
last30	0.853, 0.003	KT-H	AWMPFD
last30	0.853, 0.003	MULTI3	SDI
last40	0.840, 0.005	KT-H	AWMPFD
last40	0.840, 0.005	MULTI3	SDI
last50	0.949, 0.000	KT-H	AWMPFD
last50	0.949, 0.000	MULTI3	SDI
last52	-0.914, 0.001	CHHi	SDI
last_fire	-0.837, 0.005	KT-S	SDI
last_fire	0.837, 0.005	PC2	SDI
last_fire	0.837, 0.005	KT-S	MPS
last_FFI	-0.937, 0.000	allPC3	MPFD
avg_FFI	0.949, 0.000	KT-H	AWMPFD
avg_FFI	0.949, 0.000	MULTI3	SDI

FIGURE CAPTIONS

Figure 1. Location of Saguaro National Park, Rincon Mountain District. Dashed line shows area of focus.

Figure 2 Landsat TM 742 (RGB) false color composite 13 October 1994, with study plot locations shown. a) Scene prior to topographic normalization. b) Scene following c-factor topographic normalization.

Figure 3 Grayscale versions of four original bands of SIR-C data with fire plot locations shown.

Figure 4 Grayscale versions of six ratios calculated from original bands of SIR-C data with fire plot locations shown. a) C-HH/C-HV, b) C-HH/L-HH, c) C-HH/L-HV, d) L-HH/C-HV, e) L-HV/C-HV, f) L-HH/L-HV. Plot locations are labeled in a).

Figure 5 Grayscale images from Principal Components Analysis using all original TM bands and SIR-C channels. a) PC1, b) PC2, c) PC3. Plot labels are shown in a).

Figure 6 Grayscale images from Principal Components Analysis using all derived TM bands and SIR-C channels. a) allPC2, b) allPC3, c) allPC4. Plot labels are shown in a).

Figure 7 Flow chart showing multiplication data fusion technique used in this study.

Figure 8 Flow chart showing data simplification and analysis procedures.

Figure 9 Bar chart showing mean MPS for fused data, Landsat TM, and SIR-C.

Figure 10 Scatter plots for selected image enhancements, showing relationships between landscape metrics and average fire-free interval (AVG_FFI). Y-axis on all plots is average fire-free interval in years. Image enhancements shown, obtained the strongest correlation for each landscape metric. a) Area-Weighted Mean Patch Fractal Dimension (normalized) derived from KT-Hue, b) Mean Patch Fractal Dimension (normalized) derived from allPC3 fusion enhancement, c) Mean Patch Size (normalized) derived from NDVI, d) Patch Size Coefficient of Variation (normalized) derived from KT-Hue, e) Shannon's Diversity Index (normalized) derived from MULTI3 fusion enhancement, f) Shannon's Evenness Index (normalized) derived from KT-Hue.

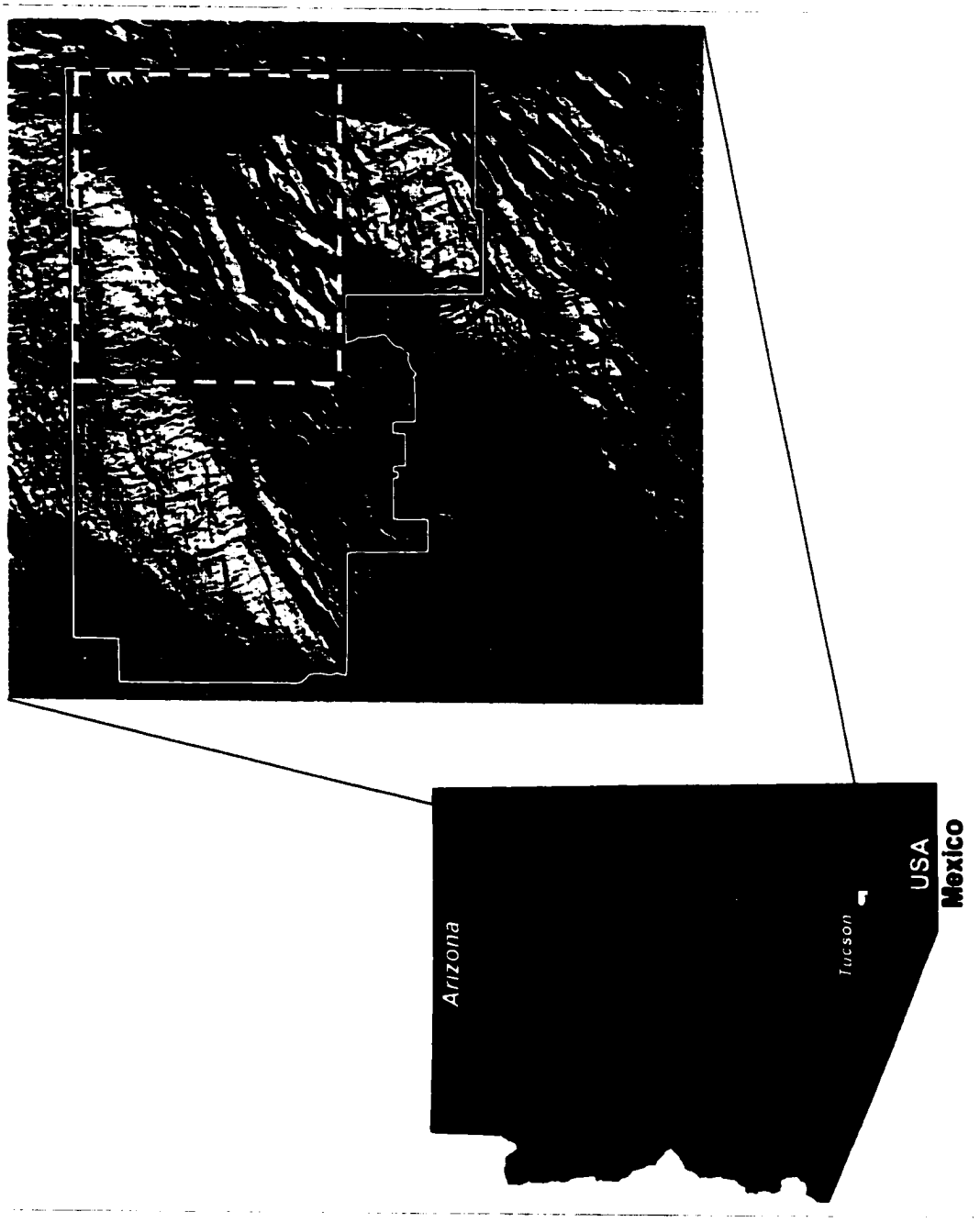

Figure 1

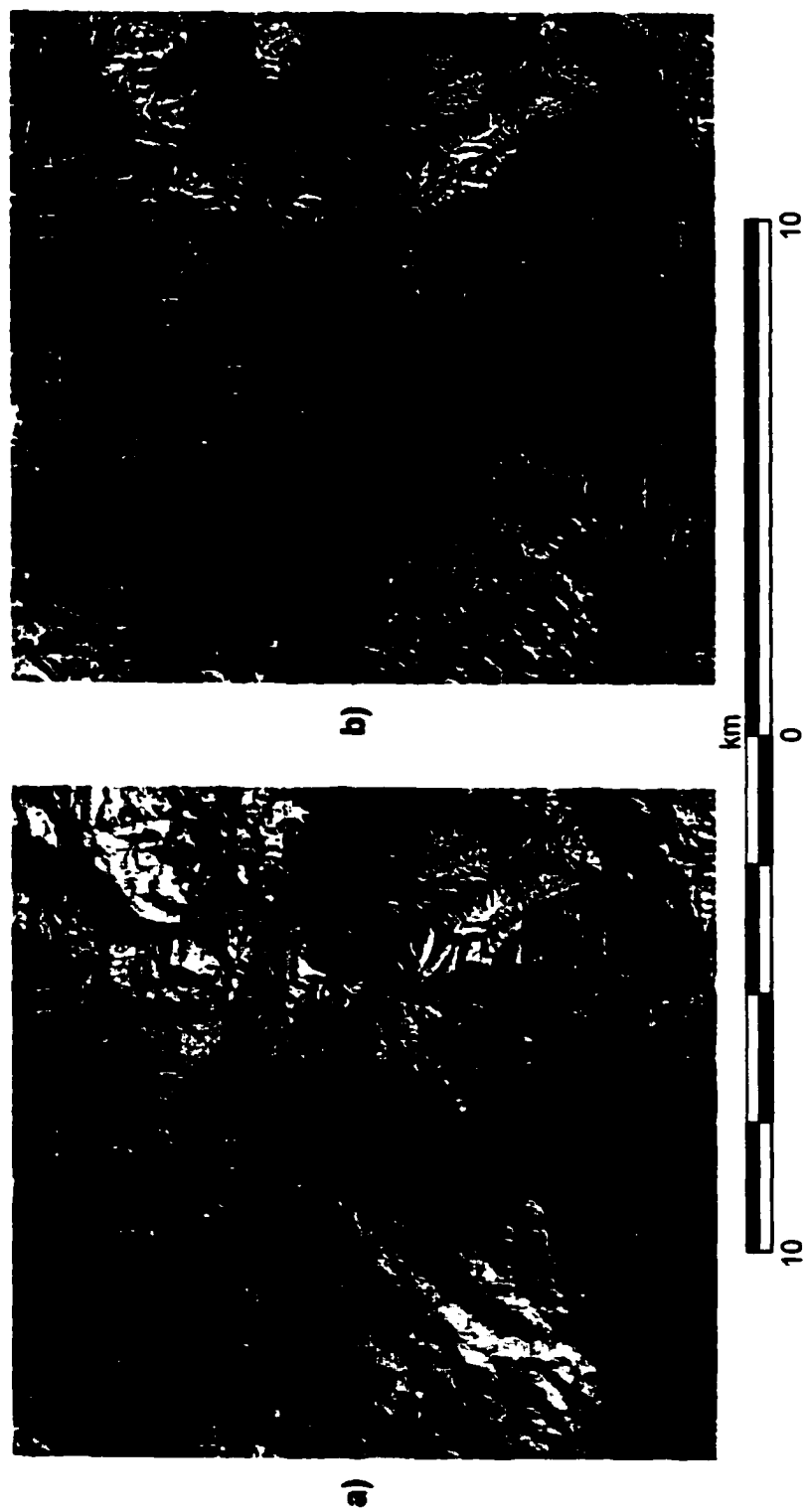

Figure 2

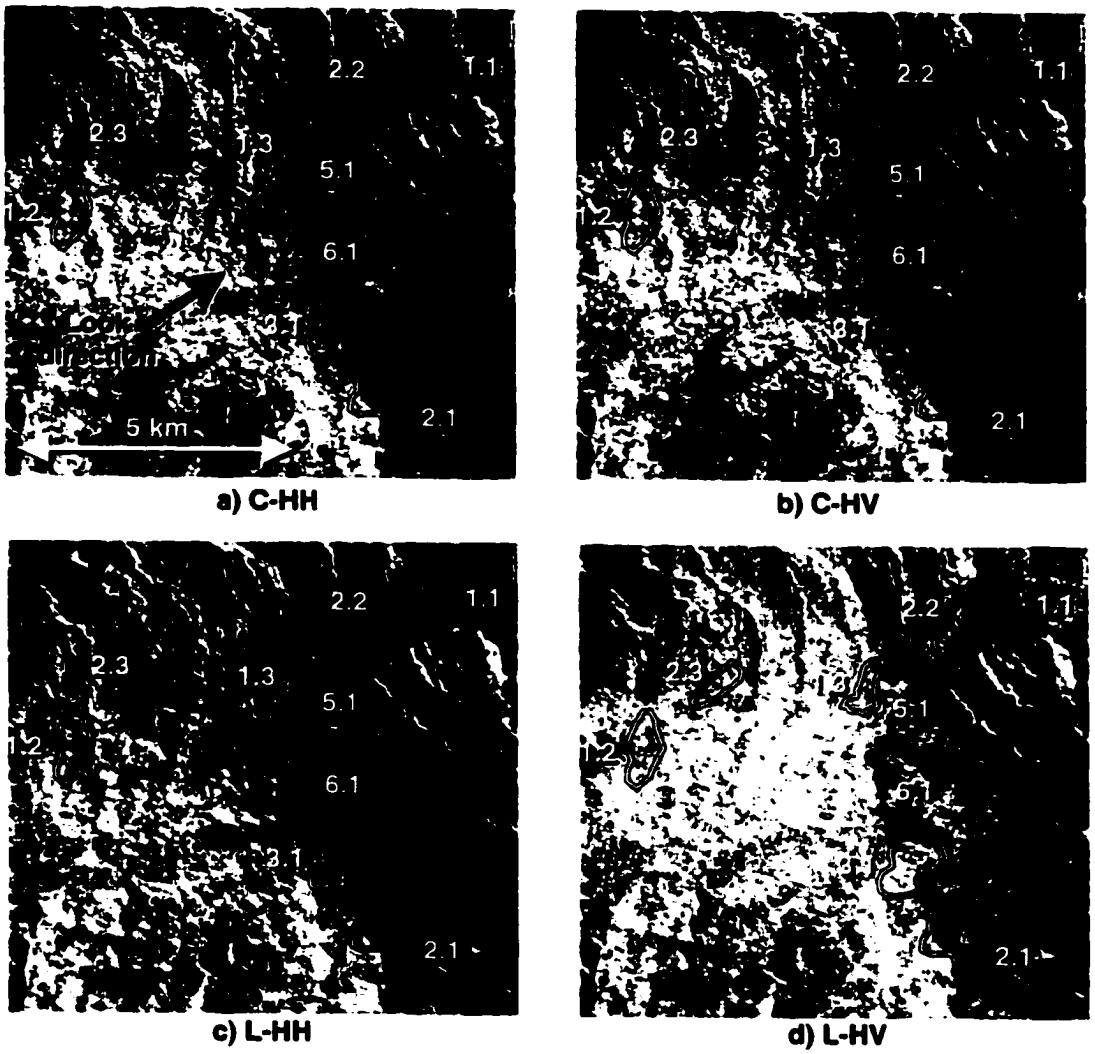

Figure 3

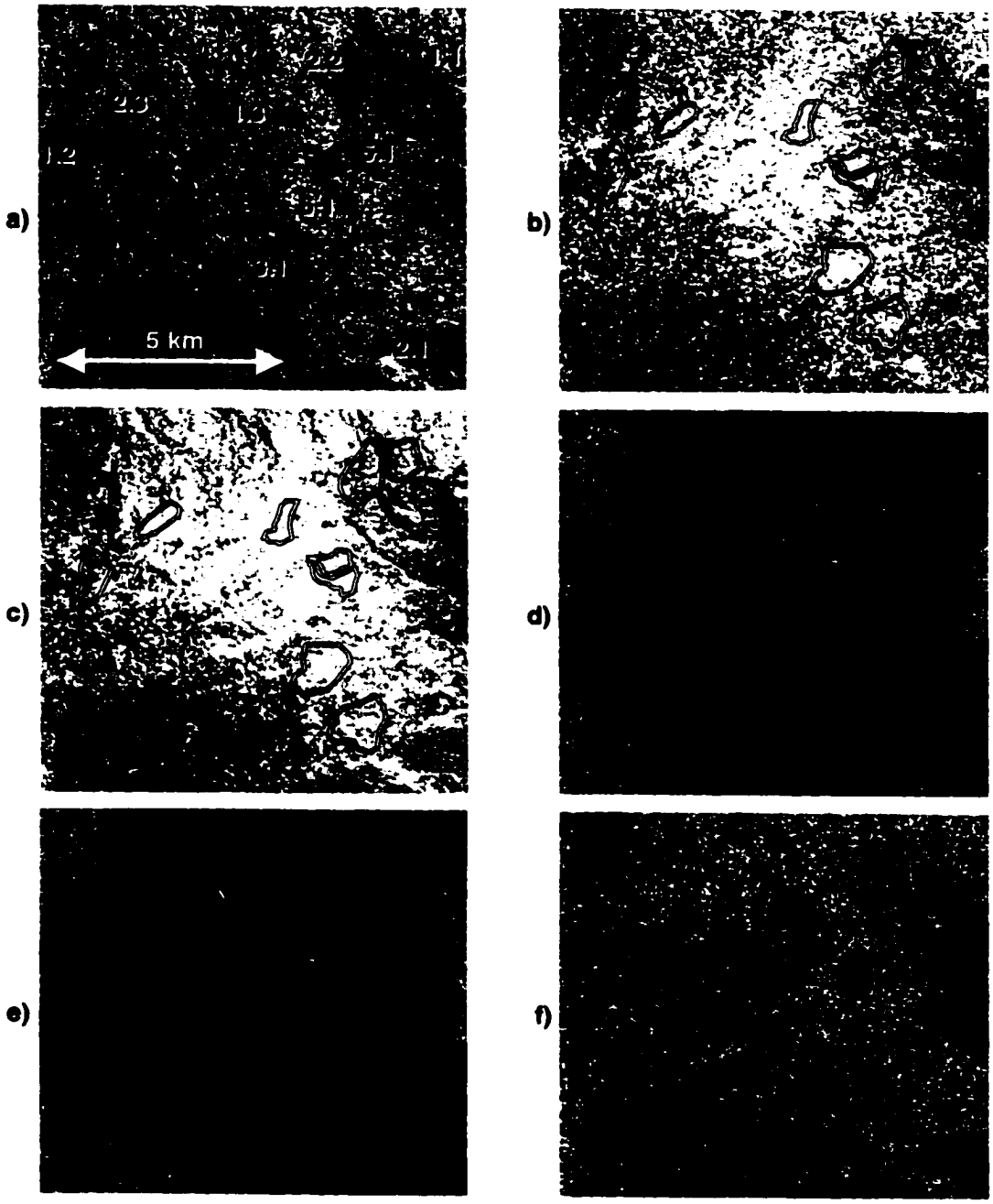

Figure 4

Figure 5

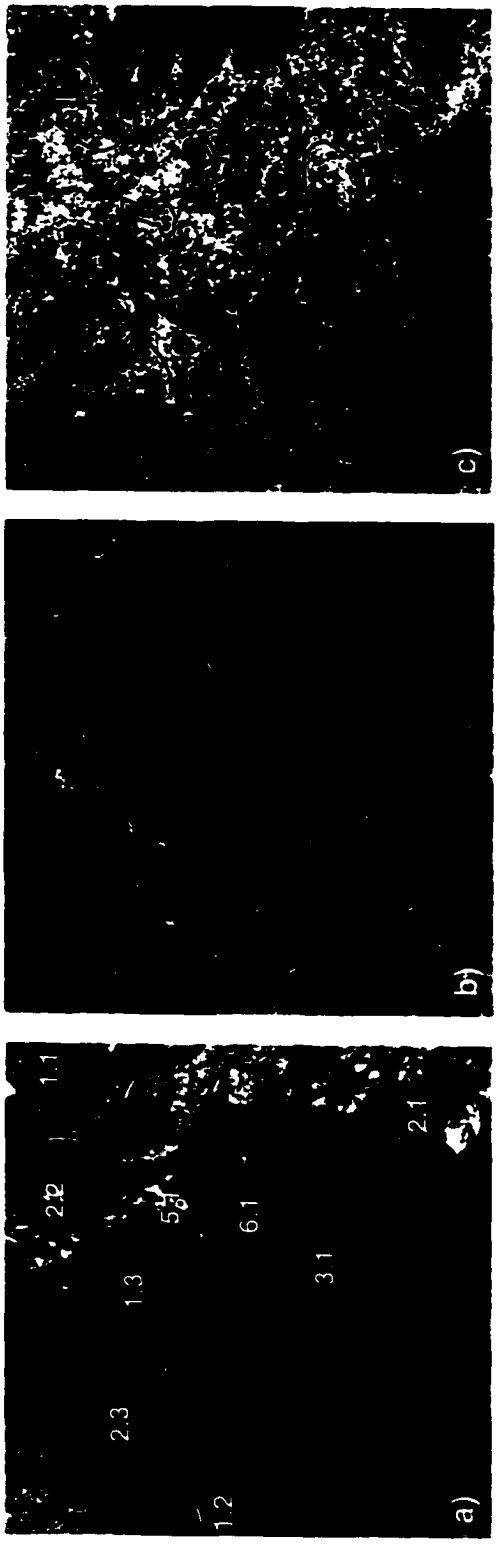

Figure 6

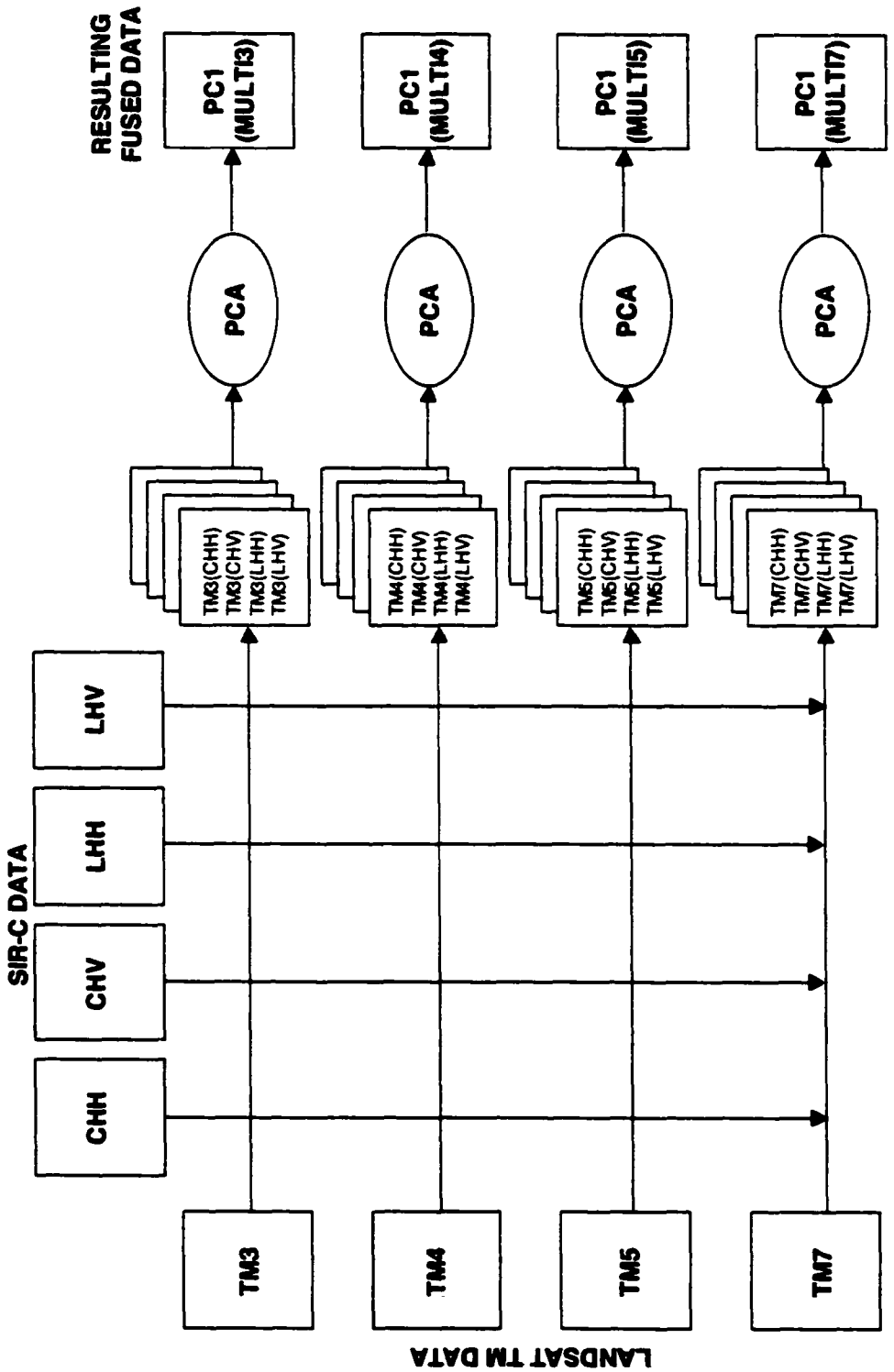
RESULTING FUSED DATA
PC1 (MULTI3)
PC1 (MULTI4)
PC1 (MULTI5)
PC1 (MULTI7)
PCA
PCA
PCA
PCA
TM3(CHH)
TM3(CHV)
TM3(LHH)
TM3(LHV)
TM4(CHH)
TM4(CHV)
TM4(LHH)
TM4(LHV)
TM5(CHH)
TM5(CHV)
TM5(LHH)
TM5(LHV)
TM7(CHH)
TM7(CHV)
TM7(LHH)
TM7(LHV)
SIR-C DATA
LHV
LHH
CHV
CHH
TM3
TM4
TM5
TM7
LANDSAT TM DATA

Figure 7

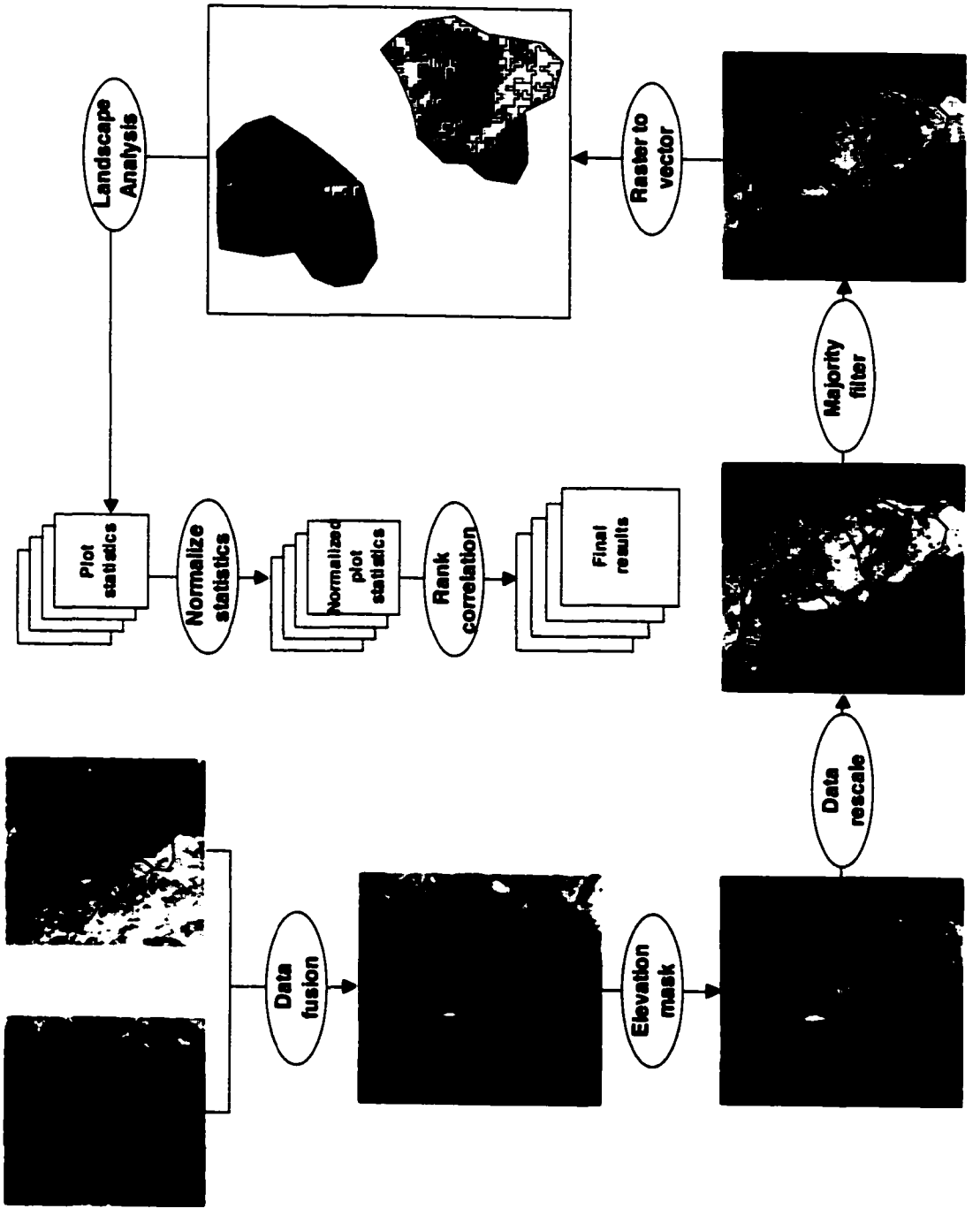
Landscape Analysis
Raster to vector
Majority filter
Plot statistics
Normalize statistics
Normalized plot statistics
Rank correlation
Final results
Data rescale
Data fusion
Elevation mask

Figure 8

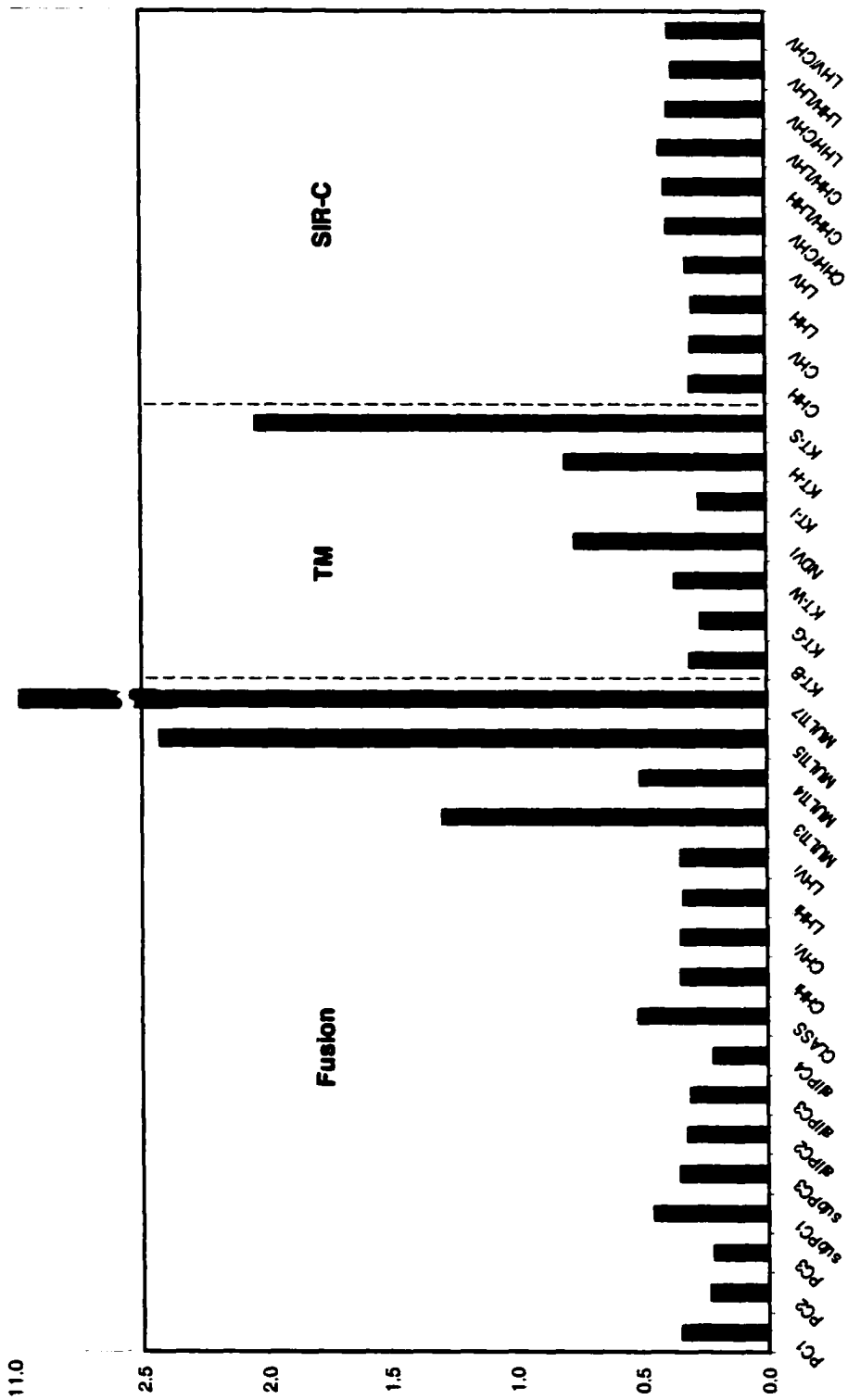
SIR-C
TM
Fusion
11.0
2.5
2.0
1.5
1.0
0.5
0.0
PC1
PC2
PC2
subPC1
subPC2
#IPC2
#IPC2
#IPC2
#IPC4
CLASS
CHI
CHI
CHI
LHI
MLT13
MLT14
MLT15
MLT17
KT-8
KT-G
KT-N
NDVI
KT-I
KT-H
KT-S
CHI
CHI
CHI
LHI
CHIHCHI
CHHLHI
CHHLHI
LHHCHI
LHHLHI
LHVCHI

Figure 9

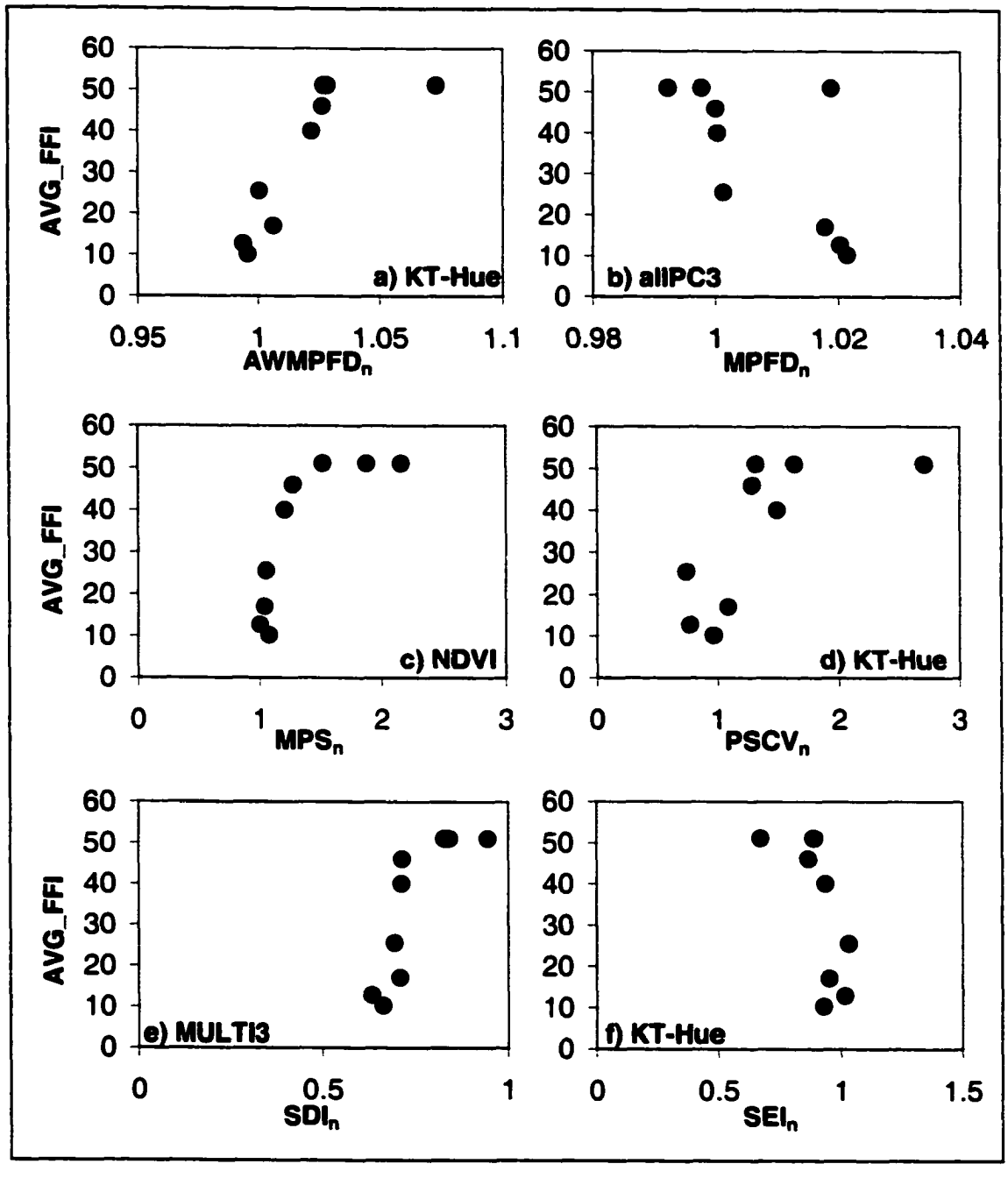
AVG_FFI
a) KT-Hue
AWMPFD$_n$
b) allPC3
MPFD$_n$
c) NDVI
MPS$_n$
d) KT-Hue
PSCV$_n$
e) MULTI3
SDI$_n$
f) KT-Hue
SEI$_n$

Figure 10